INVESTIGATION ON THE BIOACTIVE SECONDARY METABOLITES OF THE ENDOPHYTIC FUNGUS *PENICILLIUM ROSEOPURPUREUM*

A Thesis Submitted to
The Graduate School of Engineering and Sciences of
İzmir Institute of Technology
in Partial Fulfilment of the Requirements for the Degree of

MASTER OF SCIENCE

in Biotechnology

by
Berivan DİZMEN

March, 2022
İZMİR

ACKNOWLEDGMENTS

I am grateful to my advisor Prof. Dr. Erdal BEDİR for his support and immense knowledge throughout my master's study.

I would like to thank Prof. Dr. Petek BALLAR KIRMIZIBAYRAK for opening her laboratory for bioactivity studies.

I also want to thank all Bedir Group members.

I would like to thank Melis KÜÇÜKSOLAK for sharing her knowledge and experience during my research.

I'm grateful to Göklem ÜNER for supporting and assisting the bioactivity studies.

I want to thank Eyüp BİLGİ, Gamze DOĞAN, Gülten KURU, Mehmet DEMİR and Ünver KURT and all Bedir Group members for their endless help, supporting and valuable friendship.

I am deeply thankful to Berat KARABAL for his patience and support.

Finally, I am thankful to my family who have always supported me patiently all my life.

ABSTRACT

INVESTIGATION ON THE BIOACTIVE SECONDARY METABOLITES OF THE ENDOPHYTIC FUNGUS *PENICILLIUM ROSEOPURPUREUM*

In recent years, endophytic fungi have been considered as significant resources of new bioactive secondary metabolites, so they are predicted to have an important impact in drug discovery and development.

In our preliminary study, the chemical diversity and cytotoxic activity of an endophytic fungus, namely *Penicilium roseopurpureum* 1E4BS1 isolated from *Astragalus angustifolius*, have been demonstrated. Based on these data, it was aimed to obtain bioactive secondary metabolites of *P. roseopurpureum* 1E4BS1 within the scope of this thesis. Firstly, a fermentation study was carried out in a rotary shaker at 180 rpm, 25 ºC for 20 days, and the obtained broth was extracted with EtOAc. Secondly, nine metabolites were isolated from the EtOAc extract by chromatographic methods, and the structures of compounds were elucidated by spectral methods (1D-, 2D NMR, and MS). The structure elucidation studies revealed that seven metabolites had anthraquinone backbone, whereas two compounds were found to be derivatives of curvularin from macrolide group. A chemical structure search confirmed that five of the metabolites were new for nature.

Cytotoxic activity of the compounds and the EtOAc extract was tested against three cancer (DU145, LnCaP, and PC3) and normal (RPWE-1) cell lines by MTT cell viability assay. The metabolite **PR-EB-01** exhibited the highest activity with IC_{50} values of 26.0, 37.2, 24.7, and 30.9 μM against LNCaP, PC3, DU145, and RPWE-1 cells, respectively.

ÖZET

ENDOFİTİK *PENICILLIUM ROSEOPURPUREUM* FUNGUSUNDAN ELDE EDİLEN SEKONDER METABOLİTLERİ VE BİYOAKTİVİTELERİ

Son yıllarda endofitik funguslar yeni biyoaktif sekonder metabolitlerin üretimi için önemli kaynaklar olarak değerlendirilmiştir ve özellikle ilaç endüstrisi açısından ilaç keşfi ve geliştirilmesine büyük katkı sağlayacağı öngörülmektedir.

Ön çalışmamızda, *Astragalus angustifolius*'tan izole edilen bir endofitik fungus olan *Penicillium roseopurpureum* 1E4BS1'in kimyasal çeşitliliği ve sitotoksik aktivitesi gösterilmiştir. Bu verilerden hareketle, bu tez kapsamında *P. roseopurpureum* 1E4BS1'in biyoaktif sekonder metabolitlerinin elde edilmesi amaçlanmıştır. İlk olarak 20 gün boyunca 25 ºC 180 rpm'de çalkalamalı inkübatörde fermentasyon işlemi gerçekleştirilmiş ve elde edilen broth EtOAc ile ekstraksiyon işlemine tabii tutulmuştur. EtOAc ekstresinden kromatografik yöntemlerle dokuz metabolit izole edilmiş ve spektral yöntemlerle (1D-, 2D-NMR ve MS) yapıları belirlenmiştir. Yapı tayini çalışmaları yedi metabolitin antrakinon iki metabolitin ise makrolid grubu curvularin iskeletine sahip olduğunu göstermiştir. Gerçekleştirilen kimyasal yapı taraması elde edilen beş metabolitin doğa için yeni olduğunu ortaya koymuştur.

Bileşiklerin ve EtOAc ekstresinin sitotoksik etkileri, üç kanser (DU145, LnCaP ve PC3) ve bir normal (RWPE-1) hücre hattına karşı MTT hücre canlılığı testi ile araştırılmıştır. Metabolit **PR-EB-01** LnCaP, PC3, DU145 ve RWPE-1 hücrelerine karşı sırasıyla 26, 37.2, 24.7 ve 30.9 µM IC_{50} değerleri ile en yüksek aktiviteyi göstermiştir.

TABLE OF CONTENTS

LIST OF FIGURES

Figure **Page**

Figure **Page**

LIST OF TABLES

Table **Page**

LIST OF SPECTRA

Spectrum **Page**

Spectrum **Page**

ABBREVIATIONS

$CHCl_3$	Chloroform
DMSO	Dimethyl sulfoxide
EtOAc	Ethyl acetate
MeOH	Methanol
Hex	Hexane
CH_2CI_2	Dichloromethane
H_2SO_4	Sulfuric Acid
H_2O	Water
DMSO-d6	Deuterated Dimethyl Sulfoxido
PDB	Potato Dextrose Broth
PDA	Potato Dextrose Agar
PBS	Phosphate buffered saline
RP	Reversed Phase
DMEM	Dulbecco's Modified Eagle Medium
UV	Ultraviolet
IUPAC	International Union of Pure and Applied Chemistry
CC	Column Chromatography
TLC	Thin Layer Chromatography
VLC	Vacuum Liquid Chromatography
NMR	Nuclear Magnetic Resonance
1D-NMR	One-Dimensional Nuclear Magnetic Resonance
2D-NMR	Two-Dimensional Nuclear Magnetic Resonance
^{1}H-NMR	Proton Nuclear Magnetic Resonance
^{13}C-NMR	Carbon Nuclear Magnetic Resonance
HSQC	Heteronuclear Single Quantum Coherence
HMBC	Heteronuclear Multiple Bond Coherence
COSY	Correlation Spectroscopy
NOESY	Nuclear Overhauser Enhancement Spectroscopy
m	*Multiplet*
s	*Singlet*
d	*Doublet*

bs	*Broad singlet*
t	*Triplet*

CHAPTER 1

INTRODUCTION

Secondary metabolites are natural products with diverse chemical structures, not essential for growth, and possess diverse bioactivities. The discovery of new secondary metabolites has become even more important for not only pharmaceutical industry but also many other industries around the world including cosmetic, food and agriculture (Bills and Gloer 2017; Vasundhara, Sudhakara Reddy, and Kumar 2019) .

In mutualistic relationship between host plant and fungi, it is known that endophytic fungi produce beneficial metabolites that allow the host plant to survive via providing them to adapt distinct environmental stress factors (Patil, Patil, and Maheshwari 2016; Macheleidt et al. 2016) which holds a great potential for the identification of various new secondary metabolites (Thirumalanadhun et al. 2021). Although endophytic fungi isolated from plants are one of the important natural sources with new and diverse structures that are considerable for drug discovery and development studies, only a few plants have been studied in terms of endophytic fungi of which and their bioactive secondary metabolites until today (Thirumalanadhun et al. 2021; Wei and Wu 2020) and only some of them used in the commercial production of fungal bioactive compounds (Gupta et al. 2020; Bills and Gloer 2017). In recent years, endophytic fungi attracted the attention of scientists as a new source for drug discovery and development due to their rich metabolic profiles consisting of novel and bioactive compounds (Marinelli and Marcone 2019; Bills and Gloer 2017; Vasundhara, Sudhakara Reddy, and Kumar 2019).

There are two main routes for the investigation of secondary metabolites; the first is to isolate the unknown secondary metabolites, and the second is to isolate the unknown secondary metabolites with varied biological activities (Kalyanarman Rajagopal, SS, and R. 2019; Yadav et al. 2019). Therefore, to understand the true potential of endophytic fungi, the aspects of biochemical, biotechnological, chemical and related fields need to be elucidated. Within the scope of this thesis, the discovery of

new bioactive secondary metabolites produced by endophytic fungi *P. roseopurpureum* 1E4BS1 isolated from *Astragalus angustifolius/*stem were be elucidated and to obtaining excellent sources that can be used by pharmaceutical industry.

2.1. Secondary Metabolites

Secondary metabolites are heterogeneous low-molecular-weight natural compounds and distinct from the primary metabolites like lipids, amino acids, carbohydrates and nucleic acids. Secondary metabolites are not essential for growth, development, and reproduction of organism unlike primary metabolites (Brakhage 2013; Mosunova, Navarro-Muñoz, and Collemare 2020; Kumar et al. 2017a).

Secondary metabolites are synthesized by many organisms such as bacteria, fungi, and plants. The production and variation of secondary metabolites is mainly regulated by the interactions with their micro- and macro-environment (biotic or abiotic factors); thus, it can be considered that secondary metabolites have important roles in the survival of the organisms by exhibiting numerous biological activities owing to diverse chemical structures. Secondary metabolites have been an important source for scientist from different backgrounds for centuries and currently endophytic fungi attracted the attention of the experts in the field as a novel and virgin source (Mosunova, Navarro-Muñoz, and Collemare 2020; Chomel et al. 2016; Kumar et al. 2017a).

The main functions of secondary metabolites in the organisms.

I. Competitive weapons against detrimental organisms such as animals, plants, insects, and microorganisms,
II. Metal transporting agents,
III. Agents for symbiotic relation with other organisms,
IV. Reproductive agents,
V. Differentiation effectors,
VI. Agents of communication between organisms, and
VII. Interference in spore formation (not obligatory) and germination (Demain and Fang 2000; Thirumurugan et al. 2018a).

Secondary metabolites have been used for centuries due to their versatile functions as antibiotics (Narmani et al. 2019; Abdelgaleil et al. 2020), enzyme inhibitors (Gaber et al. 2016), immunosuppressive agents (Wang et al. 2018), antitumor agents (Narmani et al. 2019; Ramakrishna et al. 2021), pigments and surfactans (Barrios-González 2018; Vaishnav and Demain 2011), and nutraceuticals (Cisneros-Zevallos 2021). Additionally, secondary metabolites increase agricultural productivity as pesticides (Abdelgaleil et al. 2020), insecticides, growth promoters of plants (Ullah, Bano, and Janjua 2020), effectors of ecological competition, symbiosis and pheromones, thus secondary metabolites positively affect industrial productions by increasing the productivity (Thirumurugan et al. 2018b; Chomel et al. 2016; Vasundhara, Sudhakara Reddy, and Kumar 2019; Newman and Cragg 2020).

2.2. The Secondary Metabolism Pathways

The production of secondary metabolites begins from the primary metabolism since the necessary precursors come from the main biosynthetic pathways and regulated with specific enzymes (He et al. 2018; Grijseels et al. 2017).

Many secondary metabolites, that are structurally complex, come from structurally similar precursors. The most substantial precursors are acetyl-coenzyme A (CoA) and propionyl-CoA, creating polyketides, terpenes, steroids, and different other metabolites, and the intermediates pathways and krebs cycle help production of the secondary metabolites (Figure 1) (Sanchez and Demain 2019; Daniel 2007).

Secondary metabolites require numerous of specific enzymatic reactions for synthesis. The basis enzymes such as polyketide synthases, non-ribosomal peptide synthetases, hybrid polyketide synthase-nonribosomal peptide synthetases, terpene cyclases, and dimethylallyl tryptophan synthases catalyze simple primary metabolites involved acetyl-CoA, amino acids, or isoprene units for the production of more complex secondary metabolites which are polyketides (Bond, Tang, and Li 2016), nonribosomal peptides(Kopp and Marahiel 2007), hybrid polyketide- nonribosomal peptides (Cox, Skellam, and Williams 2018; Cox 2007), terpenoids (Ma et al. 2021; Habtemariam 2019), and alkaloids (Schläger and Dräger 2016; Hohlman and Sherman 2021),

respectively. Distinct metabolic pathways can afford different products (He et al. 2018; Keller 2019; Siddhardha and Meena 2020; Brakhage 2013).

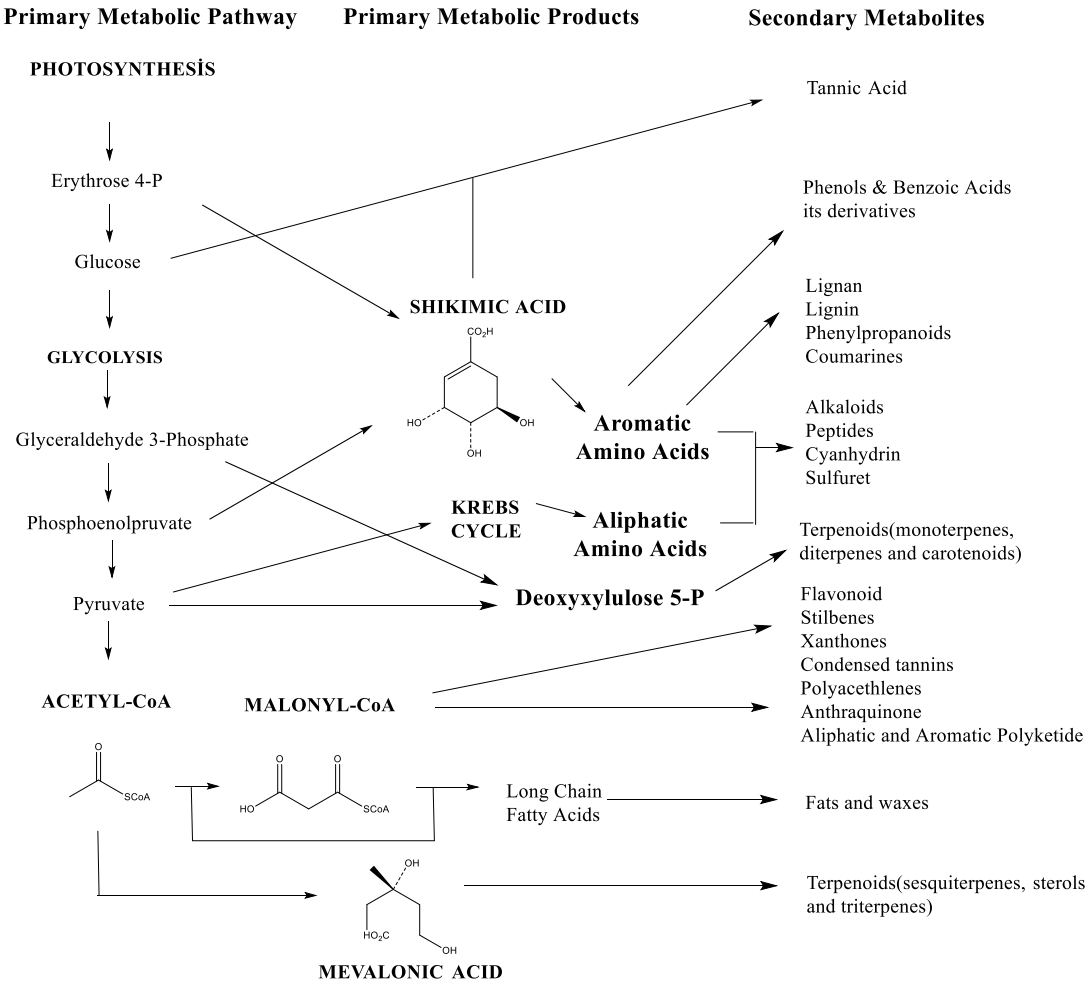

Figure 1. This diagram outlines how the secondary metabolite building blocks that occur during photosynthesis, glycolysis, and the krebs cycle are formed (Thirumurugan et al. 2018c).

2.3. Sources of Secondary Metabolite

With the discovery of new bioactive metabolites, especially antibiotics and anticancer agents, scientists have begun to investigate various natural resources (Gupta et al. 2020; Fleming 1929; Bills and Gloer 2017; Alkhulaifi et al. 2019). Numerous

bioactive secondary metabolites have been found out since 1950 (Marinelli and Marcone 2019; Bills and Gloer 2017).

In accordance with a survey conducted worldwide, about 61% of chemical compounds (535 out of 877) was isolated from nature between 1981 and 2002 and converted to drugs. In addition, 78% of antibacterial and 74% of anticancer substances were obtained from natural resources (Khan et al. 2014; Jamloki et al. 2021; Thirumurugan et al. 2018a). There are still a lot of undescribed compounds from soil, marine environments, plants or from symbiotic microorganisms with plants against variety of diseases (Marinelli and Marcone 2019; Bills and Gloer 2017; Daley, Brown, and Badal 2017).

Microorganisms and medicinal plants have important role to produce large number of secondary metabolites with pharmaceutical and biological activity (Marinelli and Marcone 2019; Demain and Fang 2000; Khan et al. 2014; Sanchez and Demain 2019; Jouda et al. 2016). More than 500 antibiotics are discovered each year, and 60% of them are acquired from the soil (Alkhulaifi et al. 2019).

As a result, there is an outstanding opportunity to discover new biomolecules from the myriad plants and microorganisms found in different kind of niches and ecosystems (Gupta et al. 2020).

2.3.1. Microbial Secondary Metabolites

Recently, natural product research has begun to intensify due to drug-resistant pathogenic microorganisms, the emergence of new diseases and side effects caused by synthetic drugs. Fungi have turned out to be a valuable resource containing important natural products with the discovery of penicillin by Alexander Fleming (Gupta et al. 2020; Fleming 1929; Bills and Gloer 2017; Alkhulaifi et al. 2019).

There are many important secondary metabolites remain undiscovered in terms of chemical diversity, and secondary metabolites produced by an estimated 99% of bacteria and 95% of fungi have not yet been investigated. The screening of these natural products may lead to the discovery of new drugs and allow the treatment of many diseases. In addition, the identification of biosynthetic gene clusters involved in the

synthesis of secondary metabolites is an crucial step for the discovery and development of microbial secondary metabolites (Marinelli and Marcone 2019; Bills and Gloer 2017; Abdelgaleil et al. 2020).

Microorganisms like small chemical factories synthesize distinct and many secondary metabolites which can be used as a antibiotic, antitumor and pigments (Table 1) (Abdelgaleil et al. 2020). The discovery studies of secondary metabolite have shown that microbial compounds have exclusive molecular structures which are not obtainable in chemical libraries, and chemists have revealed that it is not possible to synthesize many of these metabolites. Over the past fifty years, more than 50.000 novel biological active metabolites have been obtained from microorganisms, out of which 17.000 are new antibiotics (Kalyanarman Rajagopal, SS, and R. 2019; Yadav et al. 2019).

Microorganisms such as *Bacillus, Pseudomonas, Myxobacteria* and *Cyanobacteria* produce valuable secondary metabolites. It is known that most of the secondary metabolites are generated by the genus *Streptomyces.* Fungi are the most significant resources capable of producing many different secondary metabolites, and many metabolites with antibiotic properties have been obtained from fungi (Kalyanarman Rajagopal, SS, and R. 2019; Yadav et al. 2019).

Table 1. List of secondary metabolites produced by different microorganisms with their applications (Ullah, Bano, and Janjua 2020).

Activities	**Microbial Secondary Metabolites**
Antibiotics	Bacilysocin, Thuricin, Pseudomonine, Holomycine, Spiramycin, Rifamycin, Teicoplanin, Tetracycline, Mitosane, Chloramphenicol
Growth Hormon	Indoleacetic acid, Gibberellic acid, Abscisic acid, Cytokinin, Ethylene
Pigments	Astraxanthin, Monascin, Carotenoids, Flavins, Chlorophyll, Quinines, Prodigioson, Violacien
Chelating Compounds	Zincophore (ethylene diamine disuccinate), Siderophores (pyoverdines, phenol catecholates hydroxamate)
Antitumor	Anthracycline, Bleomycines, Antracenones, Epotilones, Mitomycin, Trioxacarcins, Chinikomycins A and B

2.3.1.1. Fungal Bioactive Metabolites

Fungi are somewhere between multicellular and unicellular eukaryotic structures that produce biologically active secondary metabolites. Although they are structurally apart from plants and animals, they possess some similar forms with them. Fungi can produce desired secondary metabolites by providing varied nutrients under different fermentation conditions. They can live in a wide variety of environments, including water, land/soil, plants and animals. Fungi also allow the non-living plants and animals to be recycled into organic compounds using extracellular digestive enzymes, so they can synthesize secondary metabolites with the analogous starting units, such as terpenes and polyketides (Khan et al. 2014; Bills and Gloer 2016; 2017).

In addition, development of new culturing conditions in laboratory has made it even more common to utilize fungi in experimental models. As fungi are one of the main sources of secondary metabolite production, some fungal genus such as *Penicillium*, *Aspergillus*, *Trichoderma* and *Fusarium* are the most frequently encountered microorganisms in the production of secondary metabolites (Figure 2) (Rokas et al. 2020; Kumar et al. 2017a).

Aspergillus terreus

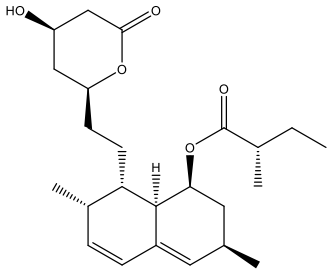

Lovastatin

Fusarium graminearum

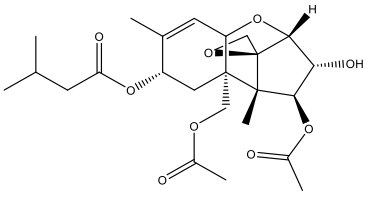

Trichothecene T-2 Toxin

Cont. on next page

Cont. of Figure 2

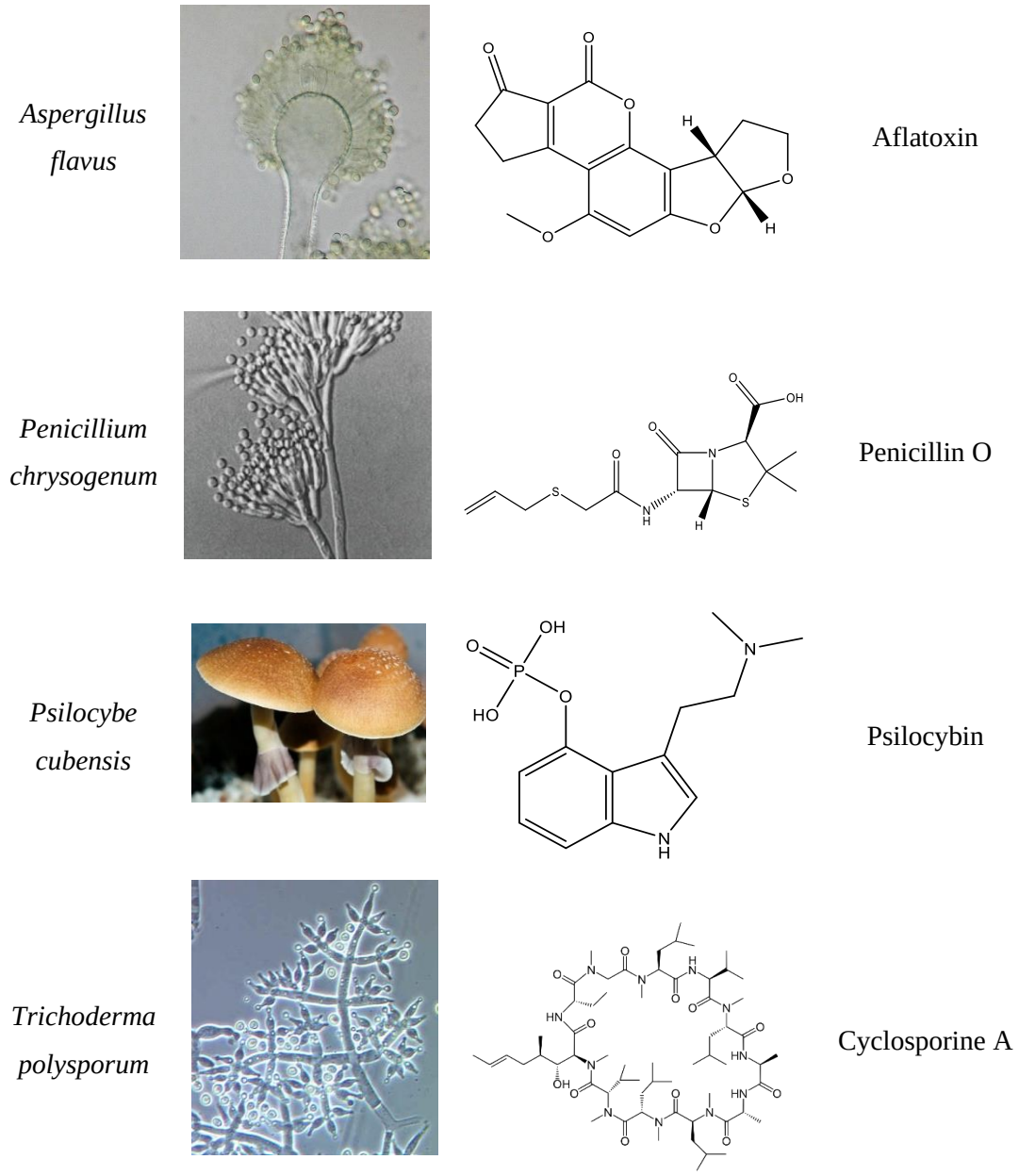

Figure 2. Some approved secondary metabolites from fungal species (Rokas et al. 2020).

Some important pharmaceuticals such as fusidic acid, cephalosporin and penicillin generated by fungi are broadly utilized in the treatment of many diseases (Alkhulaifi et al. 2019; Newman and Cragg 2020; Tallapragada and Dikshit 2017).

In studies, the fungi are used to discover not only new antibiotics, but also, antitumor, pigments, enzyme inhibitors, insecticides, immunosuppressive agents, and etc.(Kalyanarman Rajagopal, SS, and R. 2019; Yadav et al. 2019).

2.3.1.1.1. Endophytic Fungi as a Source of Bioactive Secondary Metabolites

Endophytes are microorganisms, which colonizes in the internal and distinct tissues of the host plants (Figure 3) (Mazumder et al. 2021; Ogbe, Finnie, and van Staden 2020a). As an endophytic microorganism, it uses nutrients from the plant (Patil, Patil, and Maheshwari 2016; Macheleidt et al. 2016a).

Each plant hosts one or more endophytic microorganisms, and these microorganisms have symbiotic relationships with their host plants as mutualistic, commensalistic or parasitic (Mazumder et al. 2021; Ogbe, Finnie, and van Staden 2020a) depending on the characteristics of the host and endophyte (Patil, Patil, and Maheshwari 2016; Macheleidt et al. 2016). In mutualistic relationship, endophytic microorganisms provide their host plants to be resistant to varied biotic (pathogen damage) and abiotic factors (drought, salinity and temperature changes, etc.) (Patil, Patil, and Maheshwari 2016; Macheleidt et al. 2016).

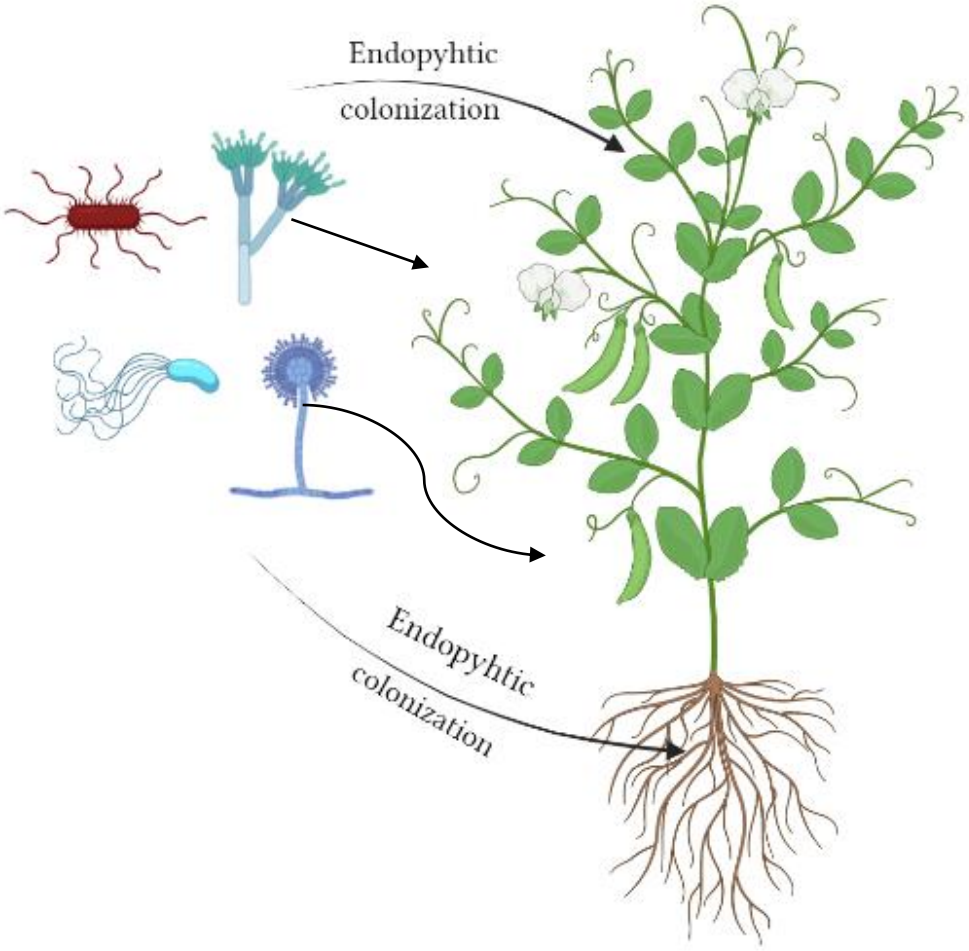

Figure 3. Endophyhtic organisms colonizes in plant or different niches (Kalyanarman Rajagopal, SS, and R. 2019).

Plants growing in Arctic, Antarctic, geothermal soils, deserts, oceans, and coastal regions provide a well opportunity for the discovery and exploration of new endophytic microorganisms. Although fungi, bacteria, actinobacteria and algae might have symbiotic associations with the plants, fungi are the most common endophytic microorganisms (Singh et al. 2021a; Patil, Patil, and Maheshwari 2016).

Many important bioactive metabolites have been discovered from endophytic fungi for the treatment of certain diseases. Therefore, it is of great importance to research and discover endophytes for the isolation of novel and bioactive compounds (Patil, Patil, and Maheshwari 2016; Jouda et al. 2016). It has been observed that some endophytes are able to produce the same or similar metabolites as host plants by mimicking host chemistry.; for example, paclitaxel (Taxol), camptothesin and its

structural analogues, jasmonic acid, ginkgolide azadirachtin, etc (Patil, Patil, and Maheshwari 2016; Singh et al. 2021a).

The past two decades, the basis of natural product screening studies has developed for the acquisition of new bioactive compounds from endophytes. In a study, it was shown that the number of new products produced by endophytic isolates (51%) is greater than the number of new products generated by soil isolates (38%) (Gloer, n.d.; Dreyfuss and Chapela 1994; "EF as a Source," n.d.). In addition, the discovery of new and bioactive compounds produced by various endophytic microorganisms has become even more important due to drug-resistant pathogenic microorganisms (Thirumalanadhun et al. 2021; Ogbe, Finnie, and van Staden 2020a).

Also, some compounds such as alkaloids, polyketides, steroids, terpenoids, quinine, and flavonoids derived from distinct endophytic fungi have been exhibited to have different biological activity (Figure 4). Phenolic, flavonoid and terpenoid compounds obtained from endophytes have also been proven to show antioxidant activity. In addition, endophytic fungi are the most preferred among the endophytic microorganisms, as they have the potential to develop antibiotics and anticancer drugs. Therefore, the discovery of fungal endophytes could aid in the discovery of new secondary metabolites with biological activities and the development of a new drug (Table 2) (Thirumalanadhun et al. 2021; Ogbe, Finnie, and van Staden 2020a; Hoffmeister and Keller 2007; Tallapragada and Dikshit 2017).

Although endophytic fungi are one of the natural sources with new and diverse structures that play a role in the development of new drugs, very few plants have been studied in terms of endophytic fungi and bioactive secondary metabolite diversity to date (Thirumalanadhun et al. 2021; Wei and Wu 2020).

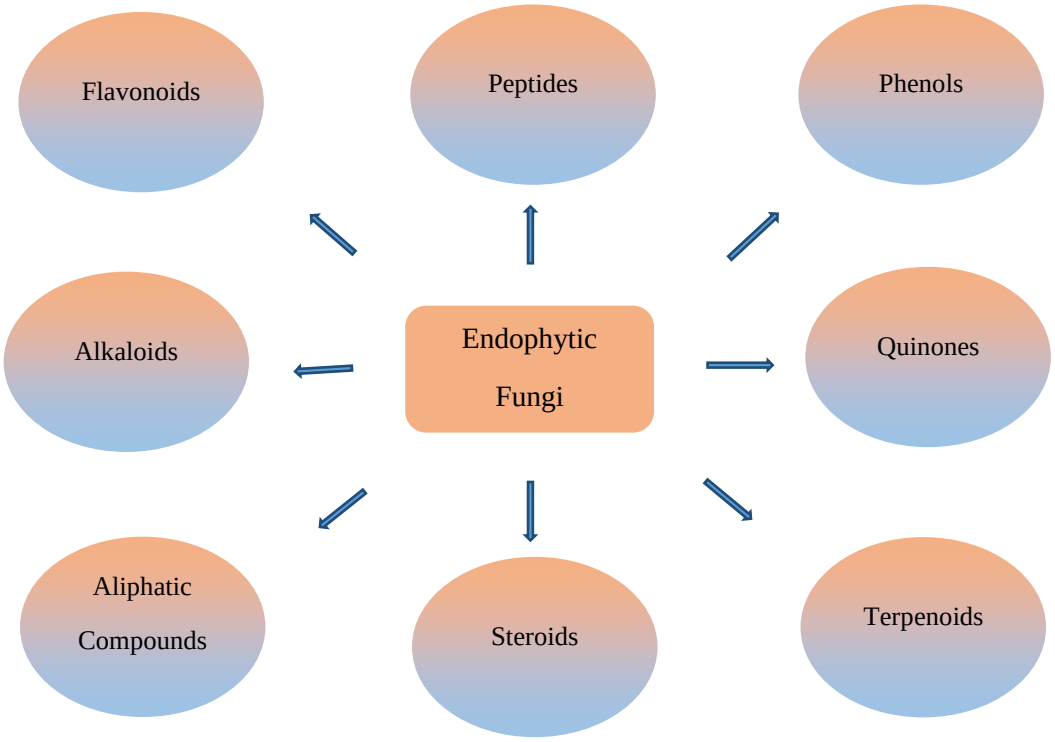

Figure 4. The chemical group of secondary metabolite produced from endophytic fungi (Singh et al. 2021b)

Despite the large amount of research on the production of bioactive compounds from fungal endophytes, the potential of this field is still in its initial stages (Gupta et al. 2020; Bills and Gloer 2017). This work will contribute to the discovery of new bioactive secondary metabolites produced by endophytic fungi that can be used by pharmaceutical industry.

Table 2. List of the known bioactive compounds produced from endophytic fungi (Kalyanarman Rajagopal, SS, and R. 2019).

S.No.	**Endophytic Fungus**	**Host Plant**	**Compound**
Anticancer Compounds			
1.	*Taxomyces andreanae*	*Taxus brevifolia*	Taxol
2.	*Pestalotiopsis microsporum*	*Torreya taxifolia*	Torreyanic acid
3.	*Entrophospora infrequens*	*Nothapodytes foetida*	Camptothecin
4.	*Fusarium solani*	*Camptotheca acuminata*	Topotecan
5.	*Aspergillus fumigates* *Philalocephala fortinii* *Fusarium oxysporum*	*Juniperus communis* *Podophyllum peltatum* *Juniperus recurva*	Podophyllotoxin
6.	Leaf Endophyte	*Mimusops elengi*	Ergoflavin

Cont. on next page

Cont. of Table 2

7.	*Mangrove Endophyte*	*Mangroves*	Secalonic acid D
8.	*Rhinocladiella sp.*	*Tripteygium wilfordii*	Cytochalasin Cytochalasin H Cytochalasin J Epoxycytochalasin
9.	*Chaetomium globosum*	*Imperata cylindrica*	Chaetoglobosin
10.	*Mycelia Sterilia*	*Catharanthus roseus*	Vincristine
11.	*Fusarium oxysporum*	*Annona squamosa*	Polyketide
12.	*Alternaria sp.*	*Taxus cuspidata*	Paclitaxel
Antioxidant Compounds			
13.	*Pestalotiopsis microspora*	*Terminalia morobensis*	Pestacin Isopectacin
14.	*Cephalosporium sp.*	*Sinarundinaria nitida*	Isobenzofurane
15.	*Fusarium sp.*	*Cajanus cajan*	Cajaninstilbene acid
16.	*Xylaria sp.*	*Ginkgo biloba*	Phenolics Flavonids
17.	*Chaetomium sp.*	*Nerium oleander*	Flavonids Phenolic acids
Immunosuppressive Compounds			
18.	*Cytonaema sp.*	*Medicinal Plant*	Cytonic acid A&B
19.	Unidentified endophyte	*Quercus coccifera*	Torreyanic acid
20.	*Pullularia sp.*	*Unidentified tree*	Pullularins A-D
21.	*Pestalotiopsis theae*	*Unidentified tree*	Pestalotheol-C
22.	*Aspergillus fumigates* *Phialocephala fortinii* *Fusarium oxysporum*	*Juniperus communis* *Podophyllum peltatum* *Juniperus recurva*	Podophyllotoxin
23.	Leaf Endophyte	*Mimusops Elengi*	Ergoflavin

1.1.1.1.2. Secondary Metabolites of The Genus Penicillium

Filamentous fungal genus *Penicillium*, which has more than 483 species, is widely found in nature due to its high adaptation to environmental changes and conditions. *Penicillium* is an anamorphic ascomycete. *Penicillium* species are the most studied species due to their prevalence and capacity to produce a wide range of secondary metabolites with known bioactivities. The active metabolites include antifungal and antibacterial agents, immunosuppressants, cholesterol-lowering agents, anticancer and potent mycotoxins. Roquefortine produced by *Penicllium* is a mycotoxin as a neurotoxic compound and inhibits digestive system enzymes and the activities of cytochrome P-450. Alkaloids, diketopiperazines, quinolines, quinazolines, and polyketides are some examples of biologically active compounds (Grijseels et al. 2017; Tallapragada and Dikshit 2017).

Penicillium produce the best-known secondary metabolite, penicillin (Fleming 1929), discovered by Fleming, and which is now produced on a large scale under better production conditions using *P. rubens*. Griseofulvin with antifungal properties (Oxford, Raistrick, and Simonart, n.d.), mycophenolic acid with immunosuppressant properties (Regueira et al. 2011), and cholesterol-lowering drug compactin/mevastatin (Brown et al., n.d.) are only a few examples of important pharmaceutical compounds produced by *Penicillium* species. These examples show that *Penicillium* sp. have great importance as sources of bioactive compounds in medical applications. In addition, *Penicillium* species can also produce mycotoxins such as citrinin, ochratoxin, and patulin (Frisvad et al. 2004), which can pose a risk to humans and animals (Grijseels et al. 2017; Tallapragada and Dikshit 2017).

Penicillium species have also been shown to produce many significant compounds such as 3-oxoquinuclidine from *Penicillium jenseii*, limonene from *Penicillium purpurogenum*, *P. olsonii*, *P. roqueforti*, *P. vulpinum*, orcinol and 1,3,8-p-menthatriene from *Penicillium canescens*, and formamidine from *Penicillium pusillum*. *Penicillium rubens*, and *Penicillium roqueforti* are utilized as cheese starters, and *Penicillium nalgiovense* is used to ferment sausages. Cellulose and hemicellulose are produced by *Penicillium waksmanii*. Moreover, all *Penicillium* species produce fatty acids and hydrocarbons (Jouda et al. 2016; Kumar et al. 2017a).

Penicillium genus is also involved in bioremediation because their members can break down phenols, halogenated phenolic compounds, oil hydrocarbons, polycyclic aromatic compounds and polychlorinated biphenyls. It can be used specifically to rearrange ecosystems contaminated with oil and its derivatives. *Penicillium* has been successfully used in various fields such as food, biotechnology, and medicines. (Kozlovsky et al. 2020; Assaf et al. 2020; Kumar et al. 2017a).

CHAPTER 2

MATERIALS AND METHODS

2.1. Materials

Biological and chemical materials together with the instruments used in this study are given below.

2.1.1. Endophytic Fungi

The endophytic fungus *Penicillium roseopurpureum* 1E4BS1 (Ac KJ775658.1) was previously isolated from the stems of *Astragalus angustifolius* as part of our ongoing studies on endophytes (funded by TUBITAK, Project No: 114Z958, PI: Prof. Dr. Erdal BEDİR), and it was utilized in this thesis.

2.1.2. Used Culture Media

In this study, two different media were utilized. Both media were sterilized by autoclave at 121 ºC (15 psi pressure) for 15 minutes (Tez et al. 2016a).

Table 3. List of used culture media.

Medium	**Preparation Procedure**	**Usage**
Potato Dextrose Agar (PDA)	39 g of the medium (Merck Millipore-110130) was mixed in 1000 ml distilled water.	The activation of fungi from stock cultures.
Potato Dextrose Broth (PDB)	24 g of the medium (Merck Millipore-110130) was mixed in 1000 ml distilled water.	The fermentation studies

2.1.3. Used Chemicals

The chemicals used in the extraction and isolation stages are listed below.

2.1.3.1. Chemicals used in the extraction and isolation studies

- Methanol (MeOH): Sigma-Aldrich
- Ethanol (EtOH): ISOLAB
- *n*-Hexane: Sigma-Aldrich
- Deuterated Dimethyl Sulfoxido (DMSO-d6):
- tert-butanol: Carlo Erba
- Chloroform ($CHCI_3$): VWR Chemicals
- Ethyl Acetate (EtOAc): VWR Chemicals
- Dimethyl Sulfoxide (DMSO): Carlo Erba
- Distilled water (dH_2O): Sartorius
- 20% Sulfuric acid (H_2SO_4): Sigma-Aldrich
- Sephadex LH-20: GE Healthcare Life Sciences
- RP-18 (Chromabond C18): Macherey-Nagel
- RP-18 F254 Thin Layer Chromatography (RP-TLC): Merck
- Kieselgel 60, F254 Thin Layer Chromatography (TLC): Merck
- Kieselgel 60, 70-230 mesh silica: Merck
- Preparative RP TLC: Merck
- Preparative Silica TLC: Merck

2.1.3.2. Used Equipments

- Nuclear Magnetic Resonance Spectrometry (NMR): Varian AS 400; Varian 600; Bruker AVANCE Neo 500
- Mass Spectrometry (MS): Thermo ORBITRAP Q-EXACTIVE

- SpeedVac Concentrator: Thermo Scientific Savant SPD 121P
- Freeze Dryer: Labconco FreeZone Freeze Dry System
- UV Imaging system: Vilber Lourmat
- Autoclave: Nuve OT 90L
- Rotavapor: Heidolph, Germany; ISOLAB
- Vacuum Pump: Labnet
- Peristaltic Pump: Thermo Scientific
- pH Meter: Mettler Toledo
- Vortex Mixer: Thermo-scientific
- Hotplate with magnetic stirrer Hotplate: ISOLAB
- Ultrasonic bath: Bandelin

2.1.4. Materials for Cytotoxicity Studies

The cell lines used for cytotoxicity studies:

DU145, PC3, LNCaP and RPWE-1 cells are human prostate cancer/normal cell lines.

2.1.4.1. Used Chemicals in Cytotoxicity Studies

- Phosphate buffered saline (PBS): Sigma-Aldrich
- Fetal Bovine Serum (FBS): Hyclone
- Dimethyl Sulfoxide (DMSO)
- Dulbecco's Modified Eagle Medium (DMEM)
- Trypan Blue Solution: Sigma-Aldrich
- EDTA-Trypsin: Sigma-Aldrich
- L-glutamine: Sigma-Aldrich
- MTT solution: Sigma-Aldrich

2.1.4.2. Equipment Used on Cytotoxicity Studies

- CO_2-Incubator: Thermo-scientific
- Light Microscope: Euromex Oxion Inverso, OX.2003-PL
- Laminar Flow Cabinet: ESCO
- Shaking Incubator: Hangzhou Miu
- Plate reader: Thermo-scientific Multiskan Sky
- Water Baths: Wisd Laboratory Instruments
- Neubauer Counting Chamber

2.2. Methods

2.2.1. Preparative Scale

Stock cultures of endophytic fungi stored at +4 °C were grown on potato dextrose agar (PDA) containing petri dishes at 25 °C for 10 days. The spore solution was prepared with 0.1% (w/v) Tween 80 and used to inoculate (2% v/v) five of 5 L Erlenmayer flasks containing 2 L potato dextrose broth (PDB). Fermentation process was carried out in a rotary shaker at 180 rpm, 25 ºC for 20 days.

To profile metabolite diversity of the fungus, a fermentation experiment in shake flask cultures was followed by a TLC analysis of the ethyl acetate extracts obtained from the samples of day 7, 14 and 20.

2.2.2. Extraction Studies

After the preparative studies, the biomass was removed from the broth by filtration using Buchner funnel system. After filtration, liquid-liquid extraction was

performed for four times using equal volume of EtOAc. The EtOAc phases were evaporated in the rotary evaporator at 35-40 ºC. The TLC analysis of the extracts were performed by using Silica gel 60 F254 and/or reversed-phase RP-C18 F254 coated aluminum plates. TLC plates were heated at 105-110 ºC for 5-10 minutes by spraying 20% aq.H_2SO_4 until the spots became visible, after UV-active compounds and non-UV-active compounds were detected at UV_{254} and $UV_{366\ nm.}$

2.2.3. Isolation and Purification Studies

For profiling the EtOAc extracts, the normal phase silica gel TLC analysis were used with the following solvent systems *n*-Hex:EtOAc:MeOH (10:10:2; 10:10:5), $CHCI_3$:MeOH (95:5; 90:10); and for the RP-C18 TLC analysis MeOH:H_2O (90:10; 85:15). In accordance with the TLC profiles, chromatographic methods were selected for isolation studies. In prefractionation and isolation steps, Open Column Chromatography and Vacuum Liquid Chromatography (VLC) were used. During this study, silica gel 60, RP C-18 and Sephadex LH-20 were used as the adsorbent/stationary phase. The chemical structures of purified metabolites were elucidated by spectral methods (1D-, 2D-NMR and MS).

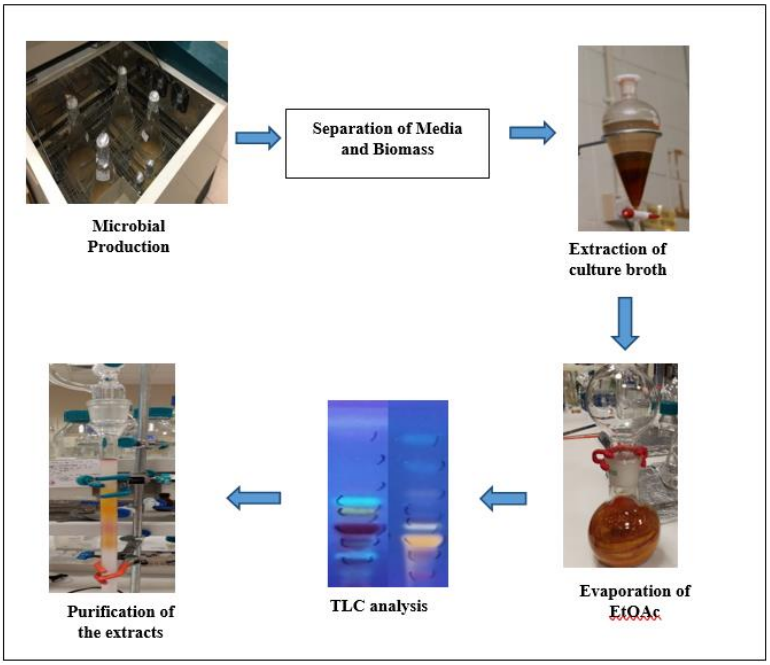

Figure 5. Illustration of general methodology

Isolation studies on the EtOAc extract (599.8 mg) started with a 135 g silica gel using open column chromatography (Figure 6). First, the extract was dissolved in $CHCl_3$:MeOH mixture and impregnated with silica gel and dried. Subsequently, the dried silica containing the extract applied to the silica column equilibrated with $CHCl_3$. The column was eluted with $CHCl_3$:MeOH (100:0 → 0:100). Collected fractions showing similar profiles were pooled together, and 22 main fractions were obtained (Figure 7-8).

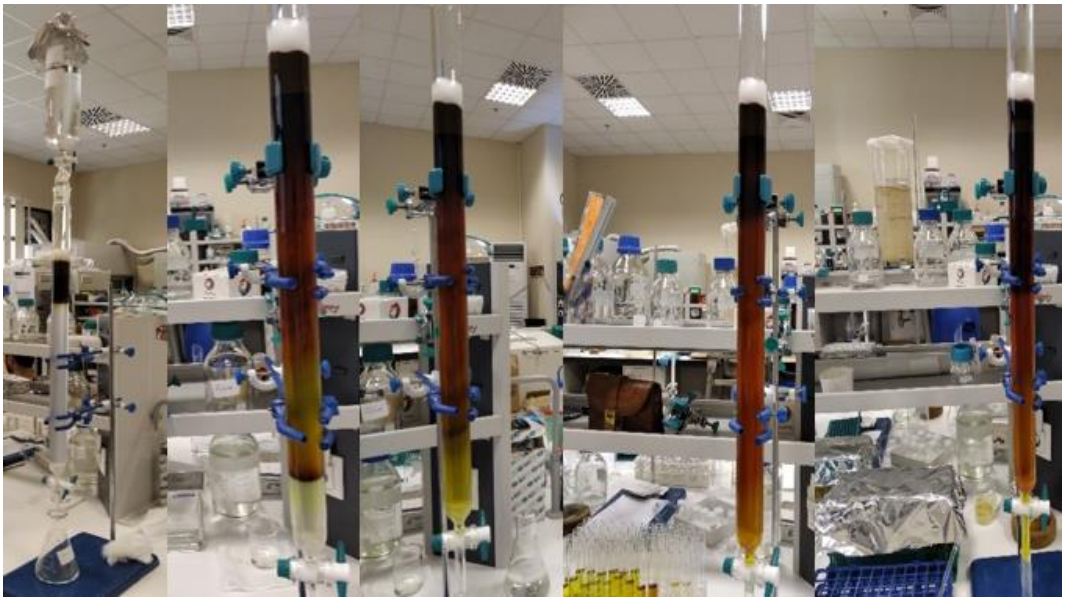

Figure 6. Images of the first column at different elution steps and main fractions collected.

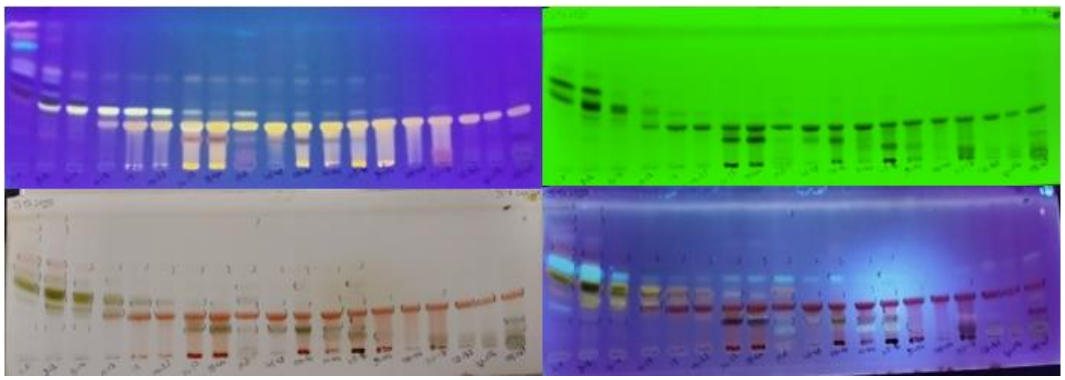

Figure 7. TLC profiles of the fractions under UV_{365} and $UV_{254\ nm}$ (EtOAc extract of *P. roseopurpureum* 1E4BS1) (Normal phase silica gel plate, Mobile Phase, 95:5; $CHCI_3$:MeOH)

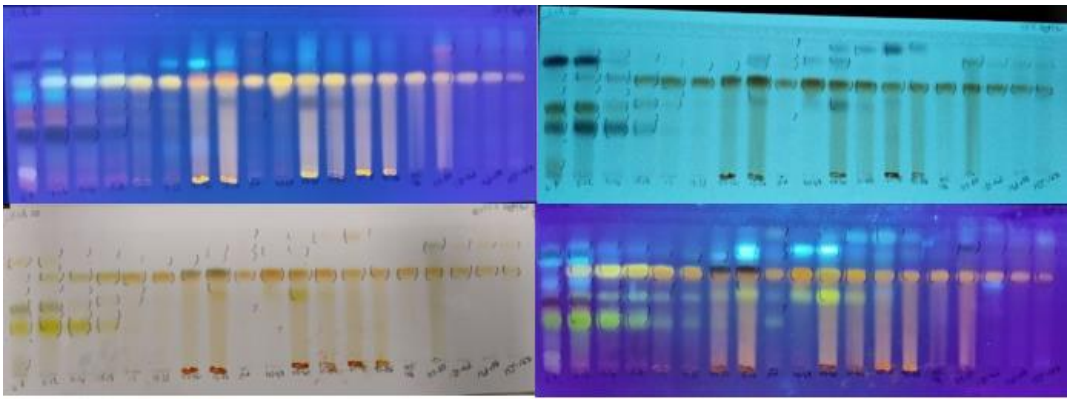

Figure 8. TLC profiles of the fractions under UV_{365} and $UV_{254\ nm}$ (EtOAc extract of *P. roseopurpureum* 1E4BS1) (Reverse phase silica gel plate, Mobile Phase, 85:15; MeOH:H_2O)

Among these 22 main fractions, 7 of them were selected for further isolation and purification studies according to TLC profiles. Detailed isolation schemes were given in below.

S4-14 (83 mg) was chromatographed over RP-C18 column (30 g) and eluted with MeOH:H_2O (50:50 → 100:0) solvent system, and sixteen subfractions were obtained. *S4-14_RP7-12* (32.8 mg) subfraction was subjected to a silica gel column (10 g) and eluted with $CHCI_3$:MeOH (99:1→0:100) solvent system. *S4-14_RP7-12* column gave **PR-EB-01** (8.3 mg) and *S4-14_RP7-12_S71-86* subfraction was further subjected to a RP-C18 column (20 g) and eluted with MeOH:H_2O (55:45) solvent system to give **PR-EB-03** (4.7 mg) (Figure 9).

S24-44 (104.4 mg) was chromatographed over a silica gel column (80 g) using *n*-Hex:EtOAc:MeOH (10:10:0.5 → 100% MeOH) solvent system, and twenty-three subfractions were obtained. *S24-44_S145-181* (31 mg) subfraction was further subjected to a Sephadex LH-20 column (15 g) and eluted with MeOH (100%) as mobile phase to give **PR-EB-04** (10 mg) and **PR-EB-05** (2.4 mg). *S24-44_S145-181_Sep15-19* and *S24-44_S145-181_Sep22-34* subfractions were combined and subjected to a Sephadex LH-20 column (15 g) using MeOH (100%) as mobile phase, which afforded **PR-EB-04** (11.2 mg) and **PR-EB-05** (3.9 mg) (Figure 9).

S65-90 (87.9 mg), one of the main fractions was chromatographed over Sephadex LH-20 column (35 g) and eluted with MeOH (100%) as mobile phase, and nine subfractions were obtained. *S65-90_Sep12-15* (6.5 mg) subfraction was further

subjected to a silica gel column (10 g) using *n*-Hex:EtOAc:MeOH (10:10:0.5→100% MeOH) as mobile phase to give **PR-EB-06** (4.2 mg) (Figure 10).

S107-131 (58.8 mg) was chromatographed over Sephadex LH-20 column (35 g) and eluted with MeOH (100%) as mobile phase, and eight subfractions were obtained. *S107-131_Sep41-52*(7 mg) subfraction was subjected to Sephadex LH-20 column (15 g) using MeOH (100%) as mobile phase, and four subfractions were obtained. *S107-131_Sep53* (2.7) and *S107-131_Sep41-52_Sep28-43* (1.7 mg) subfractions were combined to give **PR-EB-09** (4.4 mg) (Figure 10).

S170-171 (93.5 mg) was chromatographed over Sephadex LH-20 column (15 gr) and eluted with MeOH (100%) as mobile phase, and ten subfractions were obtained. *S170-171_Sep36-48* (12.6 mg) subfraction was subjected to a silica gel column (10 gr) using $CHCI_3$:MeOH (90:10→0:100) solvent system, and six subfractions were obtained. *S170-171_Sep36-48_S27* (10 mg) subfraction was subjected to a silica gel column (10 g) and eluted with *n*-Hex:EtOAc:MeOH (10:10:4→100% MeOH) solvent system to give **PR-EB-10** (3.8 mg) and **PR-EB-11** (2.5 mg) (Figure 10).

S15-23 (43.8 mg) was chromatographed over Sephadex LH-20 column (30 g) and eluted with MeOH (100%) as mobile phase, and ten subfractions were obtained. *S15-23_Sep7-21* (14.5 mg) subfraction was subjected Prep TLC (RP-C18) with MeOH:H_2O (85:15) solvent system. *S15-23_Sep7-21_Prep1* was further subjected Sephadex LH-20 column (10 g) and eluted with MeOH (100%) as mobile phase to give **PR-EB-17** (1.7 mg) (Figure 11).

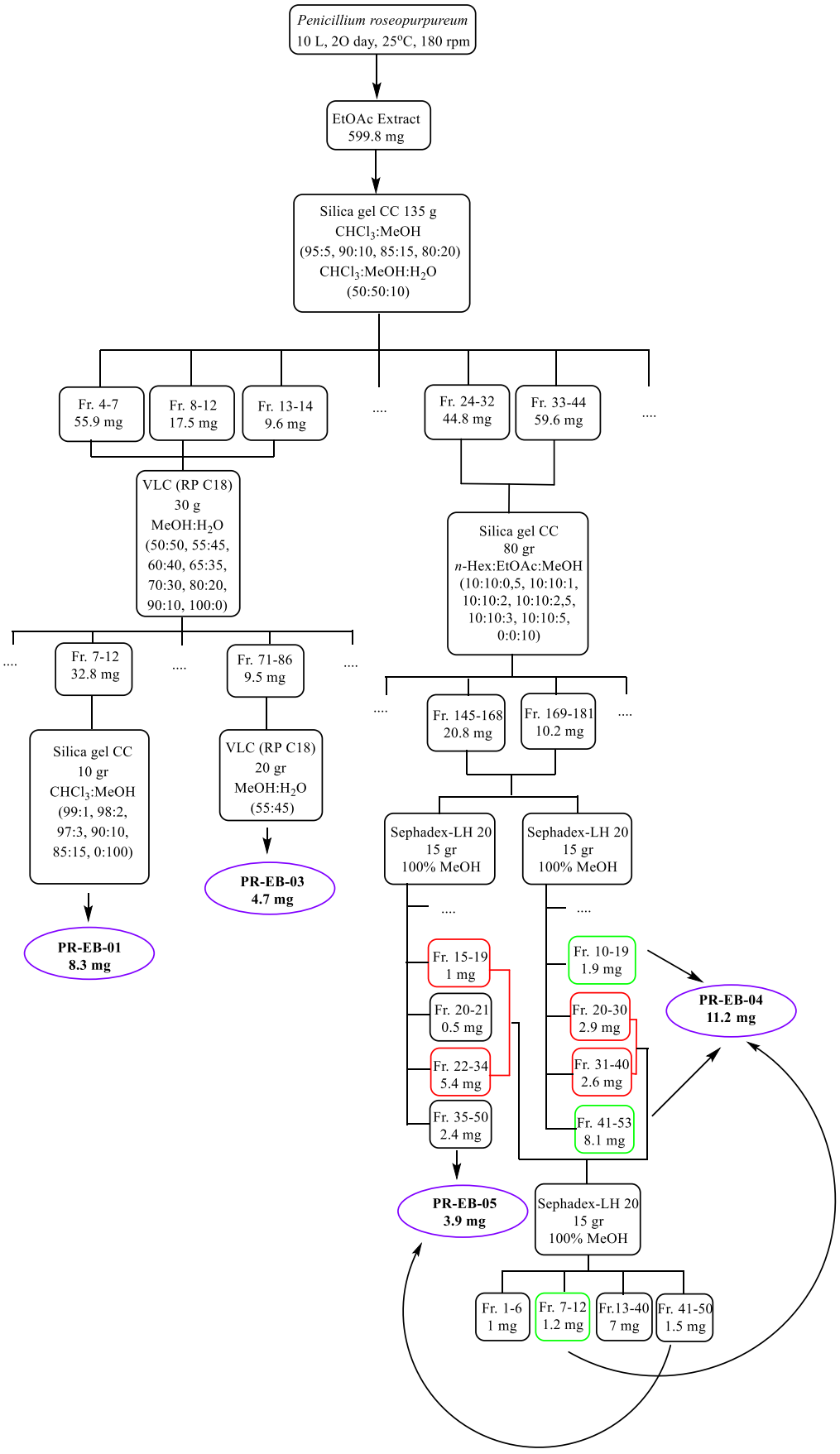

Figure 9. The isolation scheme of PR-EB-01, PR-EB-03, PR-EB-04 and PR-EB-05.

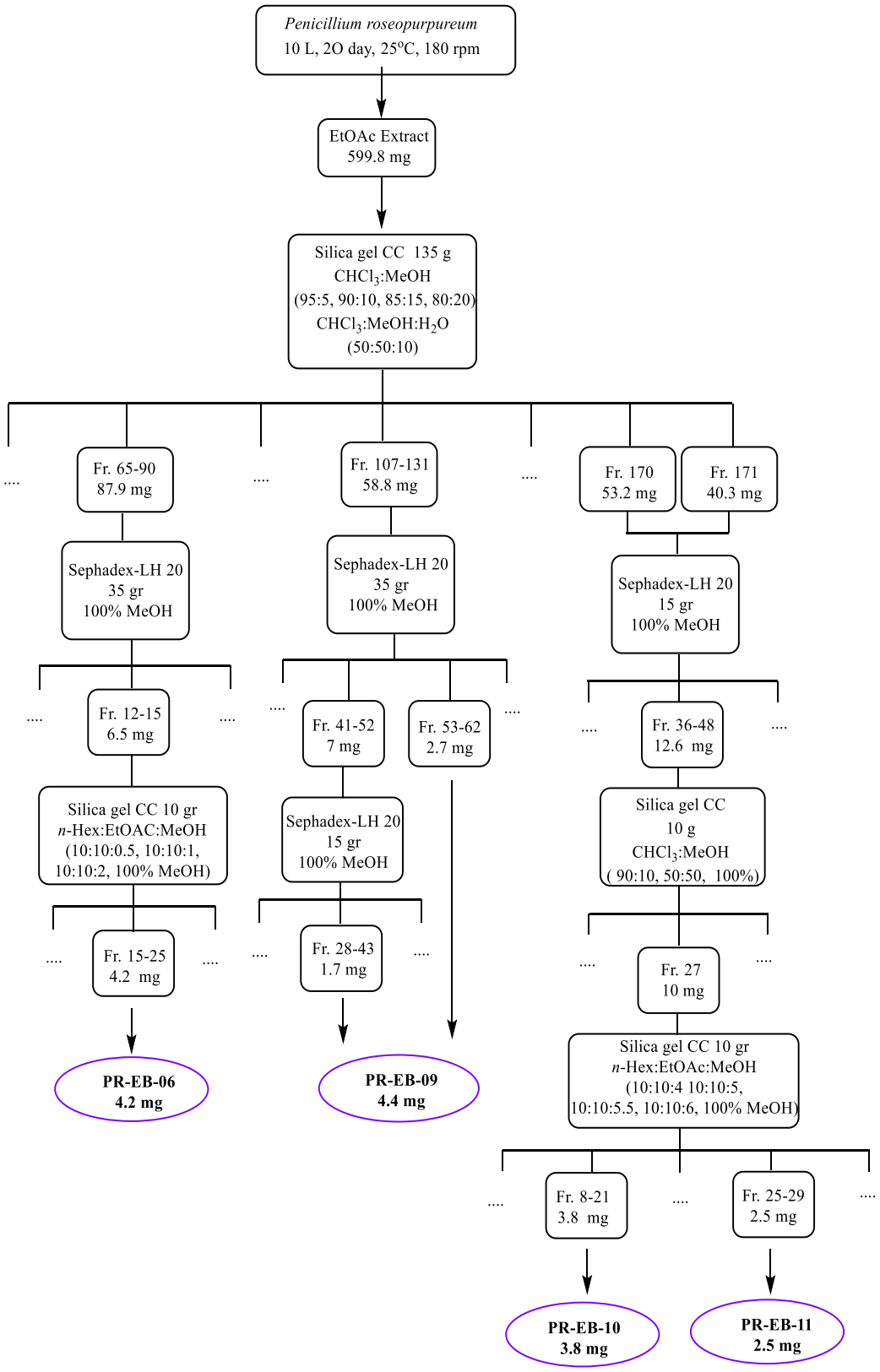

Figure 10. The isolation scheme of PR-EB-06, PR-EB-09, PR-EB-10 and PR-EB-11.

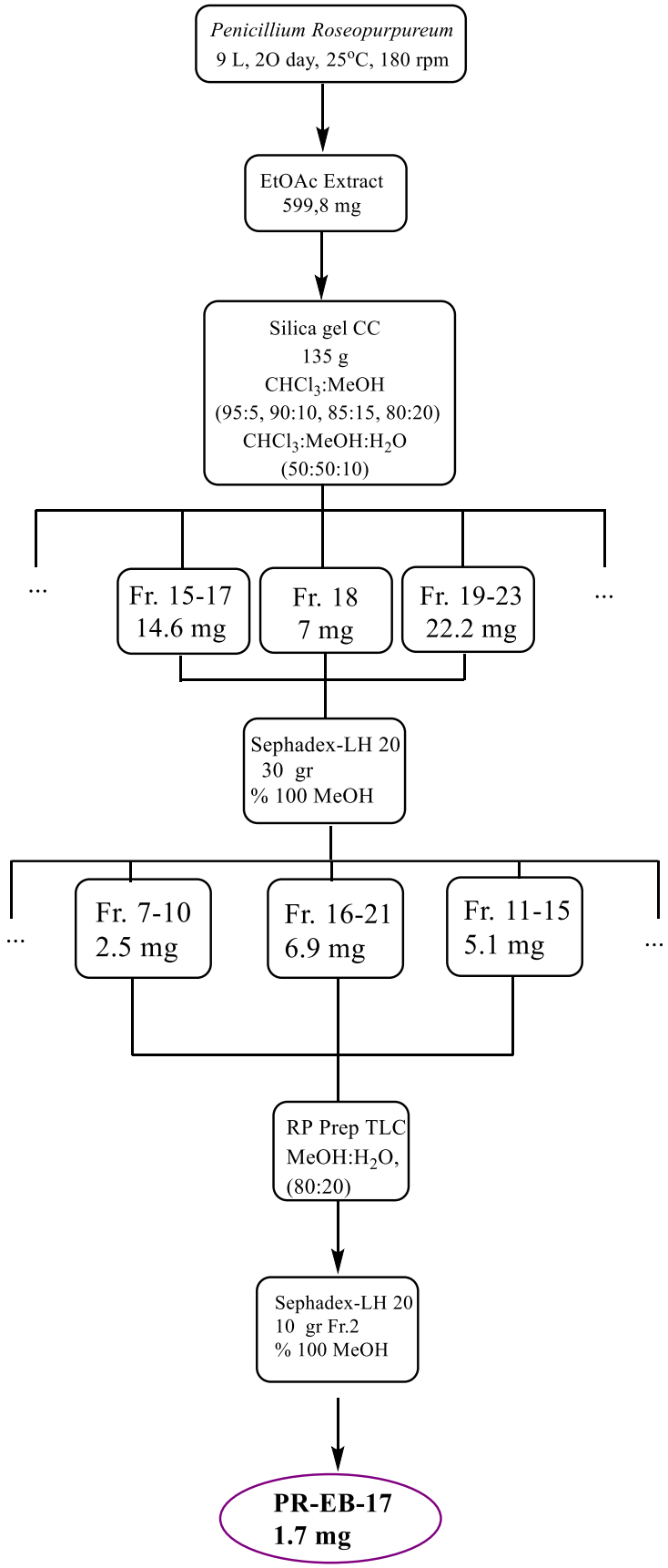

Figure 11. The isolation scheme of PR-EB-17.

2.2.4. Bioactivity Studies

The cytotoxicity of molecules was investigated by the 3-(4,5-dimethylthiazol-2-yl)-2,5-diphenyltetrazolium bromide (MTT) test, which is one of the most widely used methods for cell viability. In this section, the bioactivity method was explained.

2.2.4.1. Cell Culture studies

LNCaP cells were maintained with RPMI with 10% FBS while PC3 and DU145 cell lines cells were grown in petri dishes with DMEM containing 10% FBS. Cells were grown in petri dishes at 37 °C in humidified atmosphere with 5% CO_2. When cells reached 70% confluence, the growth medium was removed, and cells were treated with 0.05% trypsin. Then, cells were detached from surface with 0.25% trypsin at 37 °C until removal. Cells were collected with fresh medium and appropriate amount of cell suspension was transferred to a new culture dish containing fresh medium.

2.2.4.2. Cell viability (MTT assay)

After DU145 (7 x 10^3 cells/well), PC3 (6 x 10^3 cells/well) and LNCaP cells (8 x 10^3 cells/well) were seeded in 96 well plates, they were incubated to adhere at 37 °C in humidified atmosphere with 5% CO_2 for 24 h. Selected concentrations of compounds dissolved in DMSO were subjected to wells in triplicate. After 48 h of incubation, the culture medium was removed from wells and fresh media containing 10% MTT was added. Living cells transform MTT into formazan crystals with mitochondrial activity, and thus formazan crystals is used to determine percentage of viable cells by using colorimetric method. After 4 h of incubation, the medium containing 10% MTT was taken out of wells, and the formed formazan crystals were dissolved by adding DMSO.

Finally, absorbance was measured at wavelength of 590/690 nm via Varioscan flash spectrophotometer by Thermo Scientific. The data were analyzed by using GraphPad Prism to determine IC_{50} value of molecules.

CHAPTER 3

RESULTS AND DISCUSSION

3.1. Structure Elucidation of Isolated Compounds

In this thesis, *P. roseopurpureum* 1E4BS1 was used to obtain structurally diverse secondary metabolites with cytotoxic properties. After fermentation and isolation studies, ten compounds were isolated, and their structures were elucidated by using spectroscopic methods (1D NMR, 2D NMR and MS spectra). Below, structural determination of the isolates were discussed.

3.1.1. Structure Elucidation of PR-EB-01

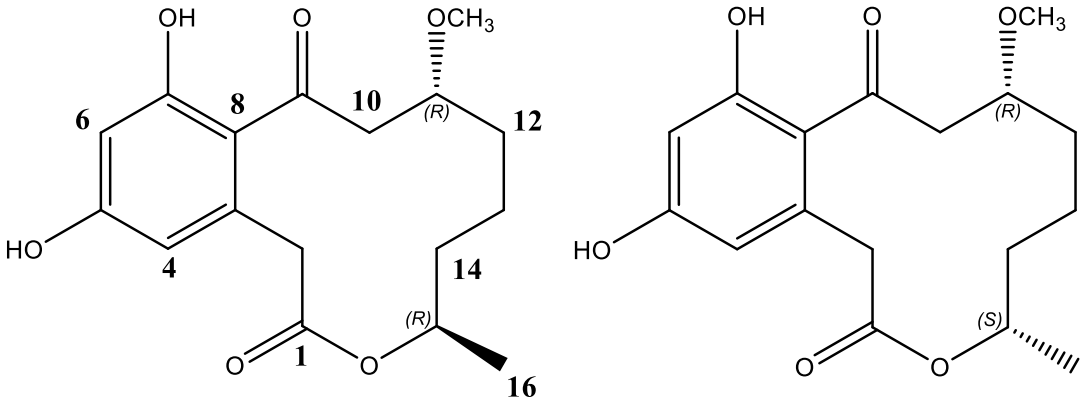

Chemical Formula: $C_{17}H_{22}O_6$
Exact Mass: 322,14164

Figure 12. Chemical structure of PR-EB-01.

The HR-ESI-MS spectrum of **PR-EB-01** exhibited a major ion peak at *m/z* 323.14845 $[M + H]^+$, (calcd. 323.14946) supported a molecular formula $C_{17}H_{22}O_{16}$ with seven indices of hydrogen deficiency.

Analysis of its ^1H and ^{13}C NMR spectra revealed that **PR-EB-01** was a mixture of two stereoisomers (**PR-EB-01A** and **PR-EB-01B**) with a macrolide structure, a common secondary metabolite group in *Penicillium* species. Further inspection of 1D- and 2D NMR spectra and literature search suggested that **PR-EB-01** had a curvularin-type polyketide backbone (Zhan and Gunatilaka 2005; Deng et al. 2015). The difference was readily deduced to be the presence of two *O*-methyl signals in the ^1H and ^{13}C NMR spectra (δ_C 55.6 x 2; δ_H 3.18 and 3.23, **PR-EB-01B** and **PR-EB-01A**, respectively). The position of the OMe group was established to be C-11 by examining the COSY, HSQC, and HMBC spectra. By comparing the spectral data of **PR-EB-01** with those of 11-hydroxycurvularin and 11-methoxycurvularin stereoisomers, the full spectral assignment of **PR-EB-01B** and **PR-EB-01A** was accomplished., whereas the absolute stereochemistry at C-11 and C-15 was deduced (Greve et al. 2008; Ye et al. 2015; Shang et al. 2016; Zhan et al. 2004; Ha et al. 2017; Liang et al. 2007). Thus, the structures of diastereomeres were established as (4R,8R)-11,13-dihydroxy-8-methoxy-4-methyl-4,5,6,7,8,9-hexahydro-2H-benzo[d][1]oxacyclododecine-2,10(1H)-dione = **PR-EB-01A** and (4S,8R)-11,13-dihydroxy-8-methoxy-4-methyl-4,5,6,7,8,9-hexahydro-2H benzo [d] [1] oxacyclo- dodecine -2,10(1H)-dione = **PR-EB-01B**, which were previously described compounds from *Penicillium* species (Zhan et al. 2004; Ha et al. 2017; Liang et al. 2007).

Table 4. ^1H and ^{13}C NMR spectroscopic data of PR-EB-01A, a) (in DMSO-d6, ^1H:600 MHz, ^{13}C:150 MHz

Position	**δ_C (ppm)**	**δ_H (ppm), (J in Hz)**
1	170.3 s	-
2a	39.5 t	3.83
2b		3.54
3	136.6 d	-
4	111.0 d	6.16 d (2.4)
5	160.0 s	-
6	101.7 d	6.30 d (2.3)
7	158.9 s	-
8	118.2 s	-
9	202.7 s	-
10a	48.5 t	3.24 m

Cont. on next page

Cont. of Table 4

10b		2.85 m
11	76.5 d	3.50 m
12b		1.33 m
13a	17.6 t	1.28 m
13b		-
14a	30.7 t	1.42
14b		1.71
15	72.7 d	4.73 m
16	21.1. q	1.04 d
5-OH	-	9.94 s
7-OH	-	10.20 s
11-OMe	55.6 q	3.23

a) Assignments are confirmed by 2D-COSY, HSQC, and HMBC experiments.

Table 5. ^{1}H and ^{13}C NMR spectroscopic data of PR-EB-01B, a) (in DMSO-d6, ^{1}H:600 MHz, ^{13}C:150 MHz)

Position	**δ_C (ppm)**	**δ_H (ppm), (J in Hz)**
1	169.7 s	-
2a	39.5 t	3.83 d
2b		3.54 m
3	136.6 d	-
4	111.4 d	6.16 d (2.4)
5	160.0 s	-
6	101.9 d	6.30 d (2.4)
7	158.9 s	-
8	118.2 s	-
9	202.7 s	-
10a	48.5 t	3.24 m
10b		2.85 m
11	76.5 d	3.50 m
12a	30.7 t	1.51 m
12b		1.33 m
13a	17.6 t	1.28 m
13b		-
14a	30.7 t	1.35
14b		1.52
15	69.8 d	4.86 m
16	18.7 q	1.02 d
5-OH	-	9.94 s
7-OH	-	10.20 s
11-OMe	55.6 q	3.18

a) Assignments are confirmed by 2D-COSY, HSQC, and HMBC experiments.

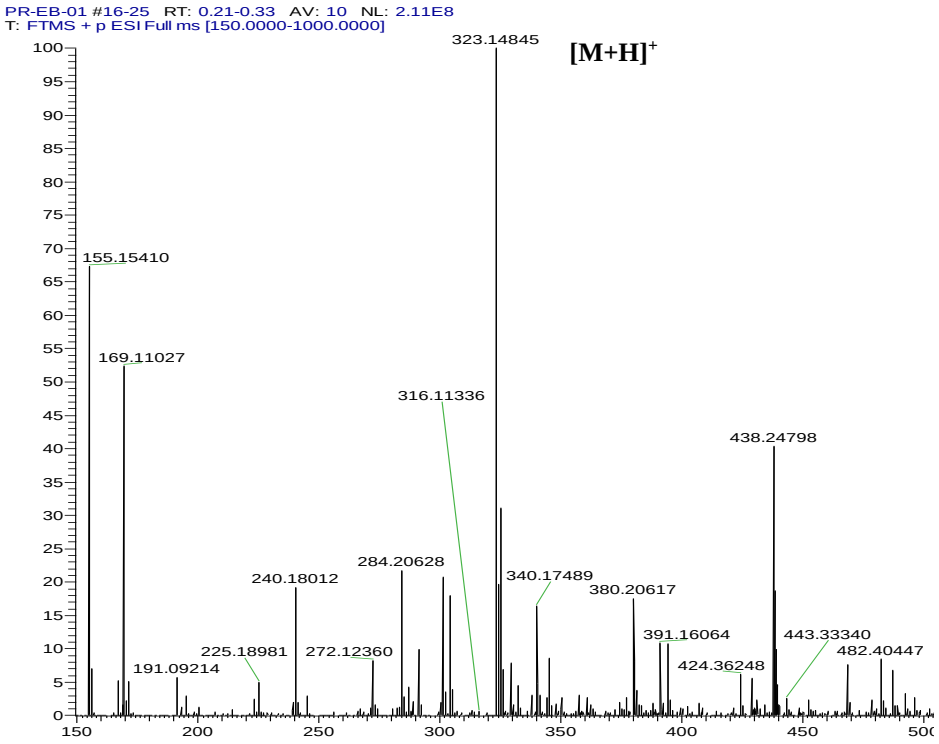

Spectrum 1. HR-ESI-MS Spectrum of PR-EB-01 (positive mode).

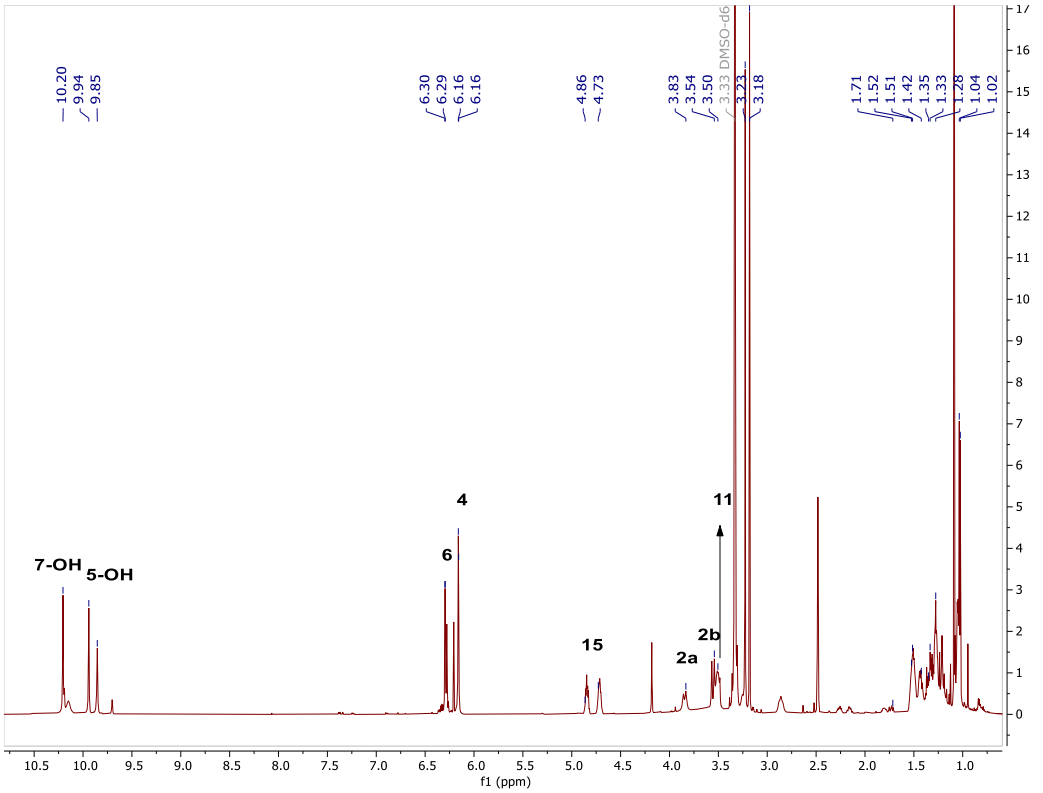

Spectrum 2. ^{1}H NMR Spectrum of PR-EB-01 (in DMSO-d6, ^{1}H: 600 MHz).

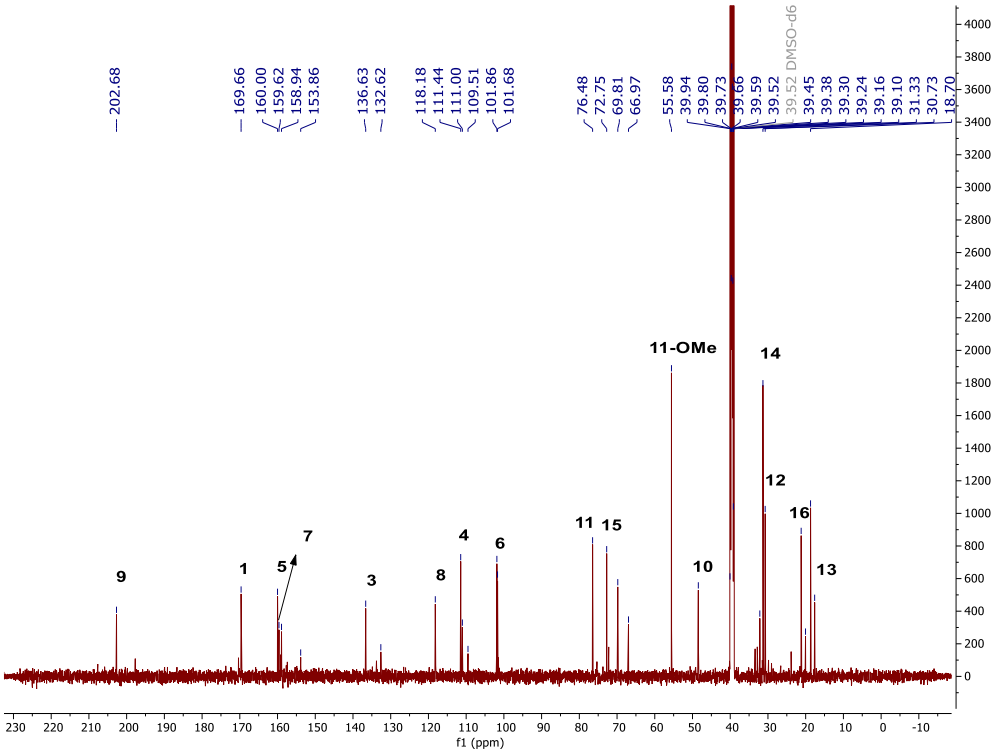

Spectrum 3. ^{13}C NMR Spectrum of PR-EB-01 (in DMSO-d6, ^{13}C:150 MHz).

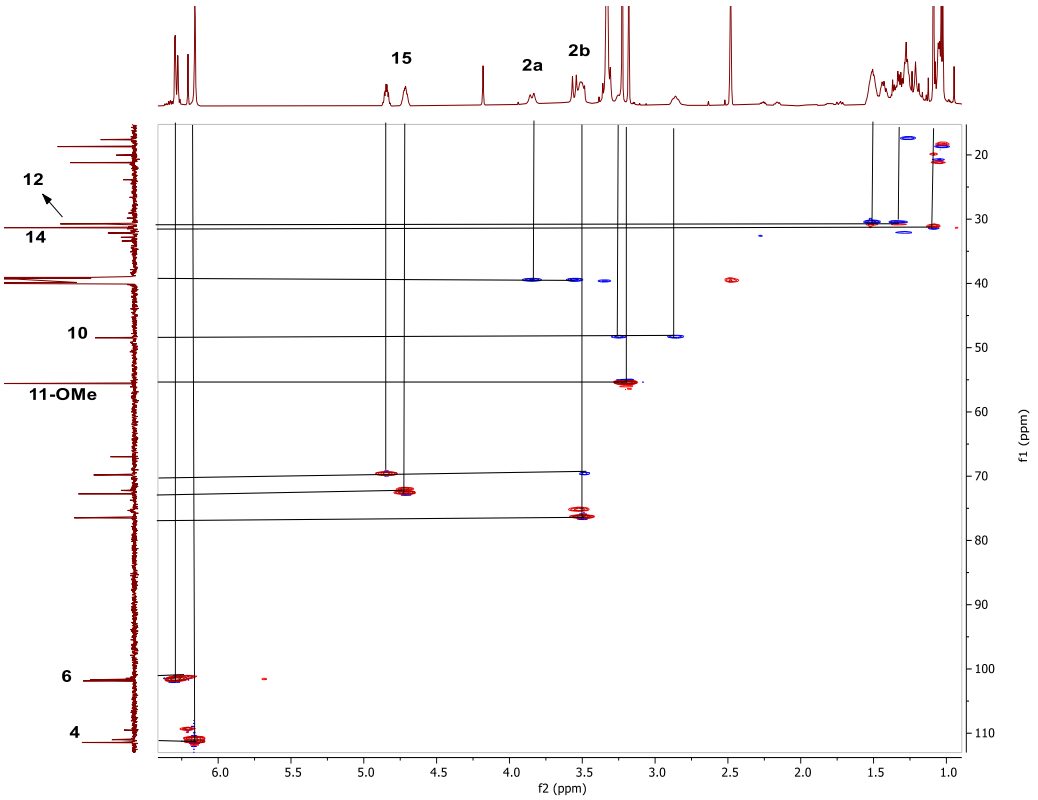

Spectrum 4. HSQC spectrum of PR-EB-01.

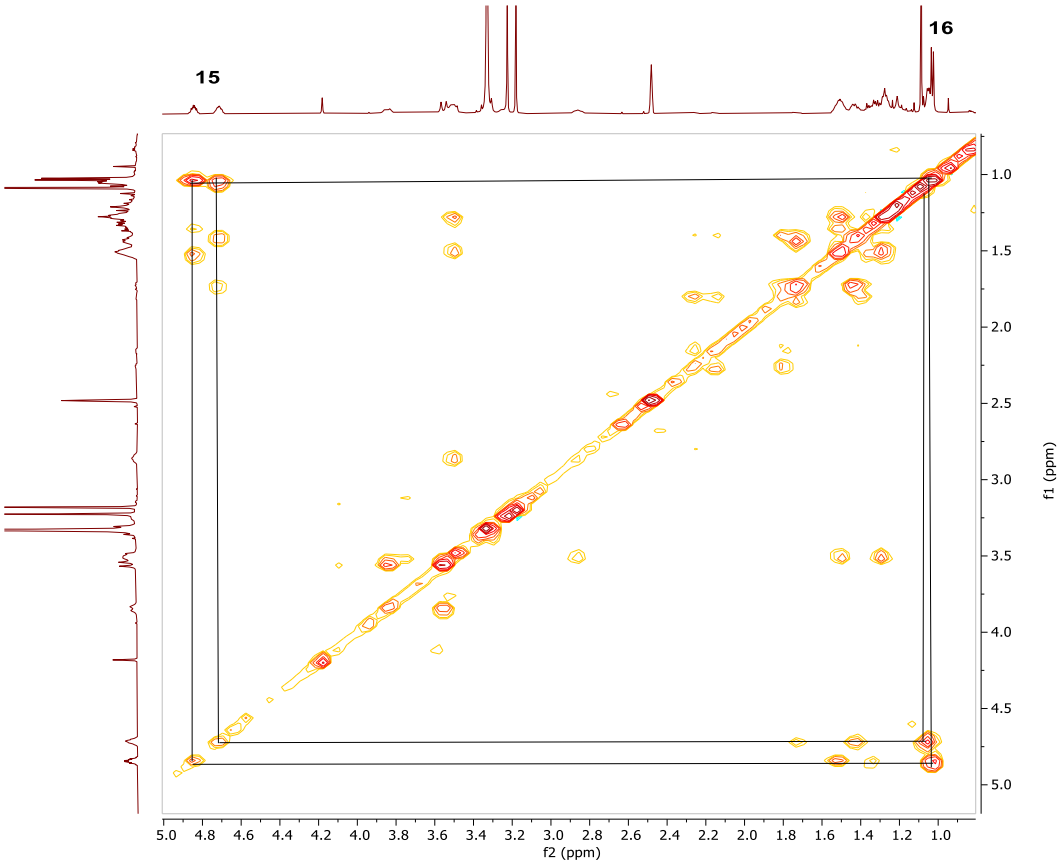

Spectrum 5. COSY spectrum of PR-EB-01.

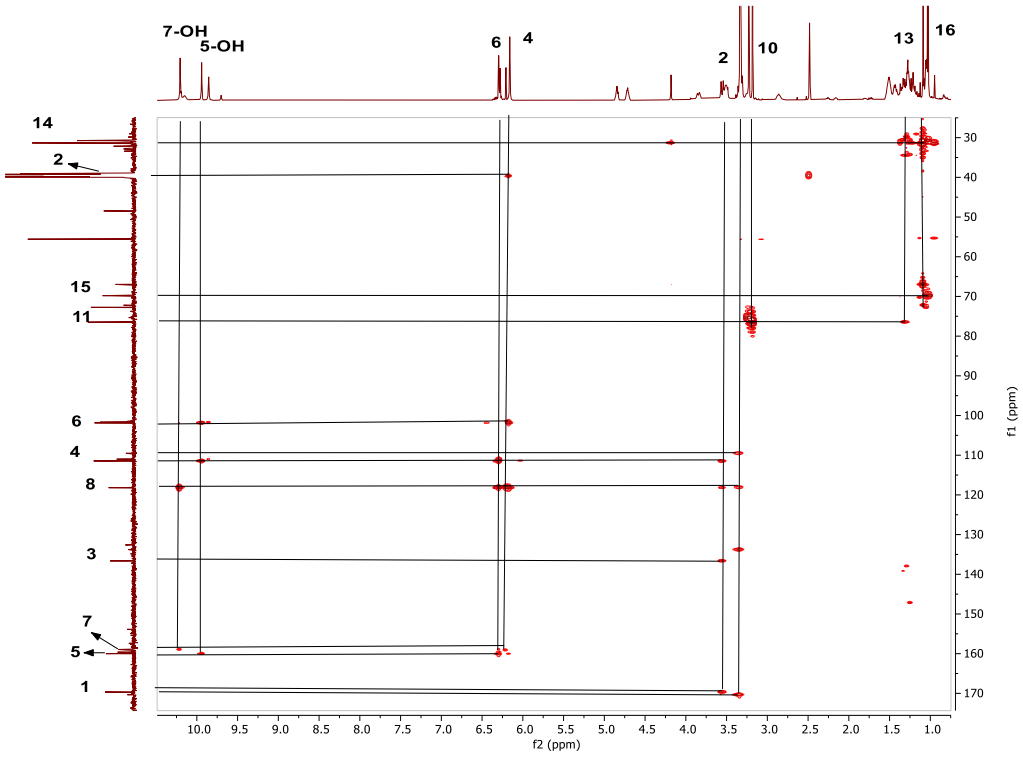

Spectrum 6. HMBC spectrum of PR-EB-01.

3.1.2. Structure Elucidation of PR-EB-03

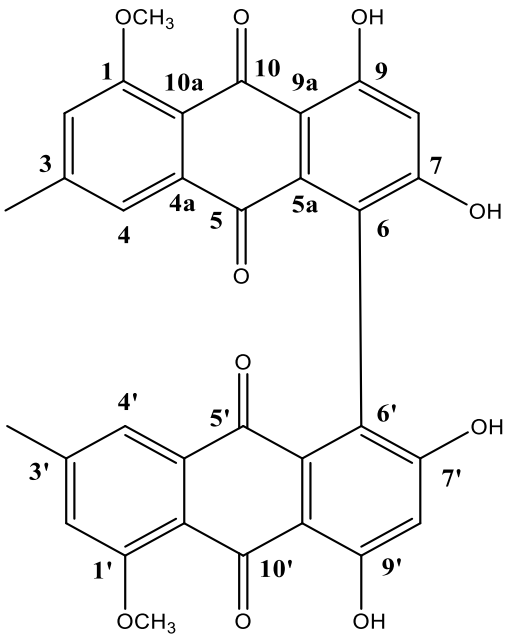

Chemical Formula: $C_{32}H_{22}O_{10}$
Exact Mass: 566,1213

Figure 13. Chemical structure of PR-EB-03.

The HR-ESI-MS spectrum of **PR-EB-03** exhibited a prominent ion peak at *m/z* 567.12799 $[M+H]^+$ (calcd. 567.12912) supported a molecular formula $C_{32}H_{22}O_{10}$ with twenty-two indices of hydrogen deficiency.

Analysis of its ^1H and ^{13}C NMR spectra revealed the presence of a methyl ($\delta_{H\text{-}11,}$ 2.32 s, $\delta_{C\text{-}11}$ 21.5q), a methoxy group (H-1-OMe: δ 3.91 s; C-1-OMe δ 56.3 s), three aromatic carbon methines ($\delta_{C\text{-}2}$ 118.5, $\delta_{C\text{-}4}$ 119.6, $\delta_{C\text{-}8}$ 107.1), and ten non-protonated carbons (six aromatic $\delta_{C\text{-}1}$ 159.6, $\delta_{C\text{-}3}$ 144.9, $\delta_{C\text{-}4a}$ 135.9 s, $\delta_{C\text{-}5a}$ 131.9 s, $\delta_{C\text{-}6}$ 127.0, $\delta_{C\text{-}7}$ 159.6, $\delta_{C\text{-}9}$ 165.0, $\delta_{C\text{-}9a}$ 106.8 s, , $\delta_{C\text{-}10a}$ 118.4 s and two keto carbons at $\delta_{C\text{-}5}$ 184.2 s, $\delta_{C\text{-}10}$ 207.3 s). Detailed inspection of the 1D-, 2D-NMR, and HR-ESI-MS spectra implied that **PR-EB-03** was a homodimeric anthraquinone, suggested to be linked through C-6 and C-6' carbons. Additionally, the monomeric unit was established as 1-O-methylemodin by comparing the spectral data with those of previous reports (Ayer and Trifonov 1994). In the ^1H NMR spectrum of **PR-EB-03**, the aromatic proton was lacking for C-6 when compared to that of 1-O-methylemodin (Ayer and Trifonov 1994), which substantiated that the monomers were coupled to each other at C-6 and C-6'. The

atropisomerism at C-6/C-6’ (S_a or R_a) for this bis-anthraquinone structure could not be determined due to insufficient spectral data. Thus, based on the data from ^{1}H and ^{13}C NMR and 2D spectra (COSY, HSQC and HMBC), the planar structure of **PR-EB-03** was determined to be 2,2',4,4'-tetrahydroxy-5,5'-dimethoxy-7,7'-dimethyl-[1,1'-bianthracene]-9,9',10,10'-tetraone (IUPAC name) as the new member of anthraquinone derivatives.

Table 6. ^{1}H and ^{13}C NMR spectroscopic data of PR-EB-03, a) (in DMSO-d6, ^{1}H:600 MHz, ^{13}C:150 MHz)

Position	**δ_C (ppm)**	**δ_H (ppm), (J in Hz)**
1(1’)	159.6 s	-
2(2’)	118.5 d	7.27 s
3(3’)	144.9 s	-
4(4’)	119.6 d	-
4a(4’a)	135.9 s	7.15 s
5(5’)	184.2 s	-
5a(5’a)	131.9 s	-
6(6’)	127.0 s	-
7(7’)	159.6 s	-
8(8’)	107.1 d	6.15 s
9(9’)	165.0 s	-
9a(9’a)	106.8 s	-
10(10’)	207.3 s	-
10a(10’a)	118.4 s	-
11 (11’)	21.5 q	2.32 s
1-OMe(1’-OMe)	56.3 q	3.91 s
7-OH(7’-OH)	-	-
9-OH(9’-OH)	-	14.16 s

a) Assignments are confirmed by 2D-COSY, HSQC, and HMBC experiments.

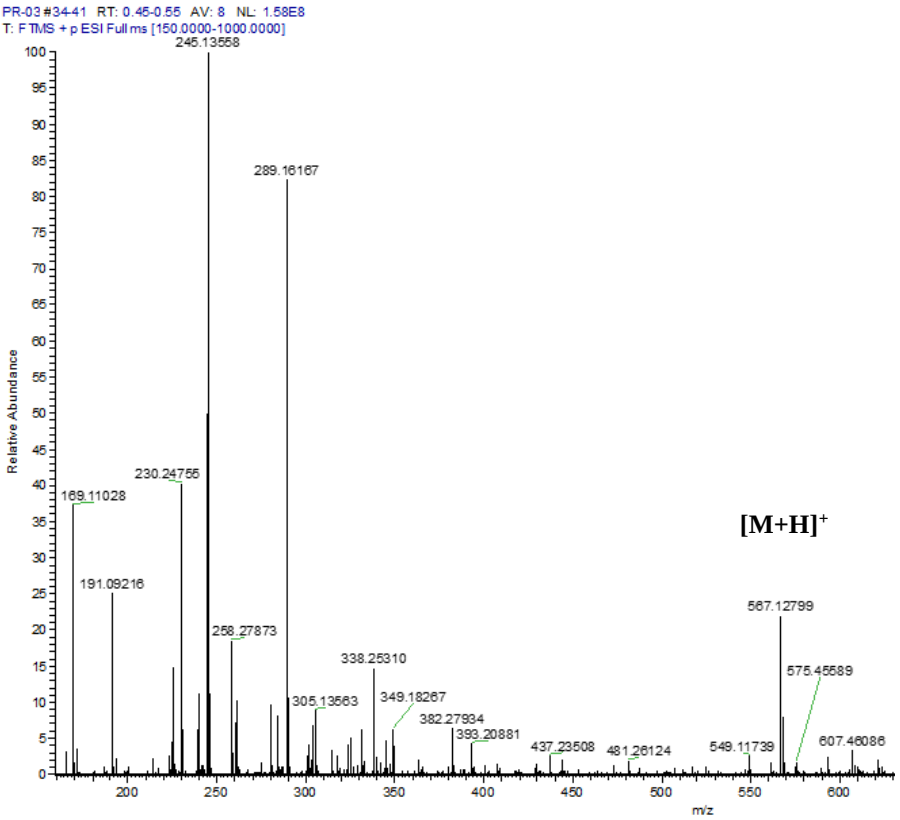

Spectrum 7. HR-ESI-MS Spectrum of PR-EB-03 (positive mode).

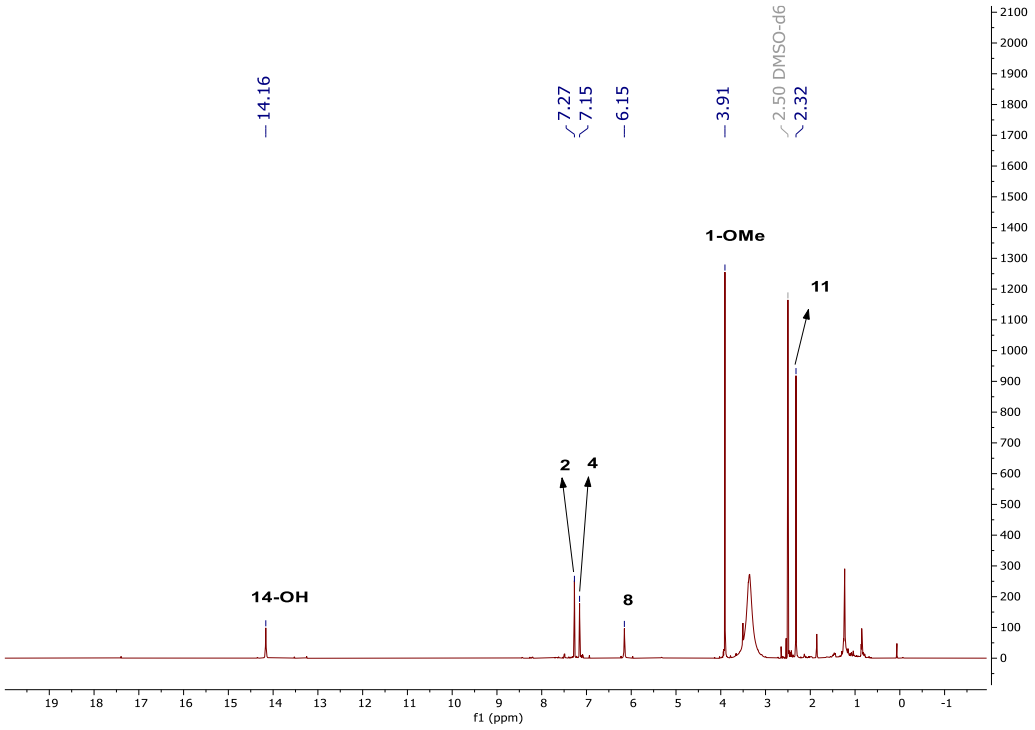

Spectrum 8. ^{1}H NMR Spectrum of PR-EB-03 (in DMSO-d6, ^{1}H: 600 MHz).

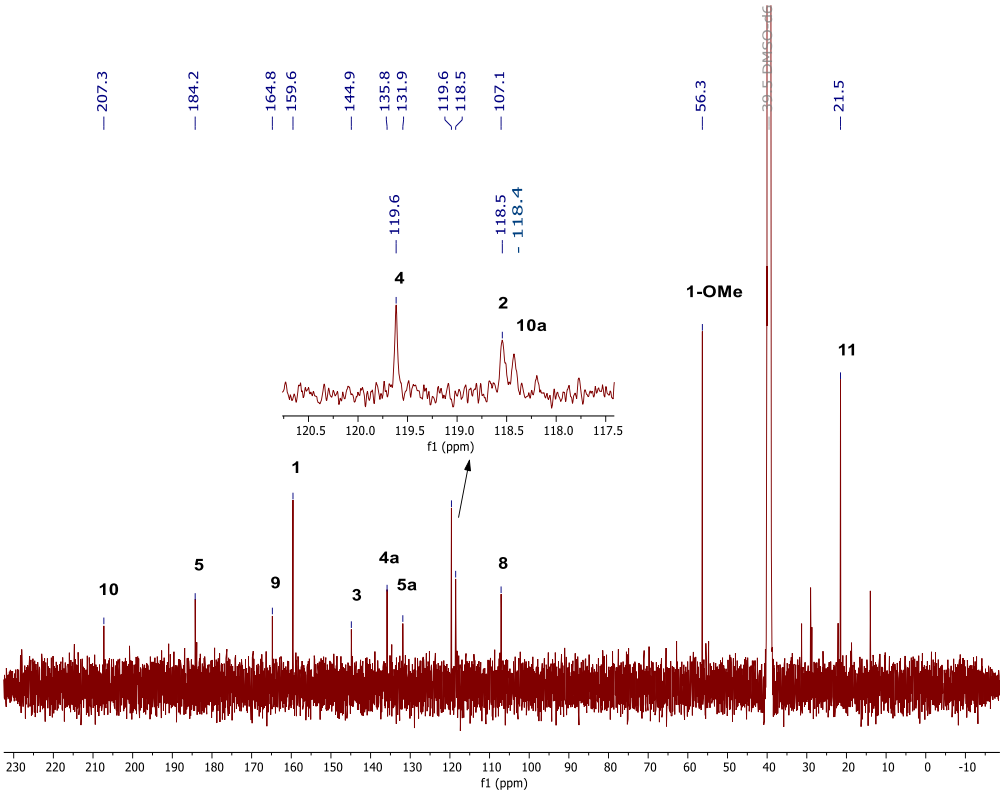

Spectrum 9. ^{13}C NMR Spectrum of PR-EB-03 (in DMSO-d6, ^{13}C:150 MHz).

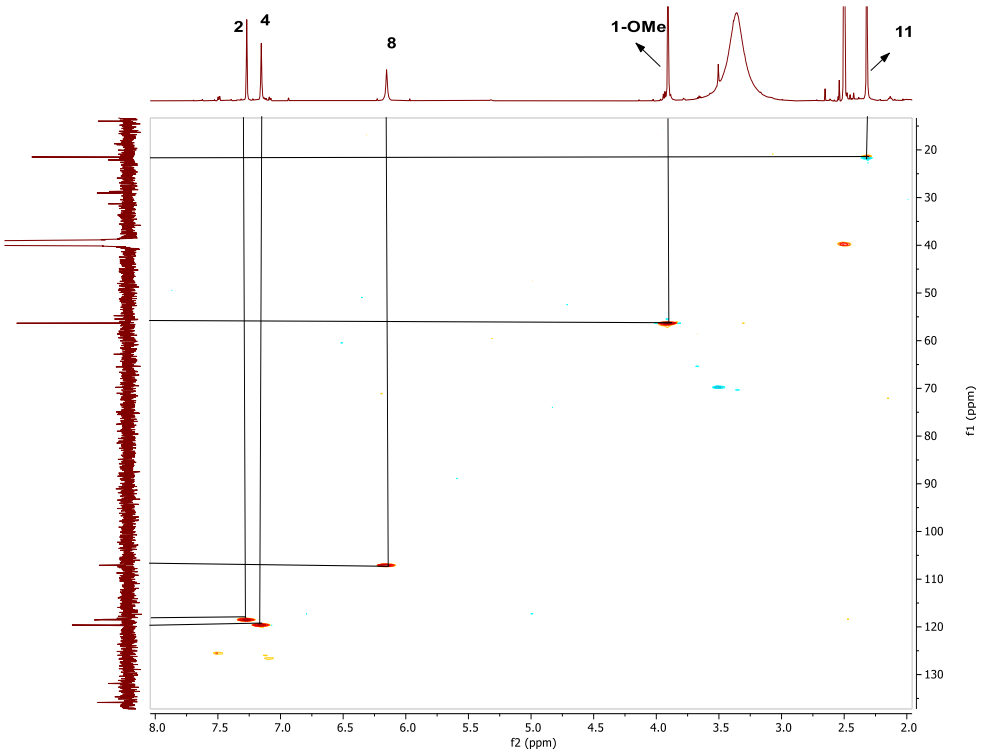

Spectrum 10. HSQC spectrum of PR-EB-03.

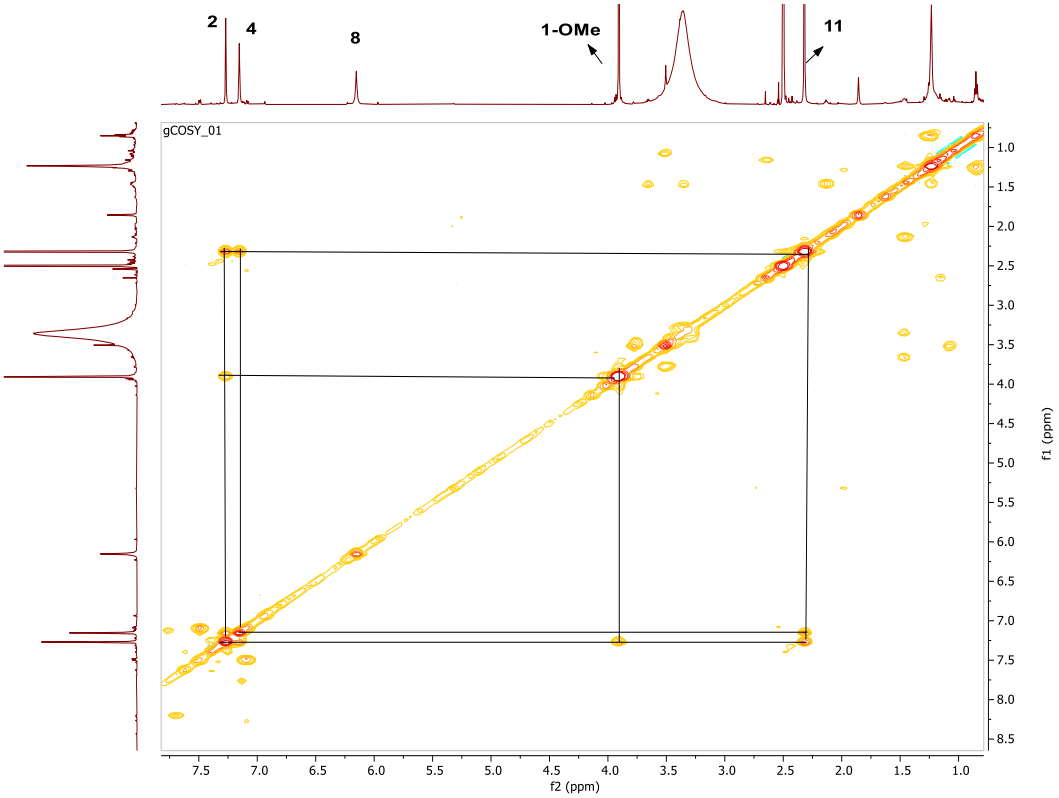

Spectrum 11. COSY spectrum of PR-EB-03.

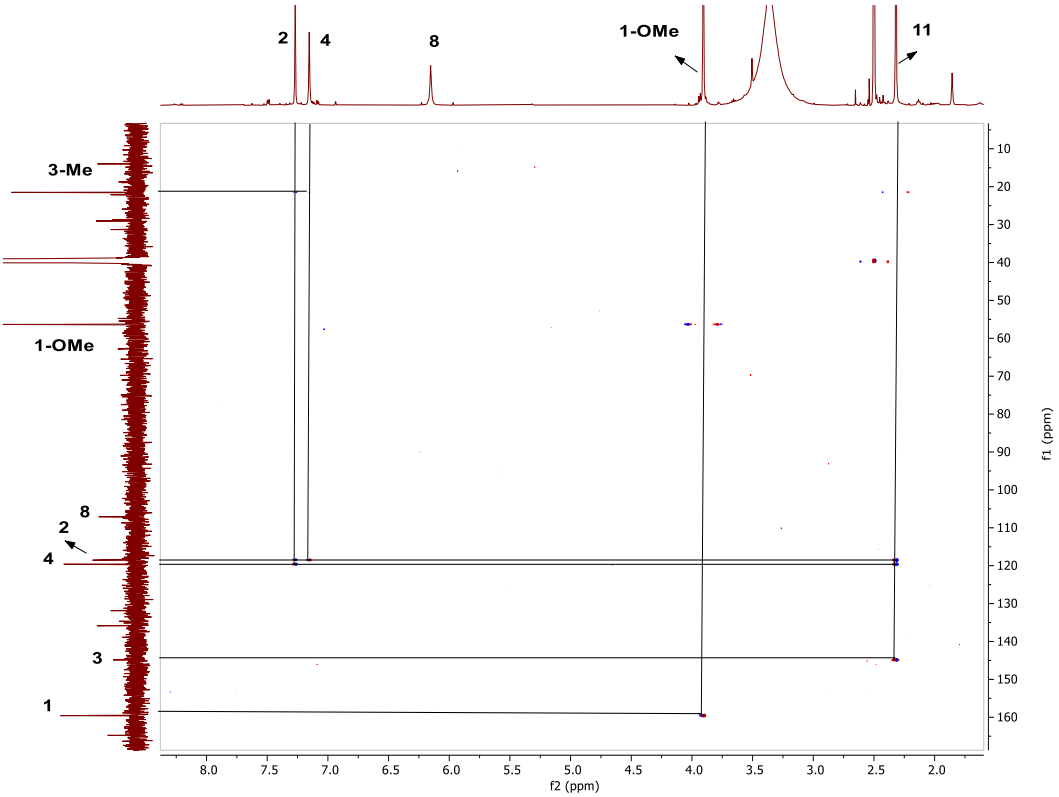

Spectrum 12. HMBC spectrum of PR-EB-03.

3.1.3. Structure Elucidation of PR-EB-04

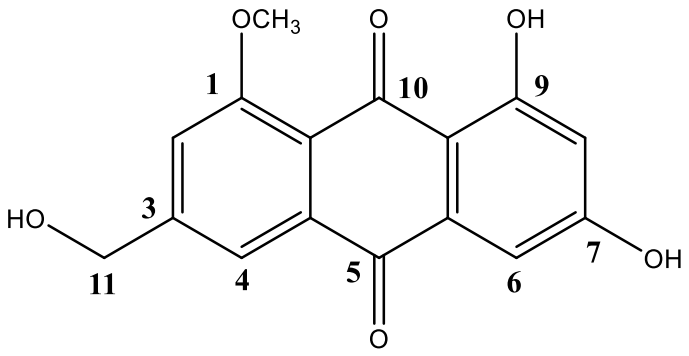

Chemical Formula: $C_{16}H_{12}O_6$
Exact Mass: 300,06339

Figure 14. Chemical structure of PR-EB-04.

The HR-ESI-MS spectrum of **PR-EB-04** exhibited a prominent ion peak at *m/z* 323.05176 $[M+Na]^+$ (calcd. 323.05316) supported a molecular formula $C_{16}H_{12}O_6$ with eleven indices of hydrogen deficiency.

The ^1H NMR and ^{13}C NMR data of **PR-EB-04** (Tables 7) showed a close structural relationship with **PR-EB-03** (Table 6). A primary alcohol group instead of the methyl group in **PR-EB-03** was evident, whereas a monomeric framework was proposed for **PR-EB-04** based on the mass data and an extra aromatic signal assigned to H-6 in the ^1H NMR spectrum.

Analysis of its ^1H and ^{13}C NMR spectra revealed the presence of a methoxy group (H-1-OMe: δ 3.93, s; C-1-OMe: δ 56.4, s), three aromatic carbon methines (δ_{C-2} 116.2 d, δ_{C-4} 116.8 d, δ_{C-6} 107.7 d, δ_{C-8} 108.4 d), and eleven non-protonated carbons (six aromatic δ_{C-1} 160.6, δ_{C-3} 151.3, δ_{C-4a} 134.7 s, δ_{C-5a} 133.9 s, δ_{C-7} 164.7, δ_{C-9} 165.4, δ_{C-9a} 109.7, δ_{C-10a} 118.4 and two keto carbons at δ_{C-5} 182.5 s, δ_{C-10} 186.0 s). Detailed inspection of the 1D-, 2D NMR and HR-ESI-MS spectra implied that the structure of **PR-EB-04** was 1,3-dihydroxy-6-(hydroxymethyl)-8-methoxy-anthracene-9,10-dione, a known compound namely carviolin. The established structure was also confirmed by comparing the spectral data with previous reports (Aly et al. 2011; Elbanna et al. 2021).

Table 7. ^{1}H and ^{13}C NMR spectroscopic data of PR-EB-04, a) (in DMSO-d6, ^{1}H:400 MHz, ^{13}C:100 MHz)

Position	**δ_C (ppm)**	**δ_H (ppm), (J in Hz)**
1	160.6 s	-
2	116.2 d	7.47 d (1.5)
3	151.3 s	-
4	116.8 d	7.72 d (1.5)
4a	134.7 s	-
5	182.5 s	-
5a	133.9 s	-
6	107.7 d	7.02 d (2.4)
7	164.7 s	-
8	108.4 d	6.52 d (2.4)
9	165.4 s	-
9a	109.7 s	-
10	186.0 s	-
10a	118.4 s	-
11	62.3 t	4.63 s
1-OMe	56.4 q	3.93 s
7-OH	-	-
9-OH	-	13.28 s
11-OH	-	-

a) Assignments are confirmed by 2D-COSY, HSQC, and HMBC experiments.

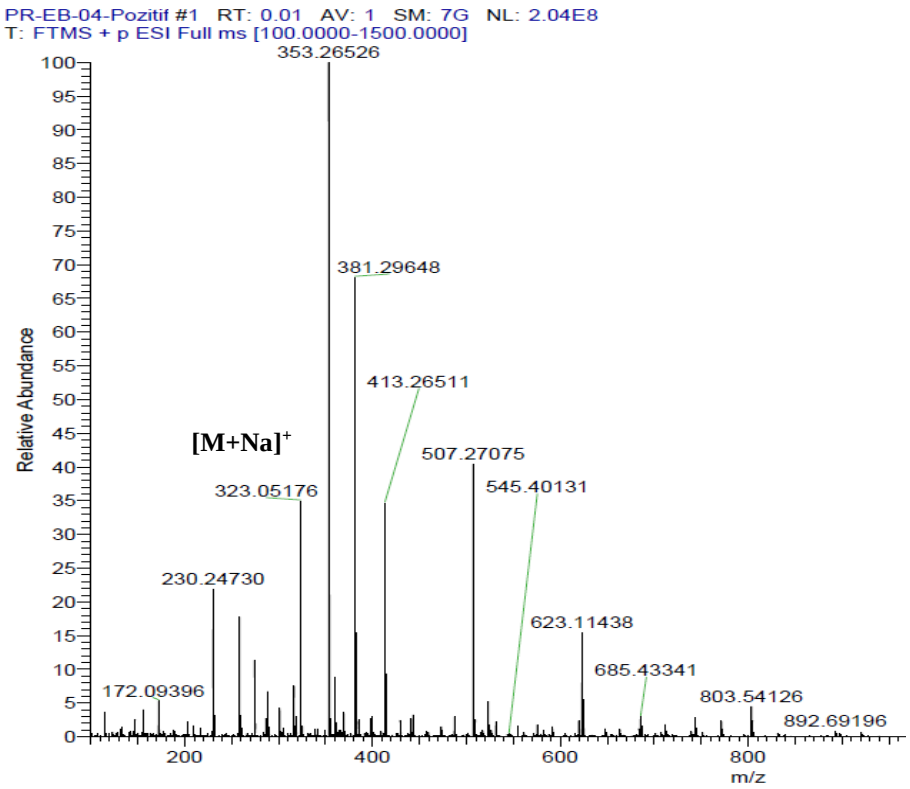

Spectrum 13. HR-ESI-MS Spectrum of PR-EB-04 (positive mode).

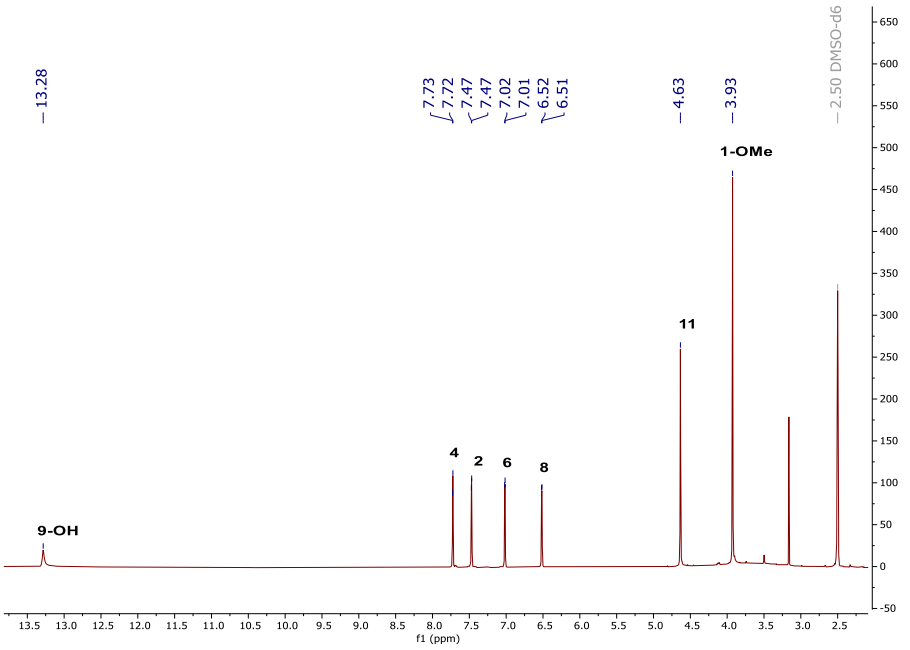

Spectrum 14. ^{1}H NMR Spectrum of PR-EB-04 (in DMSO-d6, ^{1}H: 400 MHz).

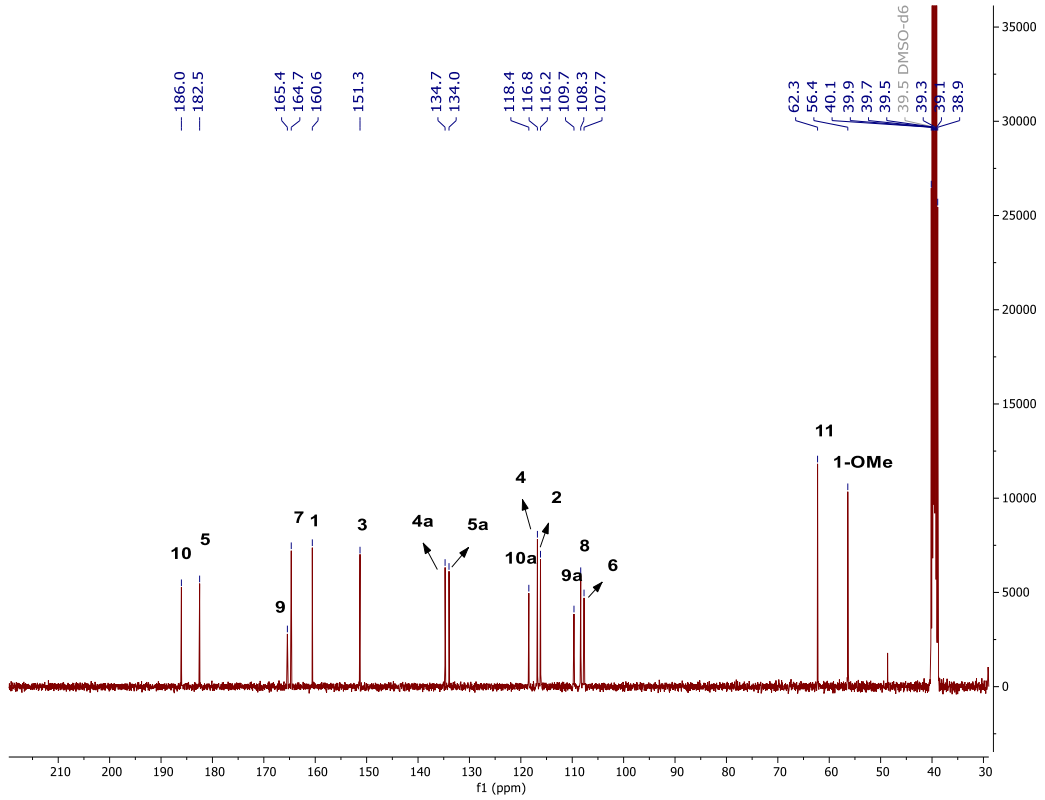

Spectrum 15. ^{13}C NMR Spectrum of PR-EB-04 (in DMSO-d6, ^{13}C:100 MHz).

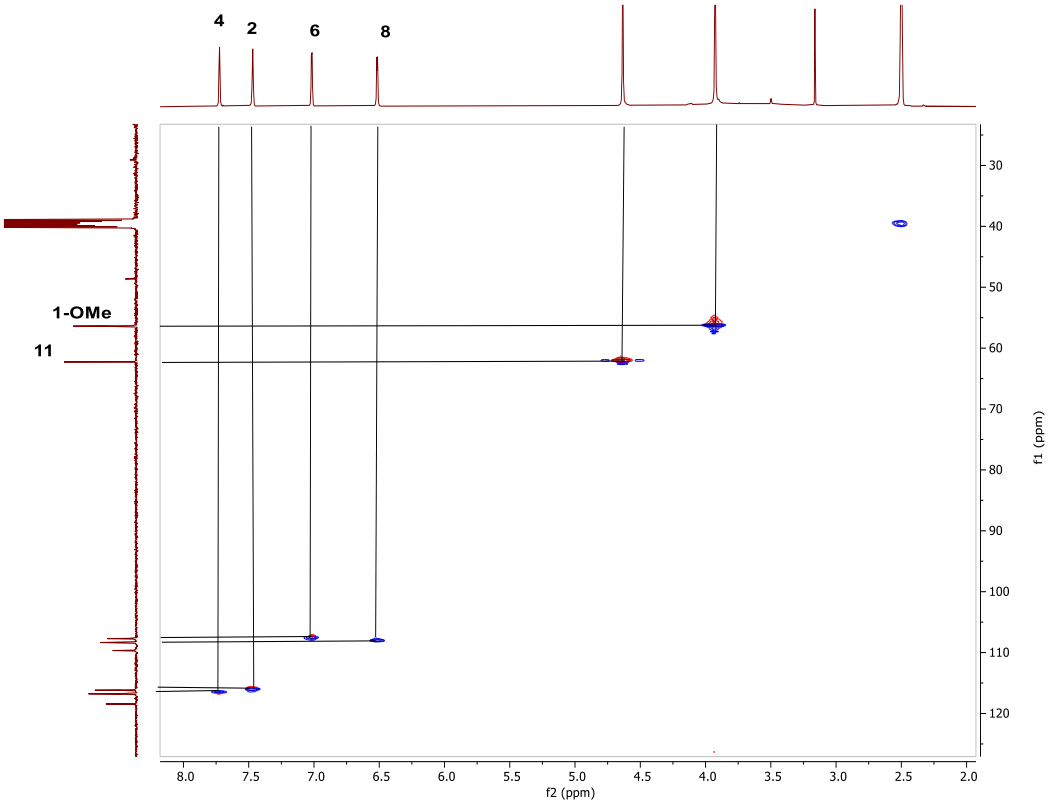

Spectrum 16. HSQC spectrum of PR-EB-04.

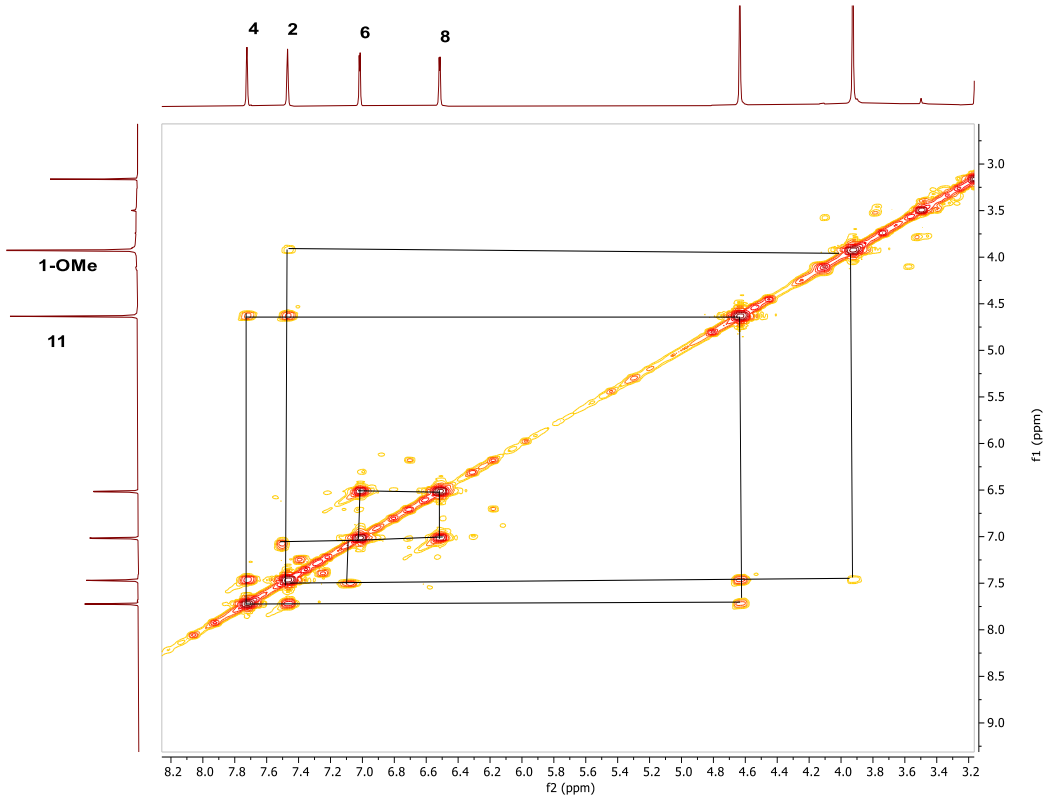

Spectrum 17. COSY spectrum of PR-EB-04.

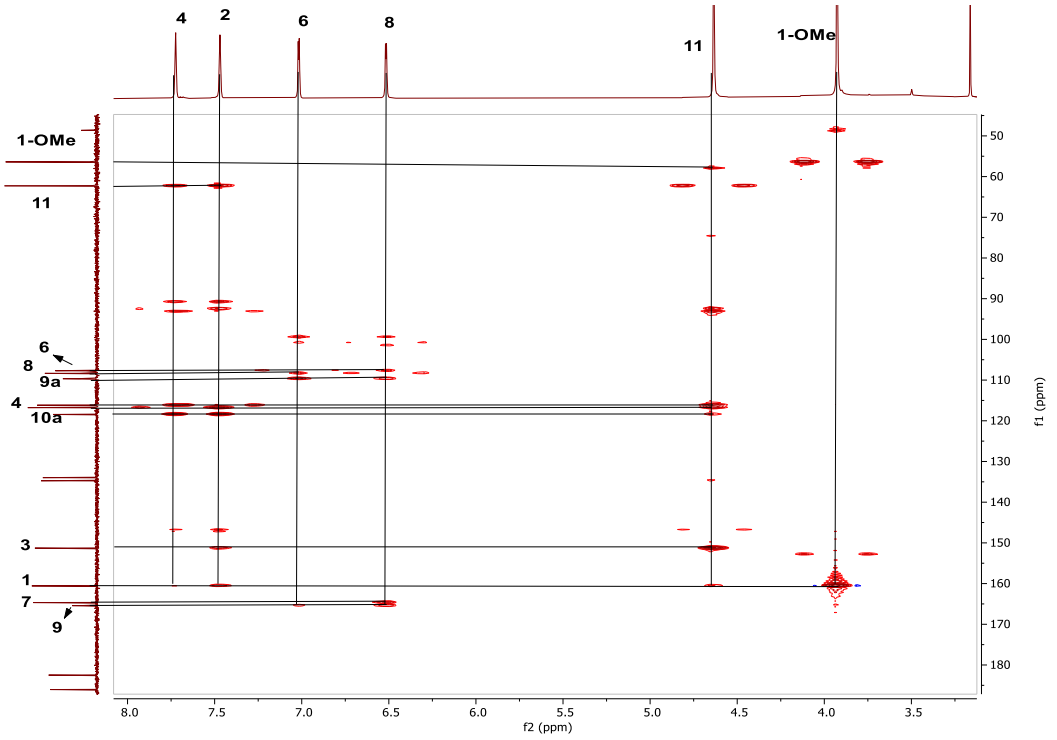

Spectrum 18. HMBC spectrum of PR-EB-04.

3.1.4. Structure Elucidation of PR-EB-05

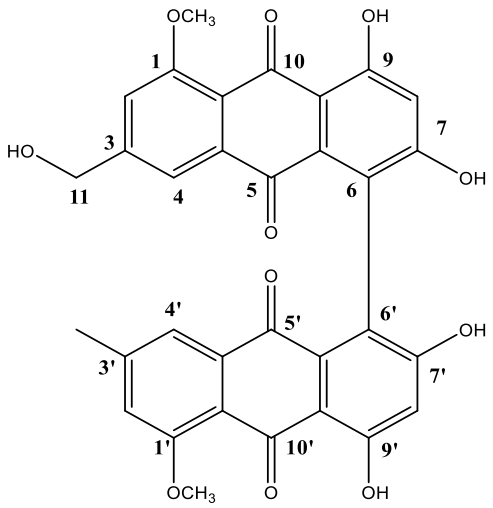

Chemical Formula: $C_{32}H_{22}O_{11}$
Exact Mass: 582,11621

Figure 15. Chemical structure of PR-EB-05.

The HR-ESI-MS spectrum of **PR-EB-05** exhibited a prominent ion peak at *m/z* 583.12300 [M+H], (calcd. 583.12404) supported a molecular formula $C_{32}H_{22}O_{11}$ with twenty-two indices of hydrogen deficiency.

The spectroscopic features suggested that **PR-EB-05** was a dimeric anthraquinone like **PR-EB-03**. **PR-EB-05** had a 16 amu (atomic mass unit) increase compared to **PR-EB-03**, implying oxygenation. In accordance, a primary alcohol group was readily assigned based on the resonances of δ 4.53 (s, 2H) and δ 62.3, in the ^{1}H- and ^{13}C NMR spectrum of **PR-EB-05**, respectively. Detailed inspection of the 1D-, 2D-NMR, and HR-ESI-MS spectra inferred that **PR-EB-05** was a heterodimer anthraquinone. One of the two monomeric units was established as 1-O-methylemodin by comparing the spectral data with those of previous reports and **PR-EB-03** (Ayer and Trifonov 1994), and the other monomeric unit was established as carviolin by comparing the spectral data with those of previous reports and **PR-EB-04** (Aly et al. 2011; Elbanna et al. 2021). As in the case of **PR-EB-03**, in the ^{1}H NMR spectrum of **PR-EB-05**, the aromatic H-6 proton was missing in both 1-O-methylemodin and carviolin substructures (Ayer and Trifonov 1994; Elbanna et al. 2021; Aly et al. 2011), signifying that monomeric moieties were linked through C6/C6'. X-Ray or circular

dichroism experiments are warranted to determine the absolute stereochemistry of **PR-EB-05**. Consequently, the planar structure of **PR-EB-05** was elucidated as 2,2',4,4'-tetrahydroxy-7-(hydroxymethyl)-5,5'-dimethoxy-7'-methyl-[1,1'-bianthracene]-9,9',10,10'-tetraone. A literature survey revealed that **PR-EB-05** was a new heterodimeric anthraquinone.

Table 8. ^{1}H and ^{13}C NMR spectroscopic data of PR-EB-05, a) (in DMSO-d6, ^{1}H: 600 MHz, ^{13}C:150 MHz)

Position	**δ_C (ppm)**	**δ_H (ppm), (J in Hz)**
1	159.9 s	-
2	115.3 d	7.40 s
3	150.2 s	-
4	116.6 d	7.40 s
4a	135.6 s	-
5	c	-
5a	131.2 s	-
6	c	-
7	c	-
8	107.2 d	6.39 s
9	164.4 s	-
9a	c	-
10	c	-
10a	119.7 s	-
11	62.3 t	4.53 s
1-OMe	56.4 q	3.93 s
7-OH	-	-
9-OH	-	13.28 s
11-OH	-	-
1-OMe	56.4 q	3.93[b] s
7-OH	-	13.40 s
9-OH	-	14.05 s
11-OH	-	5.45 bs
1’	159.9 s	-
2’	118.8 d	7.31 s
3’	145.7 s	-
4’	119.8 d	7.26 s
4’a	135.6 s	-
5’	c	-
5’a	131.2 s	-

Cont. on next page

Cont. of Table 8

6’	c	-
7’	164.4 s	-
8’	107.2 d	6.39 bs
9’	164.4 s	-
9’a	c	-
10’	180.1 s	-
10’a	118.9 s	-
12	21.6	2.34 s
1’-OMe	56.4 q	3.92[b] s
7’-OH	-	13.40 bs
9’-OH	-	14.05 bs

a) Assignments are confirmed by 2D-COSY, HSQC, and HMBC experiments.
b) Interchangeable.
c) Not observed.

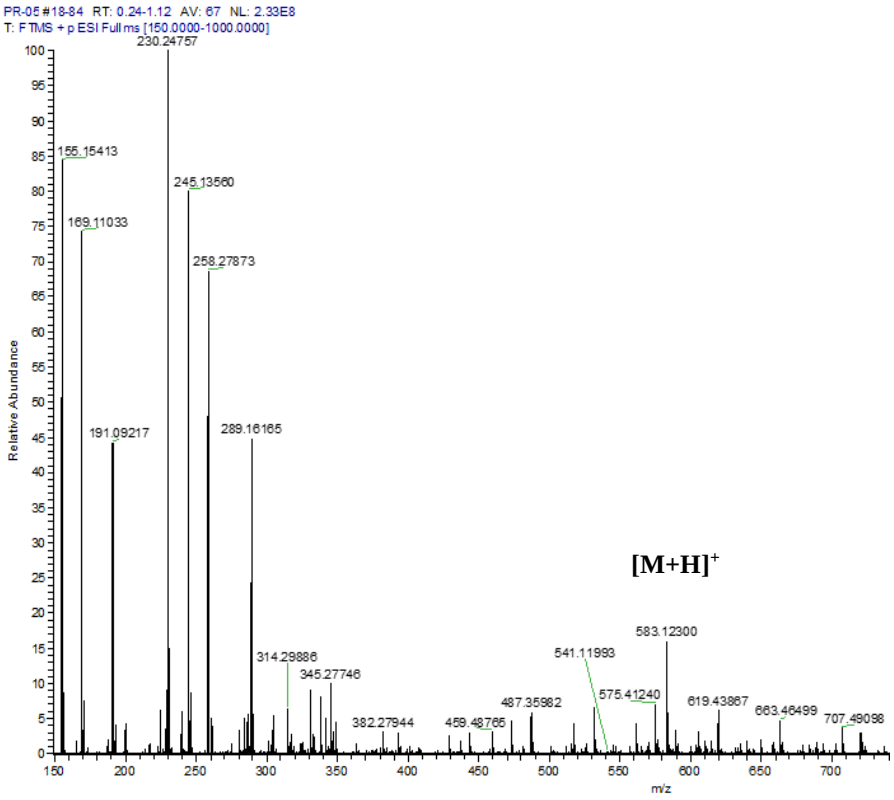

Spectrum 19. HR-ESI-MS Spectrum of PR-EB-05 (positive mode).

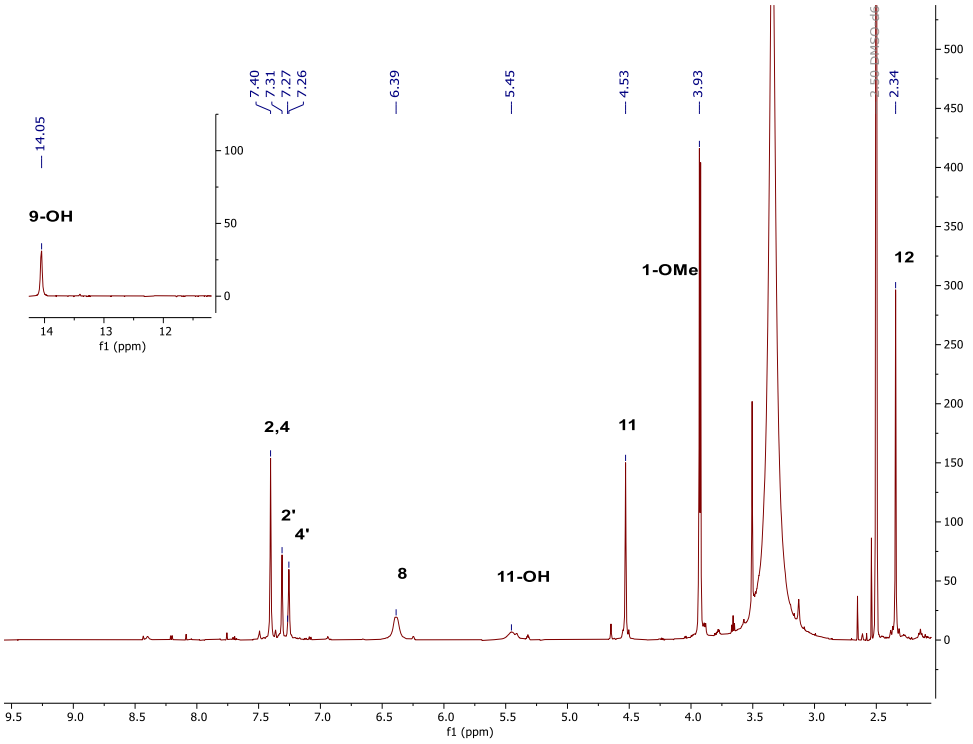

Spectrum 20. ^{1}H NMR Spectrum of PR-EB-05 (in DMSO-d6, ^{1}H: 600 MHz).

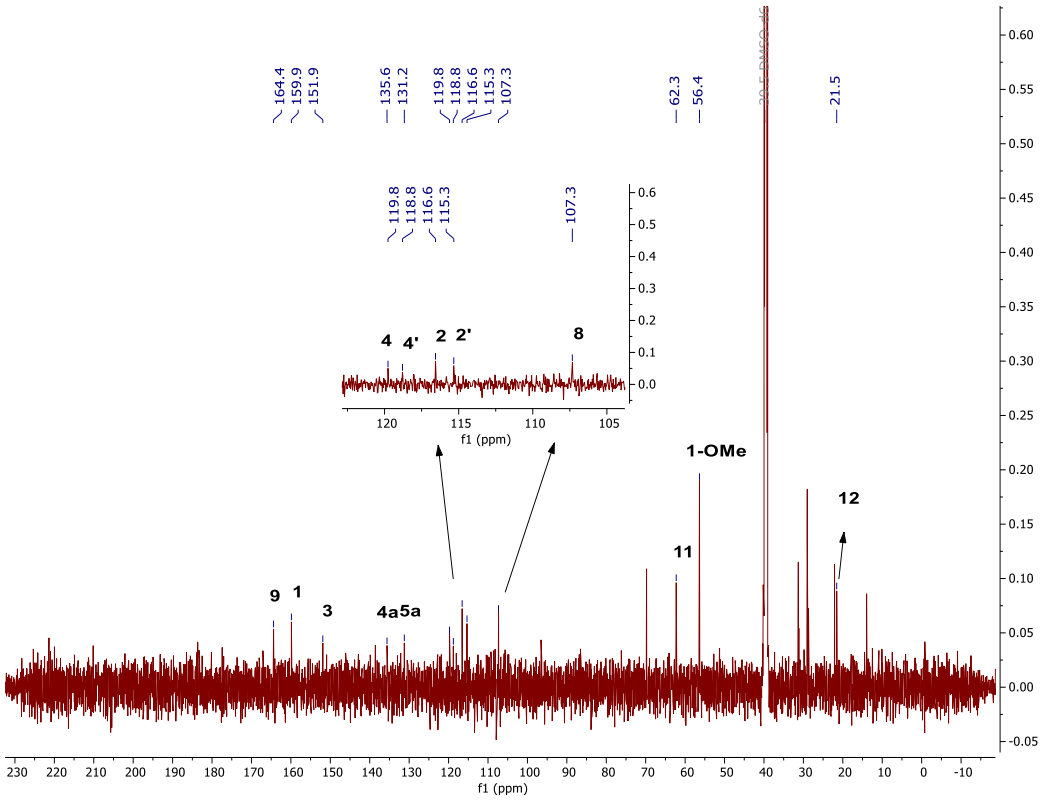

Spectrum 21. ^{13}C NMR Spectrum of PR-EB-05 (in DMSO-d6, ^{13}C:150 MHz).

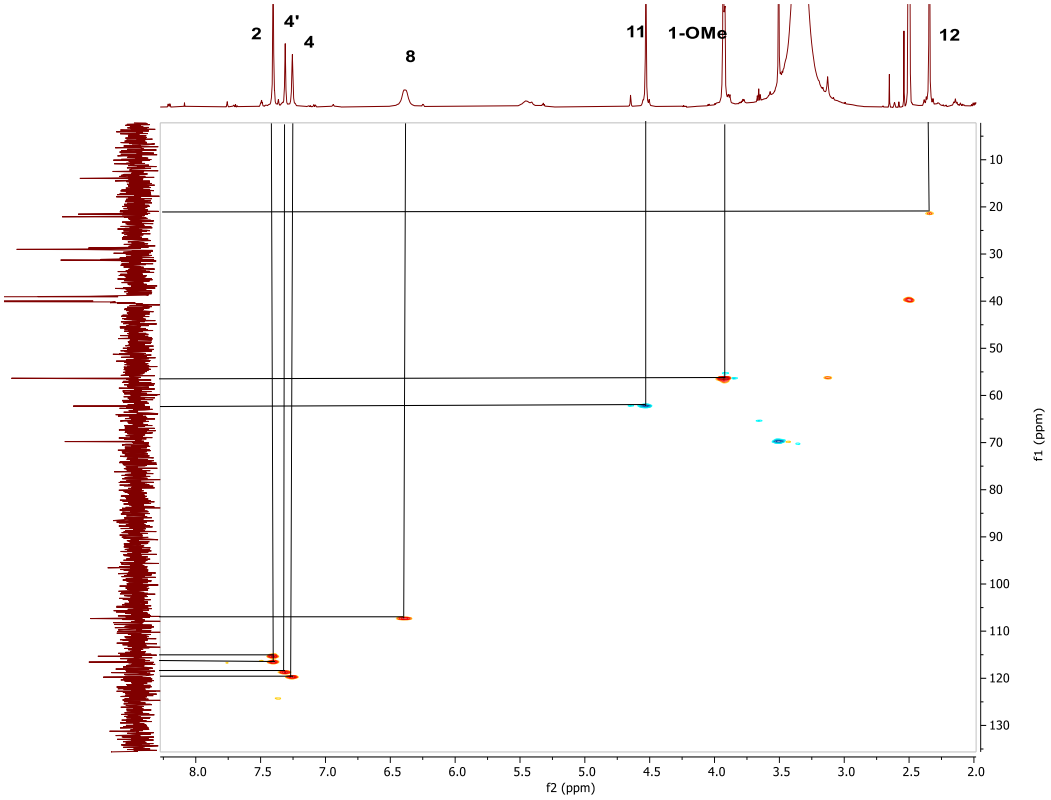

Spectrum 22. HSQC spectrum of PR-EB-05.

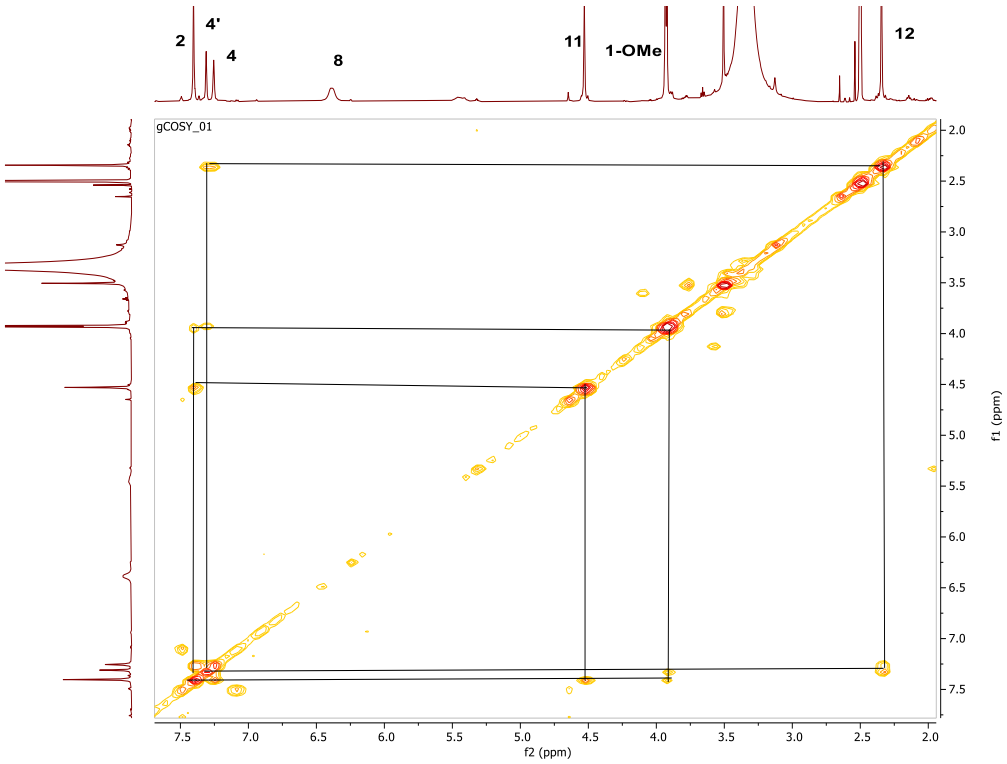

Spectrum 23. COSY spectrum of PR-EB-05.

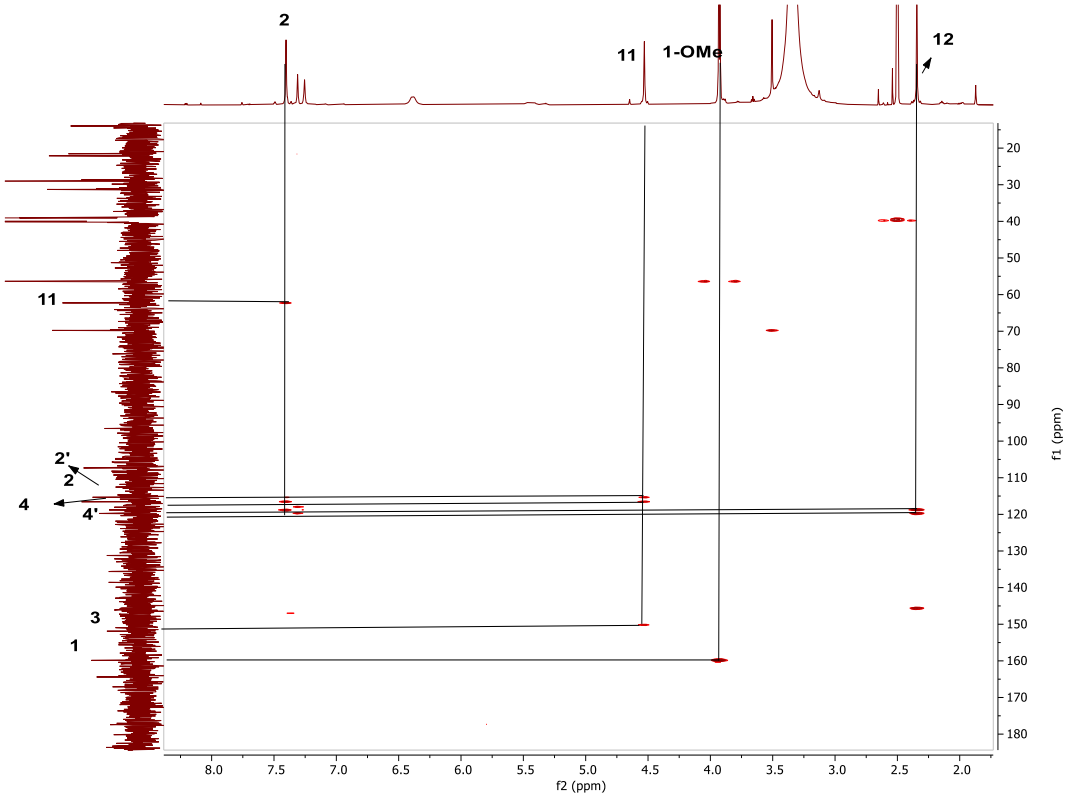

Spectrum 24. HMBC spectrum of PR-EB-05.

3.1.5. Structure Elucidation of PR-EB-06

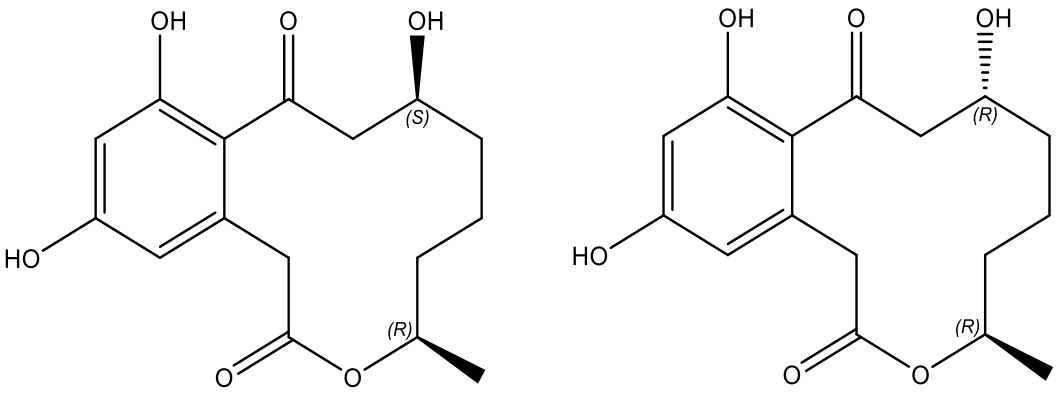

Chemical Formula: $C_{16}H_{20}O_6$
Exact Mass: 308,12599

Figure 16. Chemical structure of PR-EB-06.

The HR-ESI-MS spectrum of **PR-EB-06** exhibited a prominent ion peak at *m/z* 331.11477 $[M+H]^+$, (calcd. 331.11576) supported a molecular formula $C_{16}H_{20}O_6$ with seven indices of hydrogen deficiency.

The ^1H and ^{13}C NMR spectra of **PR-EB-06** showed a close structural relationship with **PR-EB-01**. Firstly, **PR-EB-06** was also a mixture of two diastereomers (**PR-EB-06A** and **PR-EB-06B**). Second, a hydroxy group substitution instead of the methoxy group at position 11 was proposed for **PR-EB-06** consistent with the MS data. Additionally, the presence of an exchangeable proton for each stereoisomer ($\delta_{OH\text{-}11A}$ 4.60; $\delta_{OH\text{-}11B}$ 4.58) together with the up-field shift of C-11 ($\delta_{C\text{-}11A}$ 65.0; $\delta_{C\text{-}11B}$ 65.9) about 10 ppm supported our assumption. Accordingly, the HMBC cross-peaks from C-11 and C-12 ($\delta_{C\text{-}12A}$ and $\delta_{C\text{-}12B}$ 34.4) to the exchangeable protons verified the structural deduction.

Detailed inspection of the 1D- and 2D-NMR spectra and comparison of the spectral data with those previously published established that the diastereomeric mixture was composed of (4*R*,8*S*)-8,11,13-trihydroxy-4-methyl-4,5,6,7,8,9-hexahydro-2H-benzo[d][1]oxacyclododecine-2,10(1H)-dione (**PR-EB-06A**) and (4*R*,8*R*)-8,11,13-trihydroxy-4-methyl-4,5,6,7,8,9-hexahydro-2H-benzo[d][1] oxacyclododecine-2,10(1H)-dione (**PR-EB-06B**). Both compounds were isomers of a known polyketide, namely 11-hydroxycurvularin (Greve et al. 2008).

Table 9. ^1H and ^{13}C NMR spectroscopic data of PR-EB-06A, a) (in DMSO-d6, ^1H: 600 MHz, ^{13}C: 150 MHz)

Position	**δ_C (ppm)**	**δ_H (ppm), (J in Hz)**
1	169.9 s	-
2a	38.9 t	3.77 d (13.6)
2b		-
3	136.0 d	-
4	111.4 d	6.15 d (2.3)
5	159.7 s	-
6	101.8 d	6.26 d (2.2)
7	157.6 s	-
8	119.5 s	-
9	203.5 s	-
10a	53.2 t	2.85 s
10b		3.14 s
11	65.0 d	3.87 s
12a	34.4 t	1.21 m
12b		1.47 m

Cont. on next page

Cont. of Table 8

13a	21.7 t	1.06 s
13b		1.05 s
14a	31.1 t	1.46 m
14b		1.21 m
15	70.2 d	4.84 m
16	18.0 q	1.06 s
5-OH	-	9.87 s
7-OH	-	10.03 s
11-OH	-	4.60 d (5.2)

a) Assignments are confirmed by 2D-COSY, HSQC, and HMBC experiments.

Table 10. ^{1}H and ^{13}C NMR spectroscopic data of PR-EB-06B, a) (in DMSO-d6, ^{1}H: 600 MHz, ^{13}C: 150 MHz)

Position	**δ_C (ppm)**	**δ_H (ppm), (J in Hz)**
1	170.2 s	-
2a	38.9 t	-
2b		3.56 d (15.6)
3	136.0 d	-
4	110.8 d	6.15 d (2.3)
5	159.4 s	-
6	101.7 d	6.28 d (2.3)
7	158.5 s	-
8	118.8 s	-
9	204.2 s	-
10a	53.9 t	2.85 s
10b		3.14 s
11	65.9 d	3.77 d (13.6)
12a	34.4 t	1.21 m
12b		-
13a	21.7 t	1.06 s
13b		-
14a	30.5 t	1.58 m
14b		1.32 m
15	72.8 d	4.71 m
16	18.8 q	1.06 s
5-OH	-	9.81
7-OH	-	10.09
11-OH	-	4.58 d (5.8)

a) Assignments are confirmed by 2D-COSY, HSQC, and HMBC experiments.

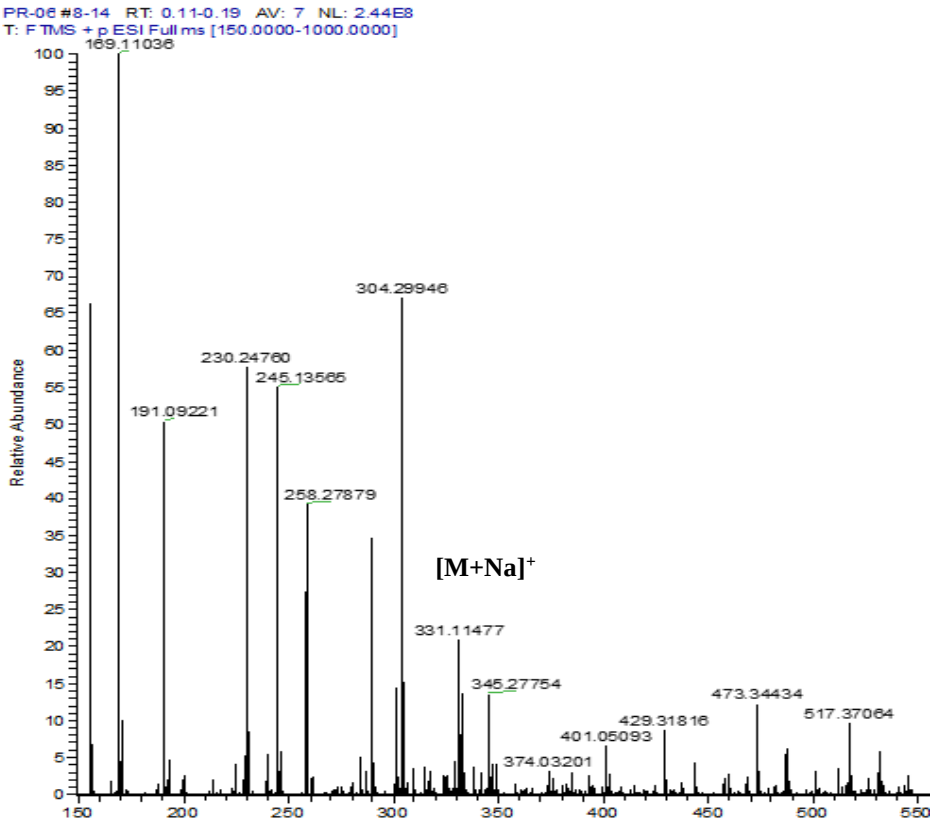

Spectrum 25. HR-ESI-MS Spectrum of PR-EB-06 (positive mode).

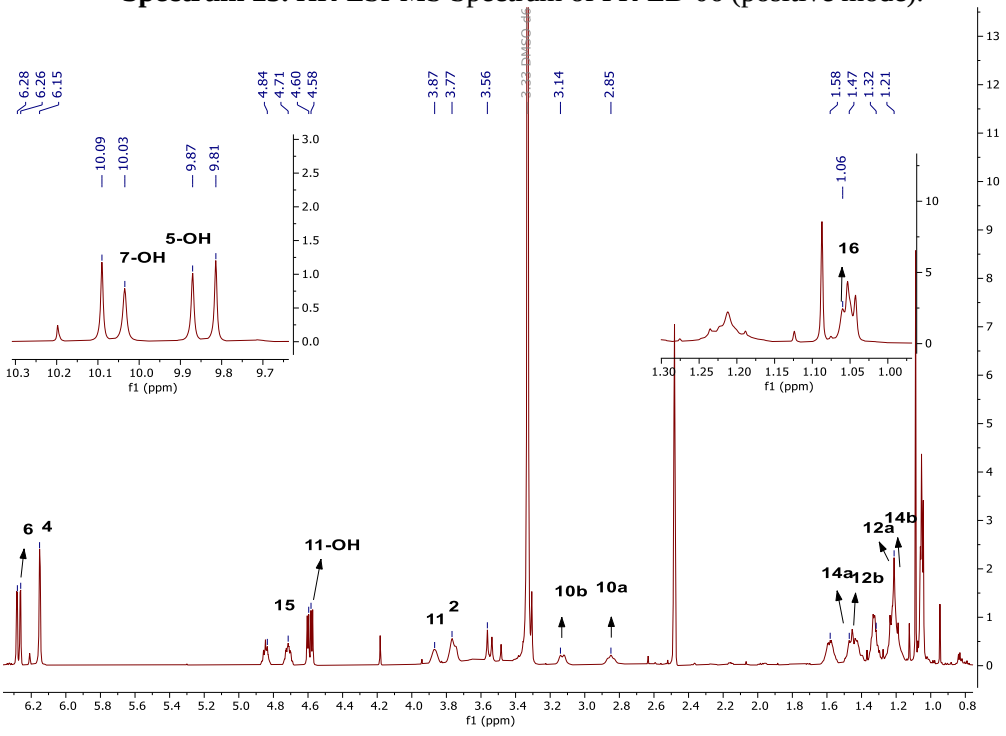

Spectrum 26. ^{1}H NMR Spectrum of PR-EB-06 (in DMSO-d6, ^{1}H: 600 MHz).

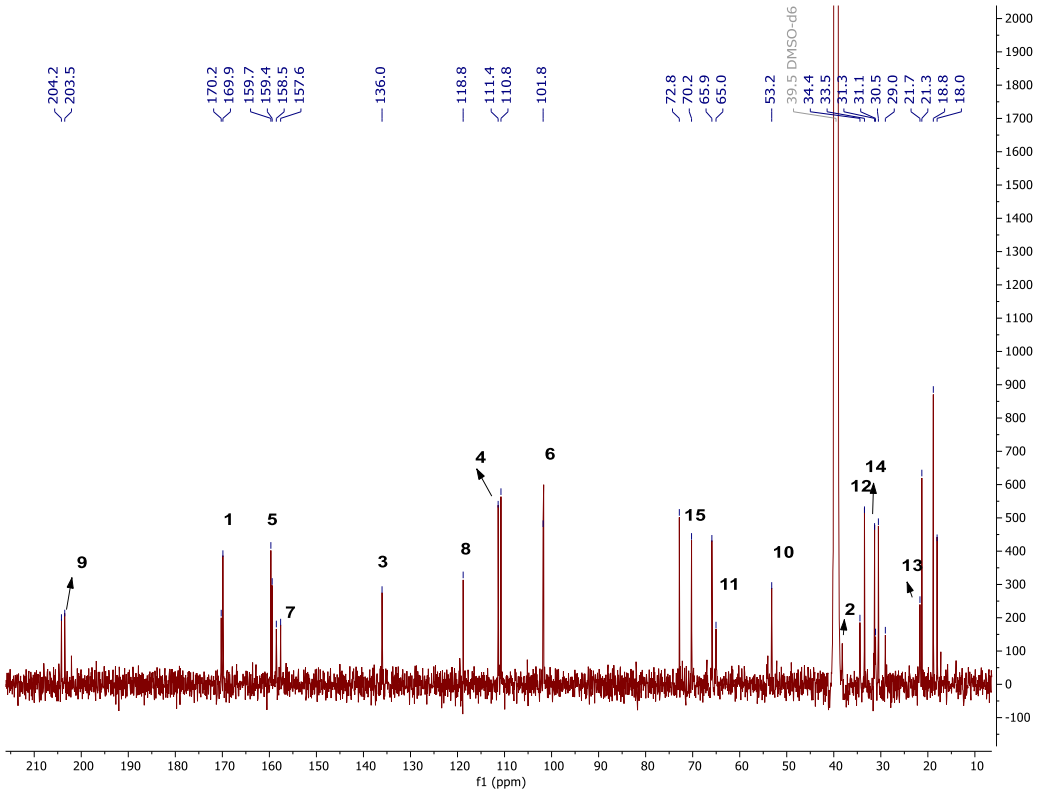

Spectrum 27. ^{13}C NMR Spectrum of PR-EB-06 (in DMSO-d6, ^{13}C:150 MHz).

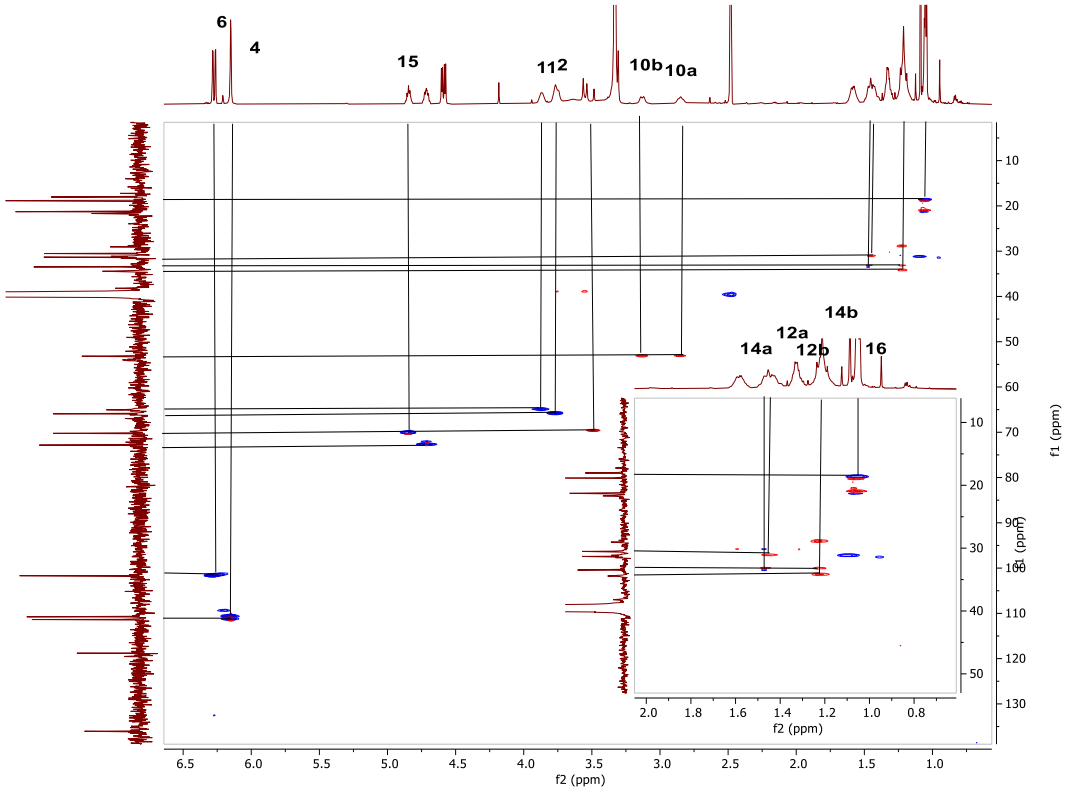

Spectrum 28. HSQC spectrum of PR-EB-06.

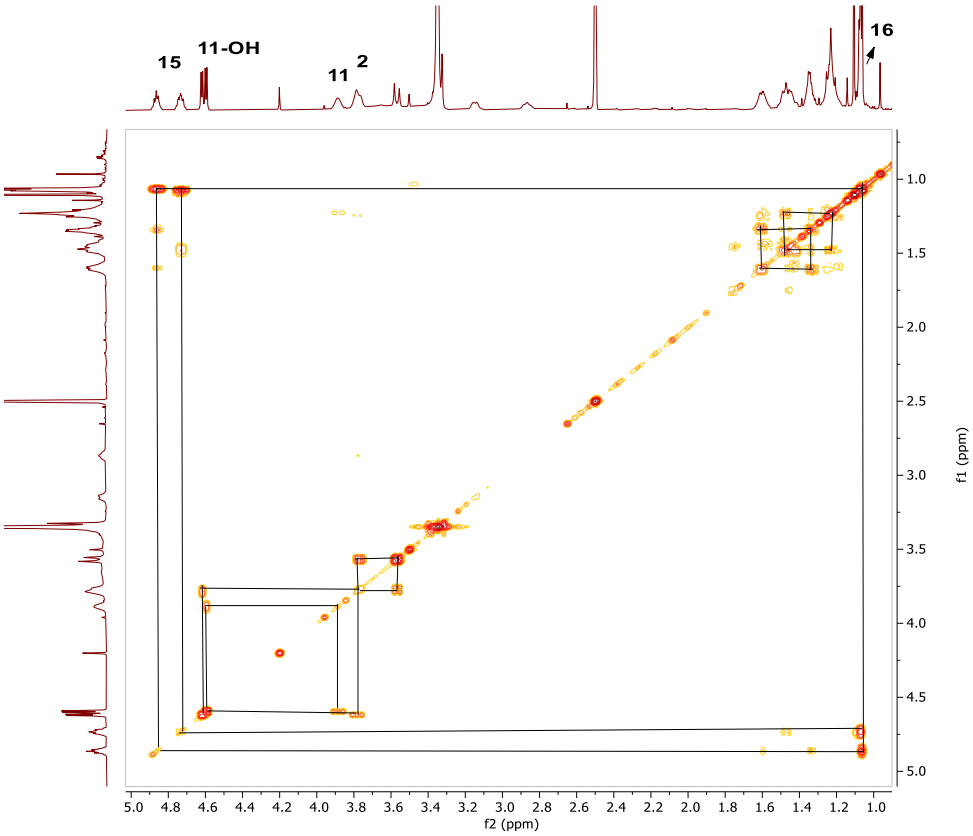

Spectrum 29. COSY spectrum of PR-EB-06.

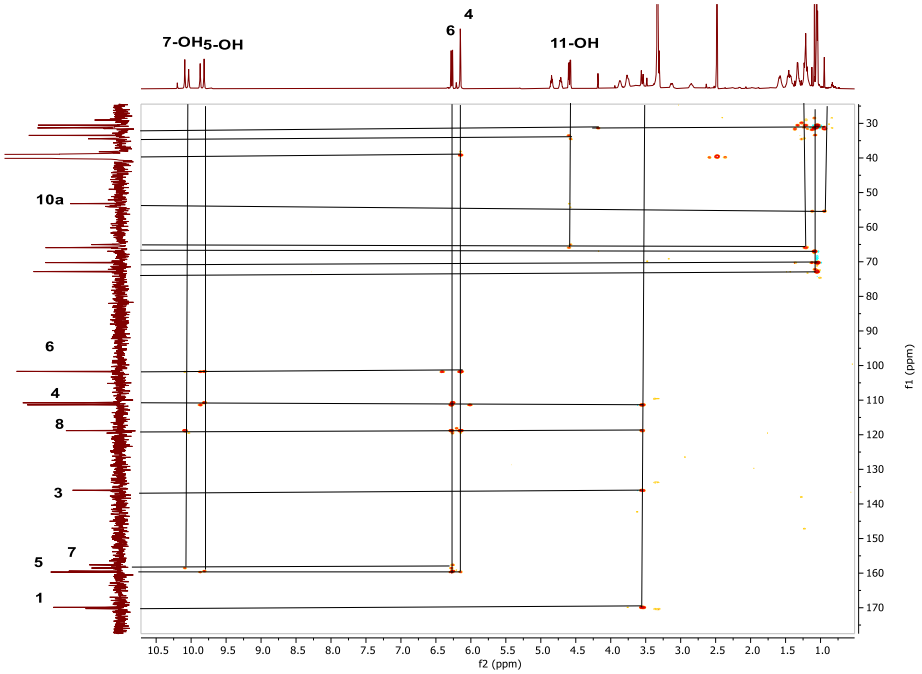

Spectrum 30. HMBC spectrum of PR-EB-06.

3.1.6. Structure Elucidation of PR-EB-09

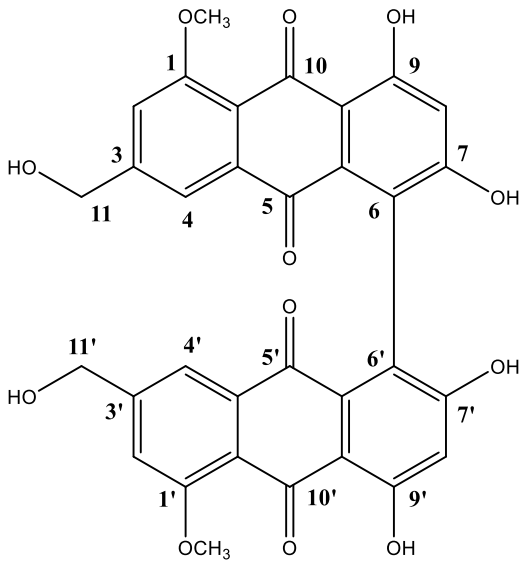

Chemical Formula: $C_{32}H_{22}O_{12}$
Exact Mass: 598,1111
Figure 17. Chemical structure of PR-EB-09.

The HR-ESI-MS spectrum of **PR-EB-09** exhibited a prominent ion peak at *m/z* 599.11768 $[M+H]^+$ (calcd. 599.11895) supported a molecular formula $C_{32}H_{22}O_{12}$ with twenty-two indices of hydrogen deficiency.

The spectroscopic features suggested that **PR-EB-09** was a dimeric anthraquinone like **PR-EB-05**. **PR-EB-09** had a 16 amu (atomic mass unit) increase compared to **PR-EB-05**, implying oxygenation. In accordance, two primary alcohol group was readily assigned based on the resonances observed at δ 4.53 (s, H_2-11, H_2-11') and δ 62.2, in the ^{1}H- and ^{13}C NMR spectra of **PR-EB-09**, respectively. Detailed inspection of the 1D-, 2D NMR, and HR-ESI-MS spectra inferred that **PR-EB-09** was a homodimeric anthraquinone. The monomeric unit was established as carviolin by comparing the spectral data with those of previous reports and **PR-EB-04** (Aly et al. 2011; Elbanna et al. 2021). As in the case of **PR-EB-05**, in the ^{1}H NMR spectrum of **PR-EB-09**, the aromatic H-6 proton was missing in carviolin substructure (Elbanna et al. 2021; Aly et al. 2011), signifying that the monomeric moieties were linked through C6/C6'. X-Ray or circular dichroism experiments are warranted to determine the absolute stereochemistry of **PR-EB-09**. Consequently, the planar structure of **PR-EB-09** was elucidated as 7,7'-diethyl-2,2',4,4',5,5'-hexamethyl-9,9',10,10'-tetramethylene-

9,9',10,10'-tetrahydro-1,1'-bianthracene. A literature survey revealed that **PR-EB-09** was a new homodimeric anthraquinone.

Table 11. ^{1}H and ^{13}C NMR spectroscopic data of PR-EB-09, a) (in DMSO-d6, ^{1}H: 500 MHz, ^{13}C: 125 MHz)

Position	**δ_C (ppm)**	**δ_H (ppm), (J in Hz)**
1(1')	160.2 s	-
2(2')	115.6 d	7.42 s
3(3')	151.1 s	-
4(4')	116.7 d	7.45 s
4a(4'a)	135.4 s	-
5(5')	183.1 s	-
5a(5'a)	130.9 s	-
6(6')	122.3 s	-
7(7')	b	-
8(8')	107.5 d	6.63 s
9(9')	164.0 s	-
9a(9'a)	109.9 d	-
10(10')	186.2 s	-
10a(10'a)	118.3 s	-
11(11')	62.2 t	4.53 s
1-OMe(1'-OMe)	56.4 q	3.88 s
7-OH(7'-OH)	-	10.82 s
9-OH(9'-OH)	-	13.87 s
11-OH(11'-OH)	-	5.47

a) Assignments are confirmed by 2D-COSY, HSQC, and HMBC experiments.
b) Not observed

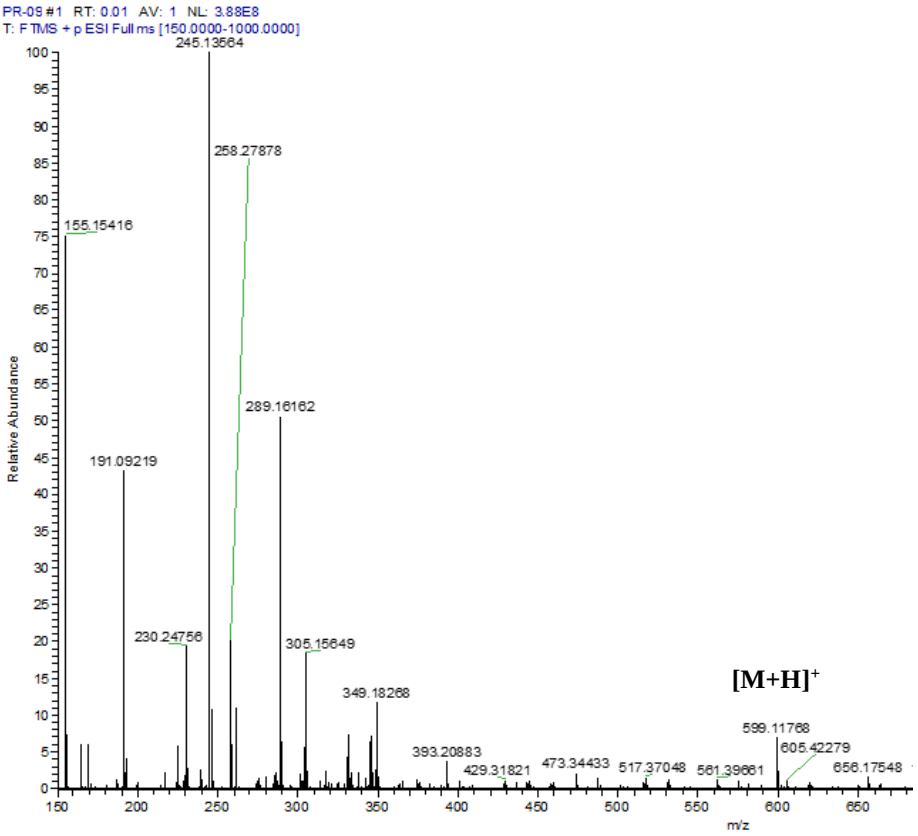

Spectrum 31. HR-ESI-MS Spectrum of PR-EB-09 (positive mode).

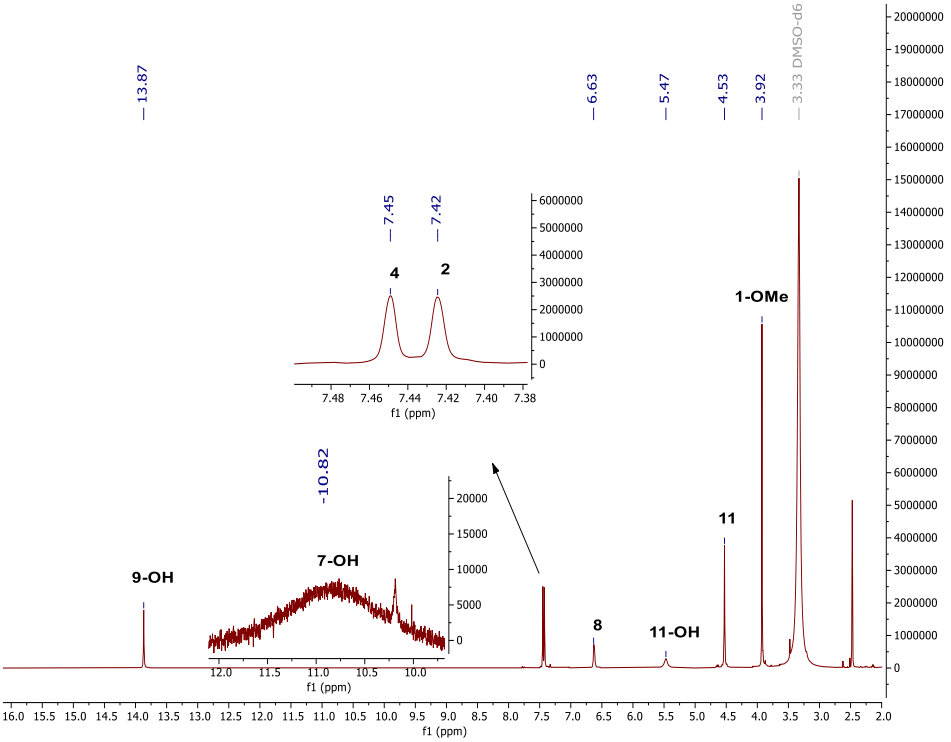

Spectrum 32. ^{1}H NMR Spectrum of PR-EB-09 (in DMSO-d6, ^{1}H: 500 MHz).

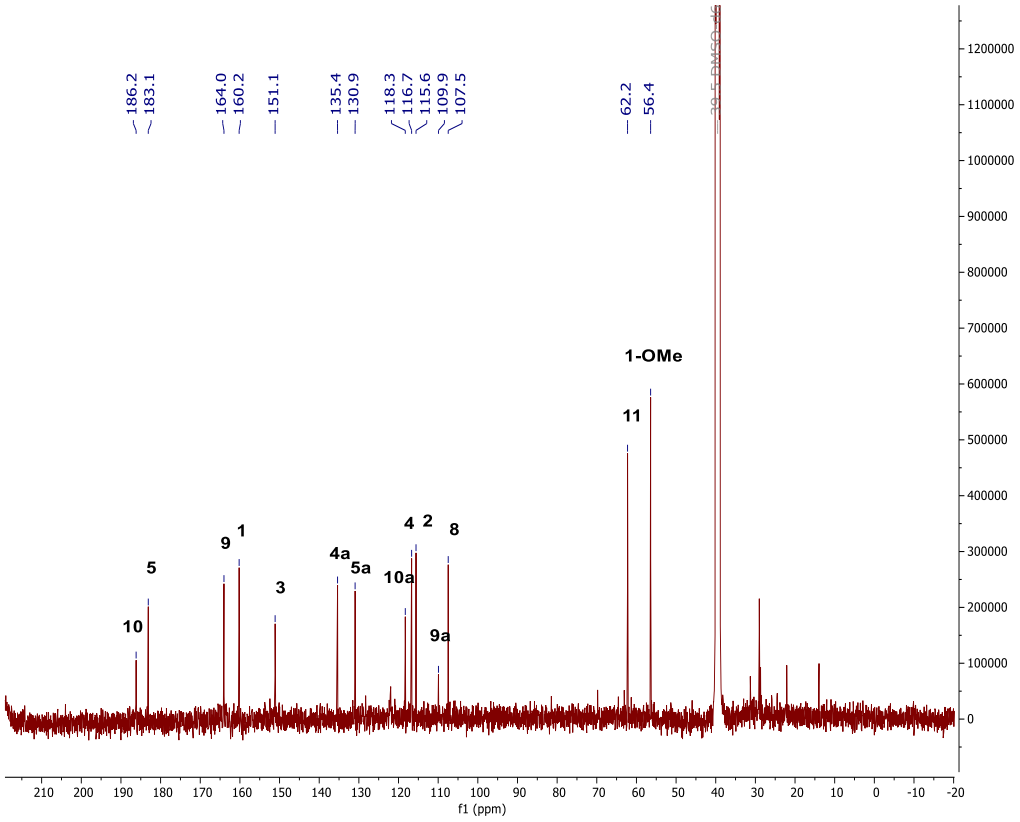

Spectrum 33. ^{13}C NMR Spectrum of PR-EB-09 (in DMSO-d6, ^{13}C:125 MHz).

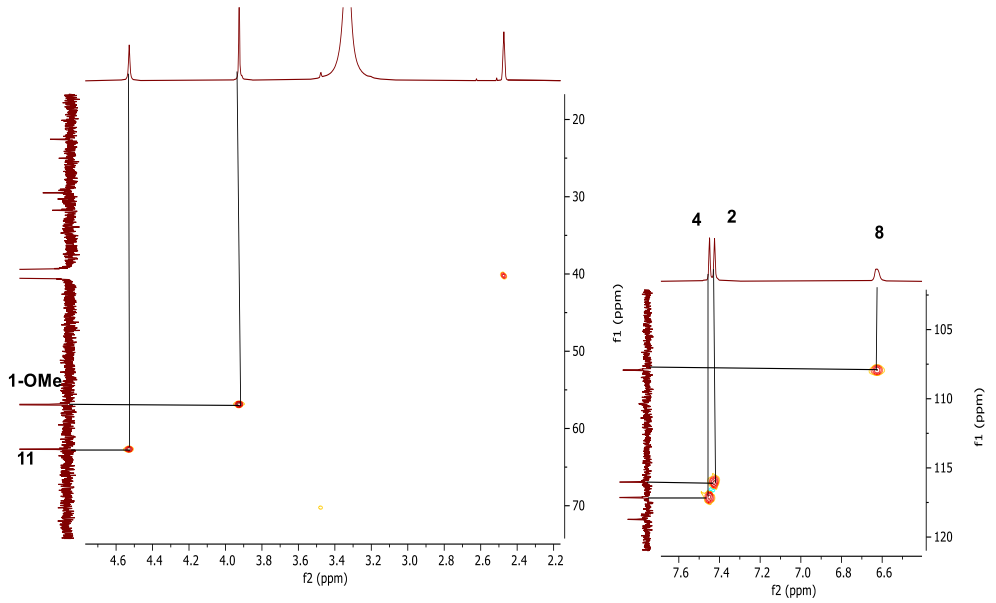

Spectrum 34. HSQC spectrum of PR-EB-09.

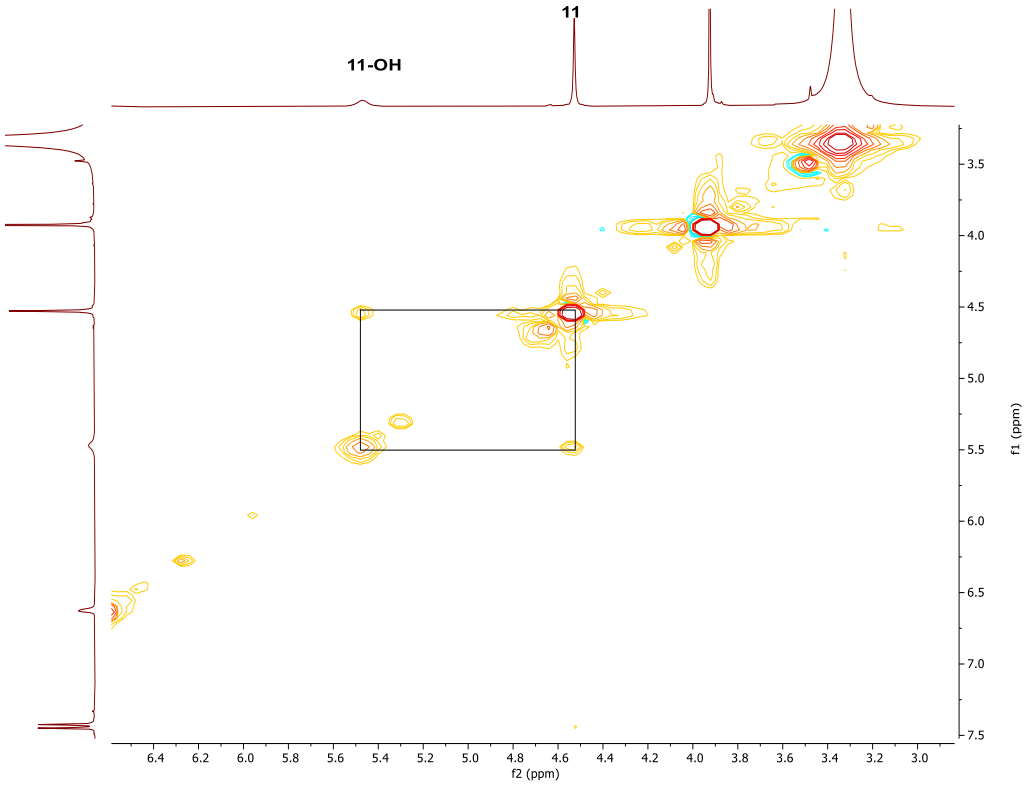

Spectrum 35. COSY spectrum of PR-EB-09.

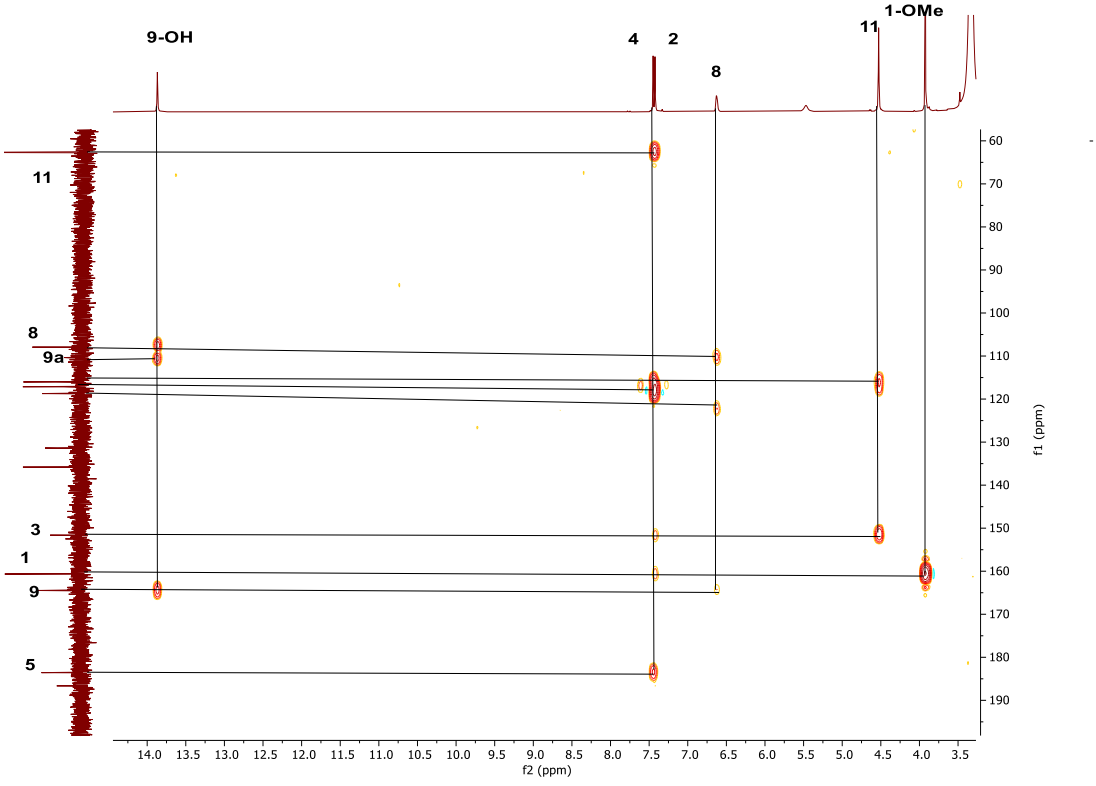

Spectrum 36. HMBC spectrum of PR-EB-09.

3.1.7. Structure Elucidation of PR-EB-10

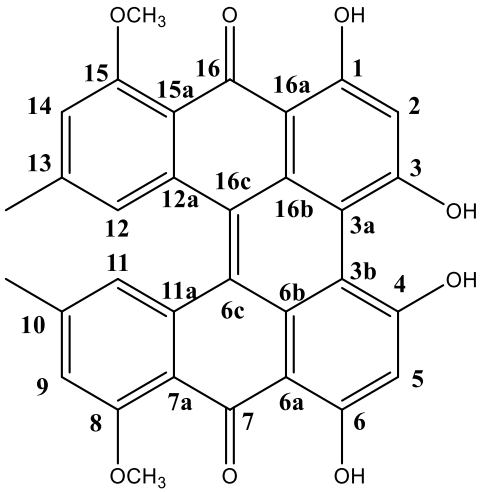

Chemical Formula: $C_{32}H_{22}O_8$
Exact Mass: 534,1315
Figure 18. Chemical structure of PR-EB-10.

The HR-ESI-MS spectrum of **PR-EB-10** exhibited a major ion peak at *m/z* 533.12463 $[M-H]^-$, (calcd. 533.12419) supported a molecular formula $C_{32}H_{22}O_8$ with six indices of hydrogen deficiency.

The ^1H NMR and ^{13}C NMR data of **PR-EB-10** (Tables 13) showed a close structural relationship with **PR-EB-03** (Table 6). The spectroscopic features suggested that **PR-EB-10** was a naphtodianthrone derivative like **PR-EB-03**. Detailed inspection of the 1D-, 2D NMR, and HR-ESI-MS spectra inferred that **PR-EB-10** was a homodimer naphtodianthrone derivative. The monomeric unit was established as 1-O-methylemodin by comparing the spectral data with those of previous reports and **PR-EB-03** (Ayer and Trifonov 1994).

In the ^1H NMR spectrum of **PR-EB-10**, the aromatic protons were lacking for C-6c, C-16c, C-3a, and C-3b when compared to that of 1-O-methylemodin (Ayer and Trifonov 1994), which substantiated that the substructures were connected through C-3a → C-3b and C-16c → C-6c bridges. (Ayer and Trifonov 1994; Elbanna et al. 2021; Aly et al. 2011). X-Ray or circular dichroism experiments are warranted to determine the absolute stereochemistry of **PR-EB-10**. Consequently, the structure of **PR-EB-10** was elucidated as 1,3,4,6-tetrahydroxy-8,15-dimethoxy-10,13-dimethyldibenzo[a,o]perylene-7,16-

dione. A literature survey revealed that **PR-EB-10** was the new member of naphtodianthrone derivatives.

Table 12. ^{1}H and ^{13}C NMR spectroscopic data of PR-EB-10, a) (in DMSO-d6, ^{1}H: 500 MHz, ^{13}C:125 MHz)

Position	**δ_C (ppm)**	**δ_H (ppm), (J in Hz)**
1	168.6 s	-
2	104.1 d	6.22 s
3	172.1 s	-
3a	118.5 s	-
3b	118.5 s	-
4	172.1 s	-
5	104.1 d	6.22 s
6	168.6 s	-
6a	101.2 s	-
6b	138.3 s	-
6c	127.7 s	-
7	182.9 s	-
7a	117.2 s	-
8	159.3 s	-
9	112.3 d	6.96 s
10	141.0 s	-
11	127.1 d	7.11 s
11a	129.3 s	-
12	127.1 d	7.11 s
12a	129.3 s	-
13	141.0 s	-
14	112.3 d	6.96 s
15	159.3 s	-
15a	117.2 s	-
16	182.9 s	-
16a	101.2 s	-
16b	138.3 s	-
16c	127.7 s	-
17	21.5 q	2.09 s
18	21.5 q	2.09 s
8-OMe	56.0 q	3.93 s
15-OMe	56.0 q	3.93 s
1-OH	-	b
3-OH	-	b
4-OH	-	b
6-OH	-	b

a) Assignments are confirmed by 2D-COSY, HSQC, and HMBC experiments.
b) Not observed.

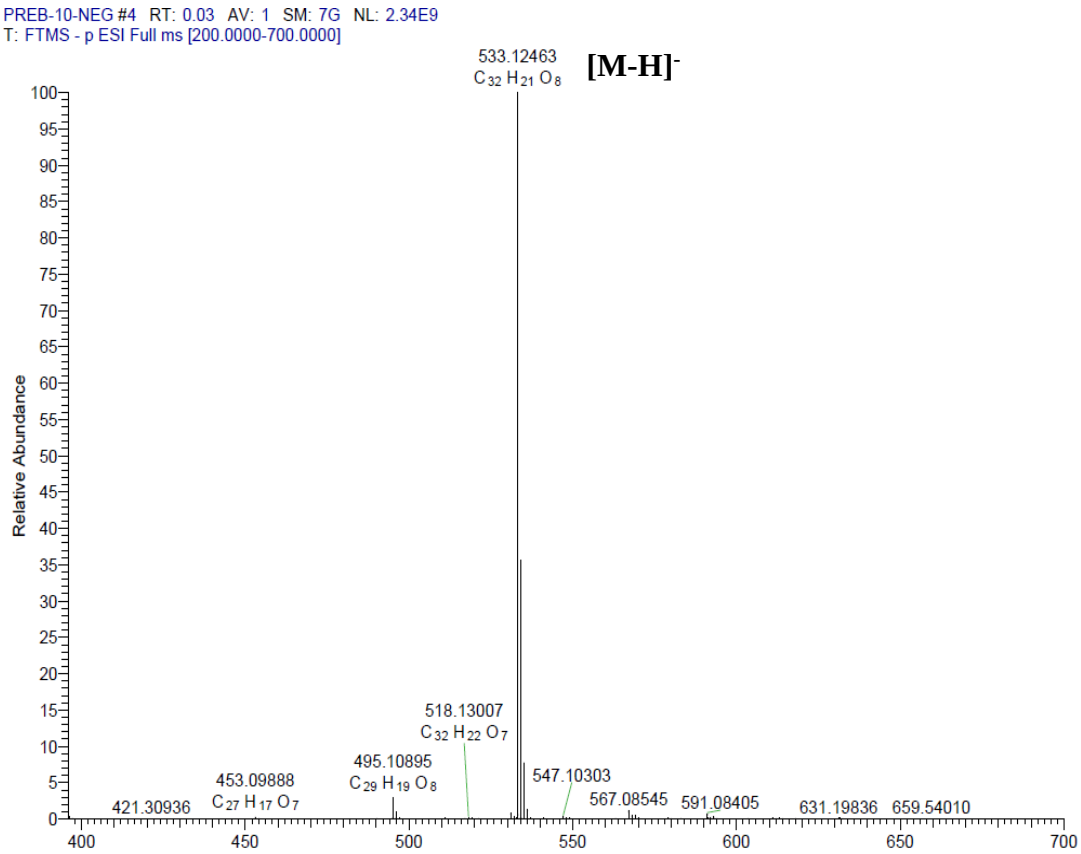

Spectrum 37. HR-ESI-MS Spectrum of PR-EB-10 (negative mode).

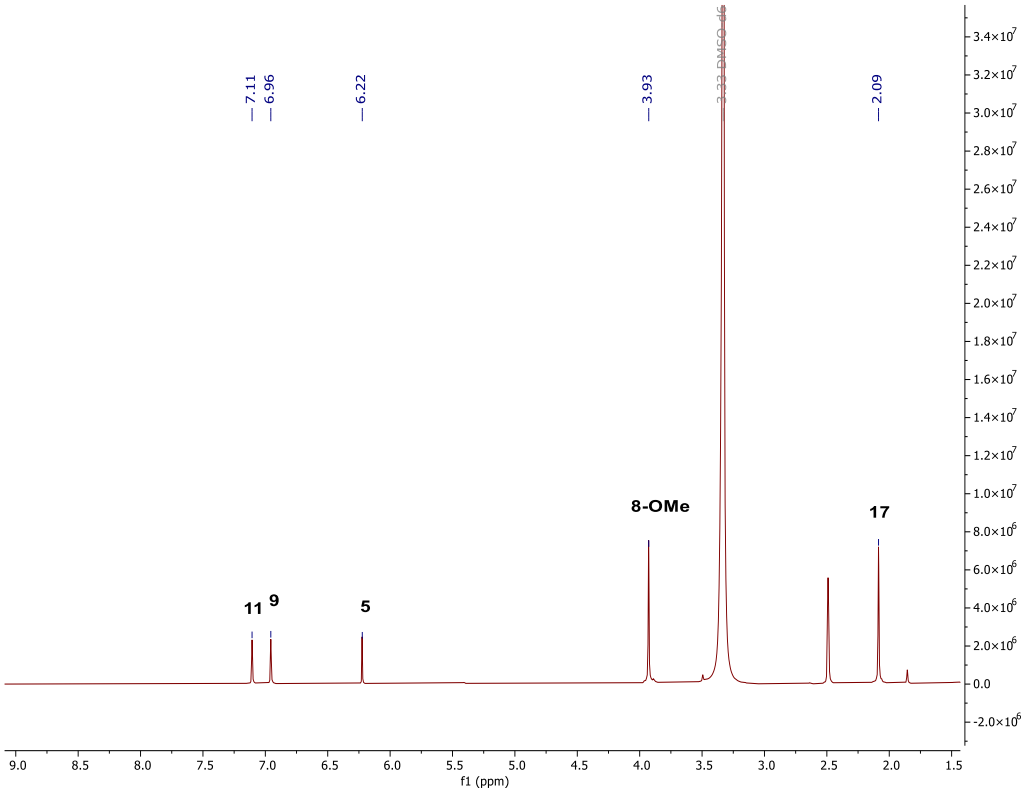

Spectrum 38. ^{1}H NMR Spectrum of PR-EB-10 (in DMSO-d6, ^{1}H: 500 MHz).

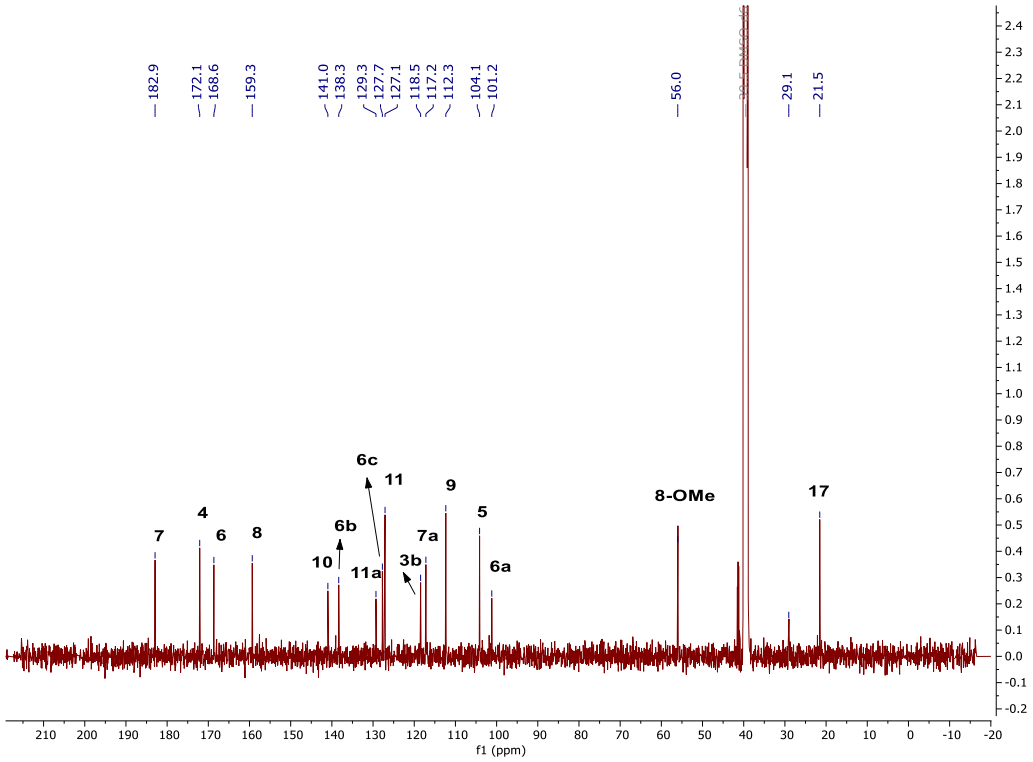

Spectrum 39. ^{13}C NMR Spectrum of PR-EB-10 (in DMSO-d6, ^{13}C:125 MHz).

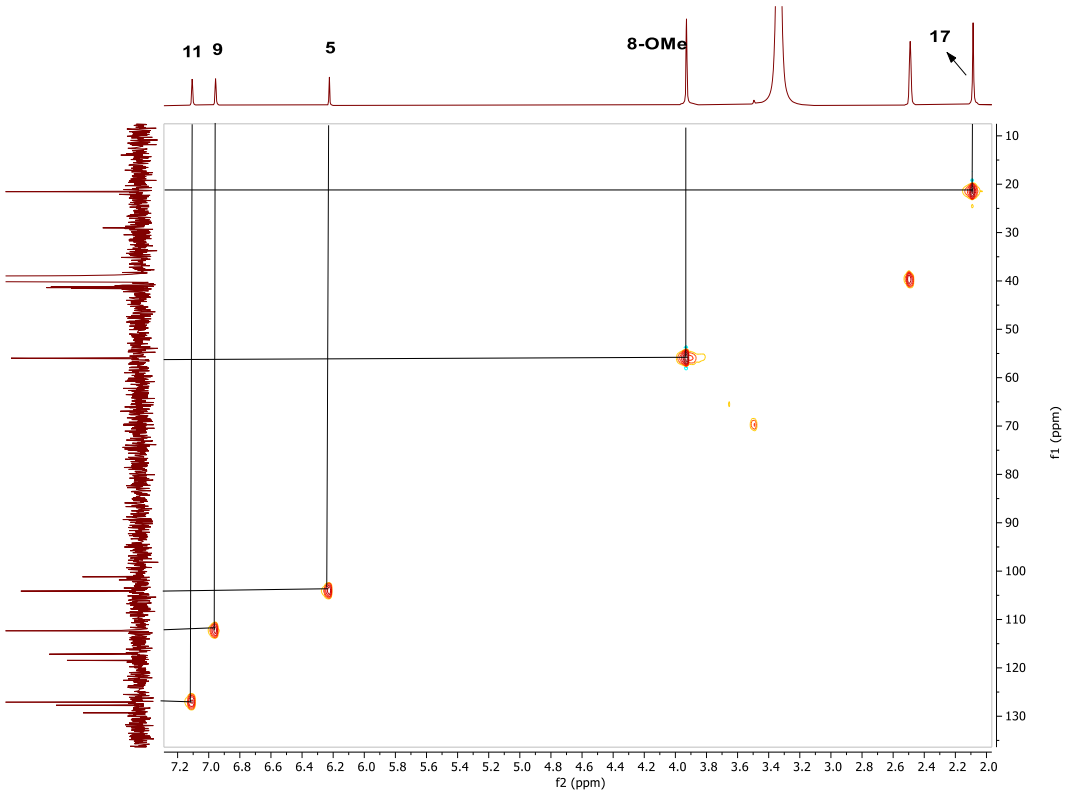

Spectrum 40. HSQC spectrum of PR-EB-10.

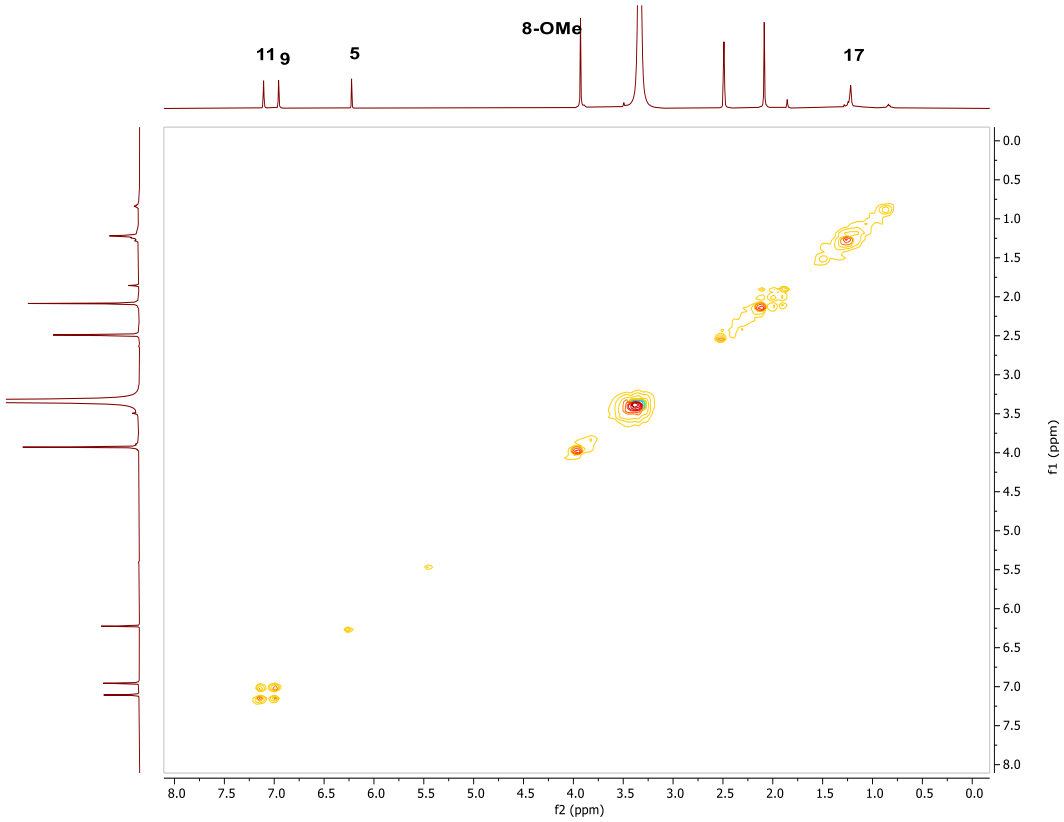

Spectrum 41. COSY spectrum of PR-EB-10.

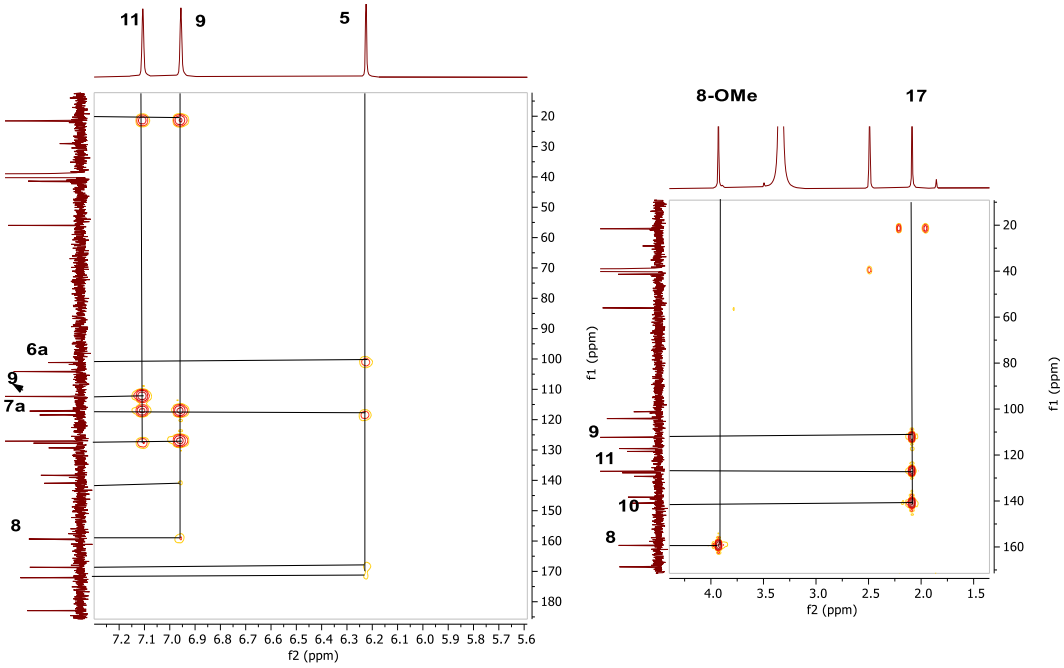

Spectrum 42. HMBC spectrum of PR-EB-10.

3.1.8. Structure Elucidation of PR-EB-11

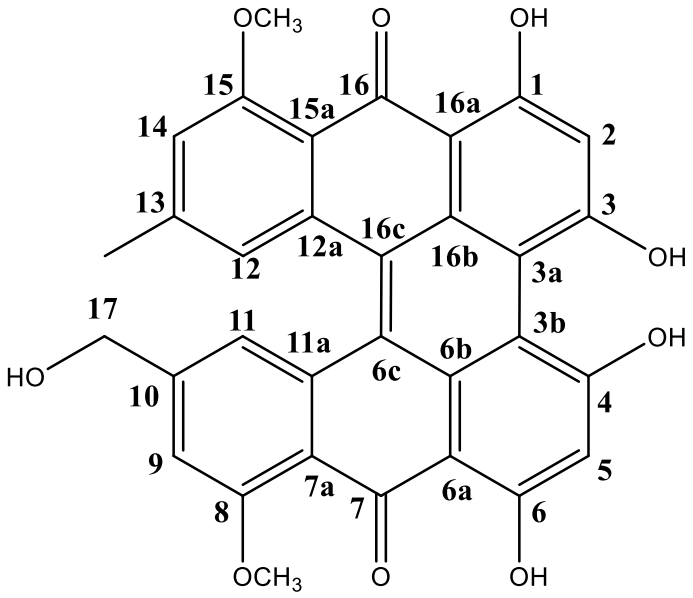

Chemical Formula: $C_{32}H_{22}O_9$
Exact Mass: 550,1264
Figure 19. Chemical structure of PR-EB-11.

The HR-ESI-MS spectrum of **PR-EB-11** exhibited a major ion peak at *m/z m/z* 549.11969 $[M-H]^-$, (calcd. 549.11910) supported a molecular formula $C_{32}H_{22}O_9$ with twenty-two indices of hydrogen deficiency.

The spectroscopic features suggested that **PR-EB-11** was a naphtodianthrone derivative like **PR-EB-10**. **PR-EB-11** had a 16 amu (atomic mass unit) increase compared to **PR-EB-10**, implying oxygenation. In accordance, a primary alcohol group was readily assigned based on the resonances of δ 4.25 (s, H_2-17) and δ 62.4, in the ^{1}H- and ^{13}C NMR spectra of **PR-EB-11**, respectively. Detailed inspection of the 1D-, 2D NMR, and HR-ESI-MS spectra inferred that **PR-EB-11** was a heterodimer naphtodianthrone. One of the two monomeric units was established as 1-O-methylemodin by comparing the spectral data with those of previous reports and **PR-EB-03** (Ayer and Trifonov 1994), and the other monomeric unit was established as carviolin by comparing the spectral data with those of previous reports and **PR-EB-04** (Aly et al. 2011; Elbanna et al. 2021). As in the case of **PR-EB-04** and **PR-EB-03**, in the ^{1}H NMR spectrum of **PR-EB-11**, the aromatic H16c/H6c and H3a/H3b protons

were missing in both 1-O-methylemodin and carviolin substructures (Ayer and Trifonov 1994; Elbanna et al. 2021; Aly et al. 2011), signifying that the substructures were linked through two bridges: C16c → C6c and C3a → C3b. X-Ray or circular dichroism experiments are warranted to determine the absolute stereochemistry of **PR-EB-11**. Consequently, the structure of **PR-EB-11** was elucidated as 1,3,4,6-tetrahydroxy-10-(hydroxymethyl)-8,15-dimethoxy-13-methyldibenzo[a,o]perylene-7,16-dione. A literature survey revealed that **PR-EB-11** was a new heterodimeric naphtodianthrone.

Table 13. ^{1}H and ^{13}C NMR spectroscopic data of PR-EB-11, a) (in DMSO-d6, ^{1}H:500 MHz, ^{13}C:125 MHz)

Position	**δ_C (ppm)**	**δ_H (ppm), (J in Hz)**
1	168.7 s	-
2	104.1 d	6.22 d
3	172.0[b] s	-
3a	118.5 s	-
3b	118.4 s	-
4	172.1[b] s	-
5	104.1 d	6.22 d
6	168.7 s	-
6a	101.1 s	-
6b	138.3[b] s	-
6c	127.8 s	-
7	182.9 s	-
7a	117.9 s	-
8	159.4 s	-
9	109.0 d	7.06 s
10	145.7 s	-
11	124.0 d	7.25 s
11a	129.3 s	-
12	127.1 d	7.10 s
12a	129.3 s	-
13	141.5 s	-
14	112.3 d	6.4 s
15	159.3 s	-
15a	117.1 s	-
16	183.0 s	-
16a	101.1 s	-
16b	138.4[b] s	-
16c	127.7 s	-
17	62.4 t	4.25 m
18	21.6 q	2.07 s
1-OH	-	16.24[b] bs

Cont. on next page

Cont. of Table 13

3-OH	-	18.5 bs
4-OH	-	16.25[b] bs
6-OH	-	5.16 t
17-OH	-	3.94[b] s
8-OMe	55.9 q	3.92[b] s
15-OMe	55.9 q	

a) Assignments are confirmed by 2D-COSY, HSQC, and HMBC experiments.
b) Interchangeable.

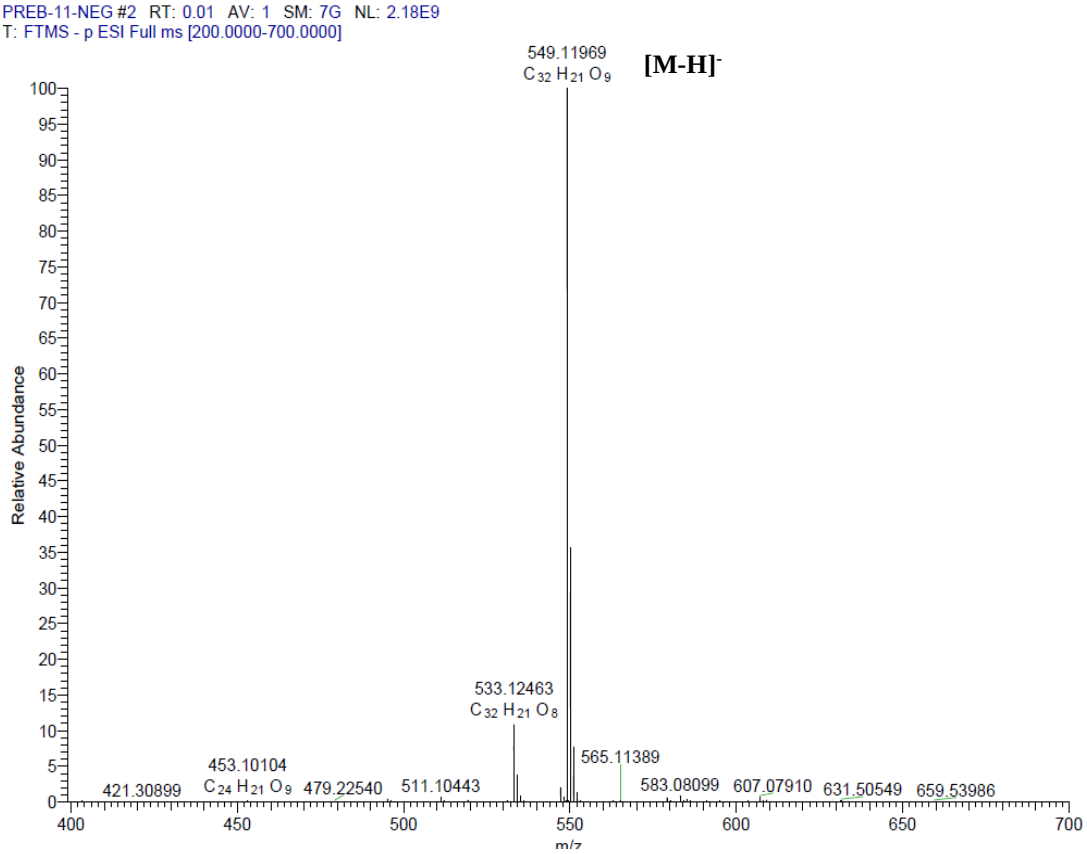

Spectrum 43. HR-ESI-MS Spectrum of PR-EB-11 (negative mode).

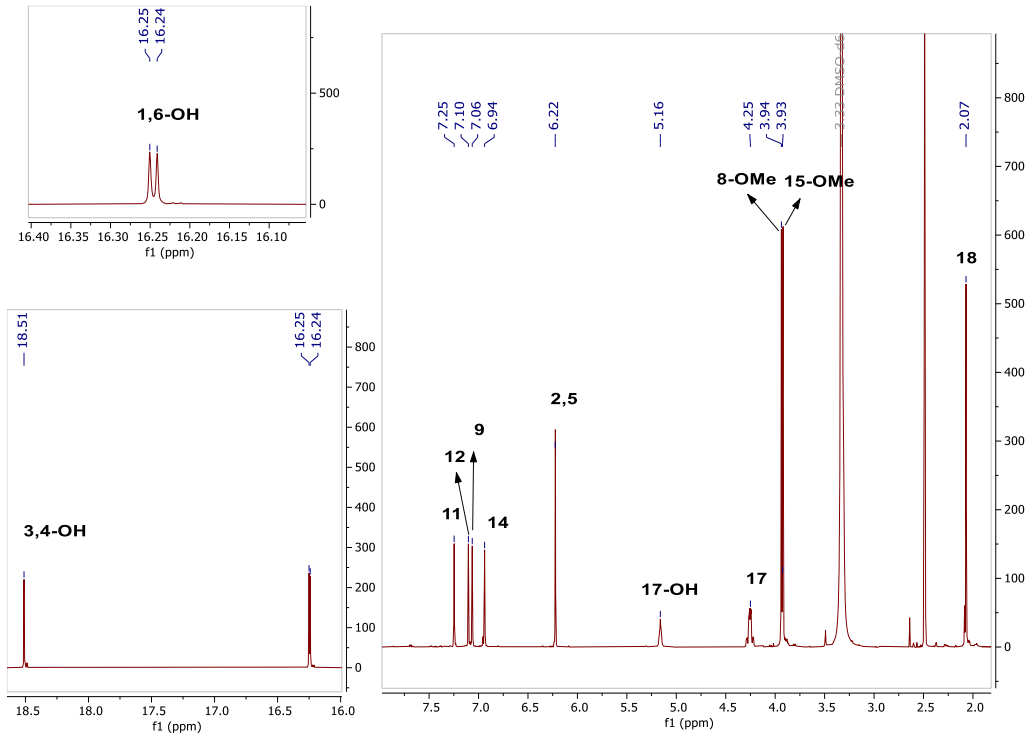

Spectrum 44. ^{1}H NMR Spectrum of PR-EB-11 (in DMSO-d6, ^{1}H: 500 MHz).

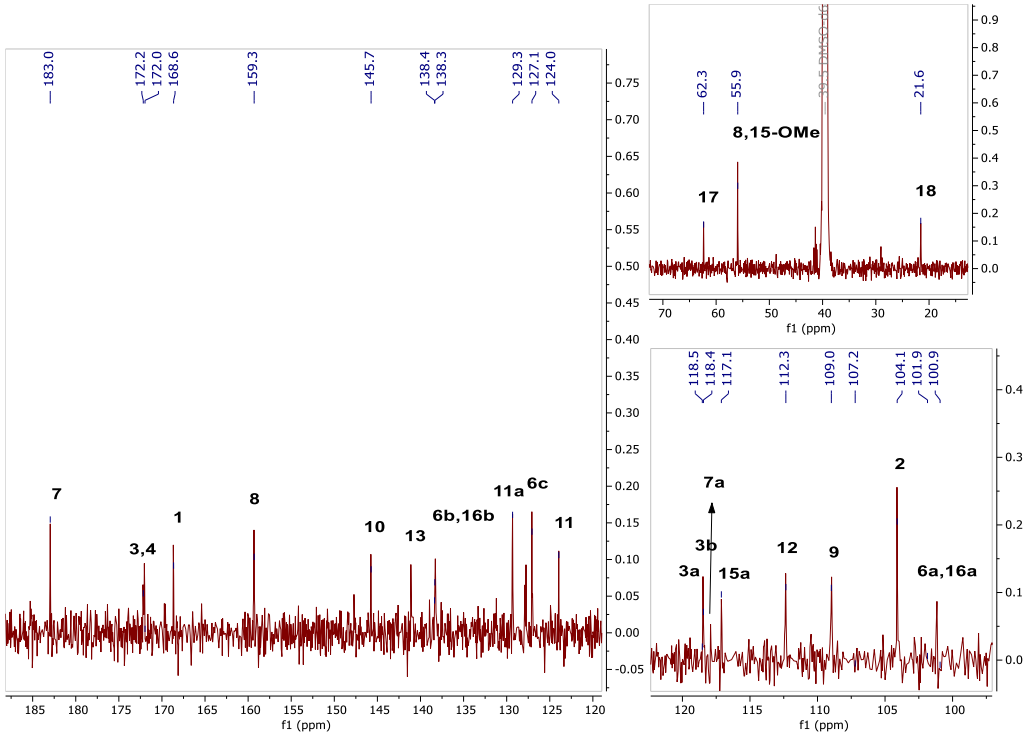

Spectrum 45. ^{13}C NMR Spectrum of PR-EB-11 (in DMSO-d6, ^{13}C:125 MHz).

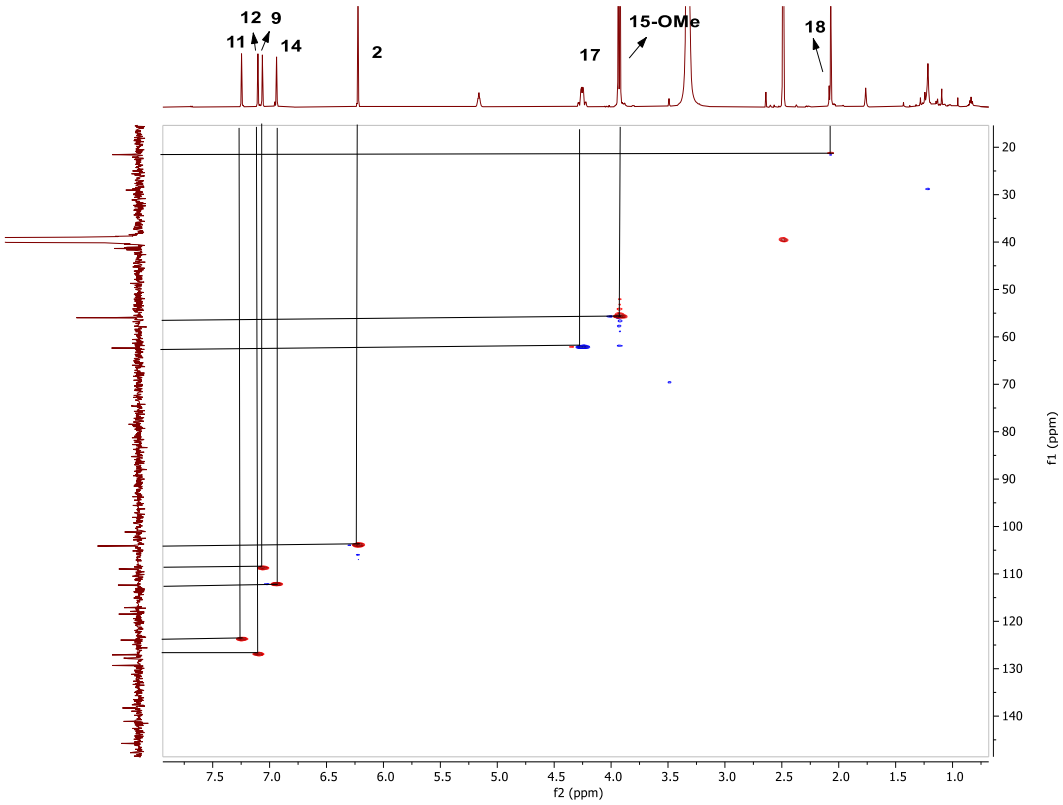

Spectrum 46. HSQC spectrum of PR-EB-11.

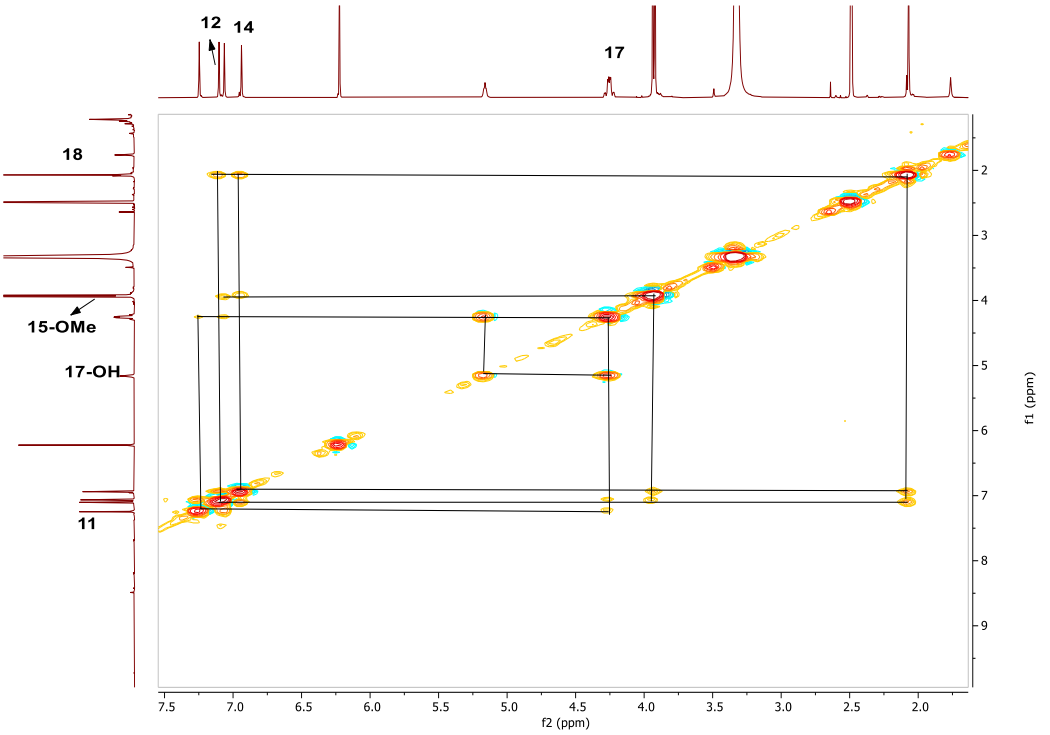

Spectrum 47. COSY spectrum of PR-EB-11.

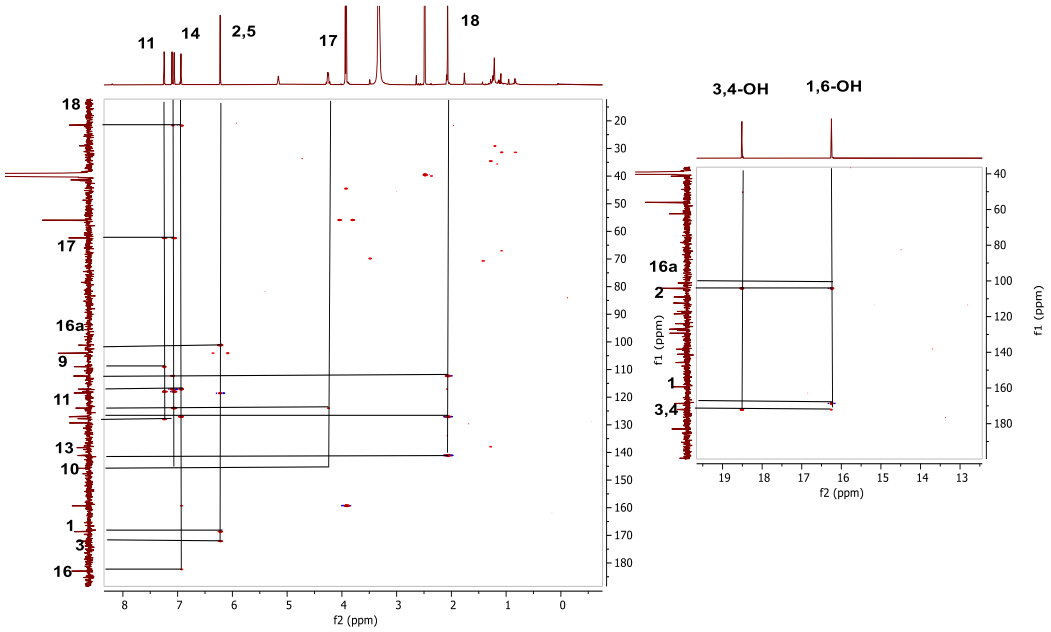

Spectrum 48. HMBC spectrum of PR-EB-11.

3.1.9. Structure Elucidation of PR-EB-17

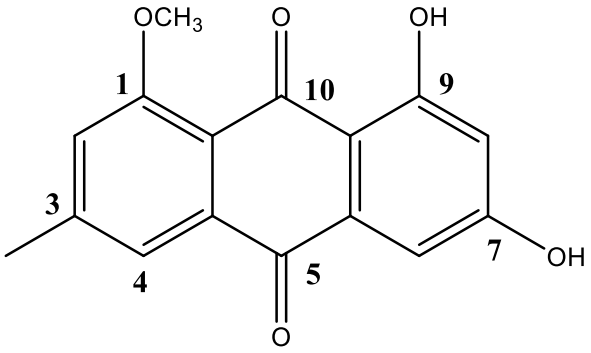

Chemical Formula: $C_{16}H_{12}O_5$
Exact Mass: 284,0685
Figure 20. Chemical structure of PR-EB-17.

The HR-ESI-MS spectrum of **PR-EB-17** exhibited a major ion peak at *m/z* 283.06140 $[M-H]^-$, (calcd. 283.1622) supported a molecular formula $C_{16}H_{12}O_6$ with eleven indices of hydrogen deficiency.

The ^1H- and ^{13}C NMR data of **PR-EB-17** (Table 14) revealed that it was another monomeric anthraquinone like **PR-EB-04** (Table 7). **PR-EB-17** had a 16 amu decrease compared to **PR-EB-04**, whereas the low-field resonance of primary alcohol group in

PR-EB-04 was missing. Instead, the appearance of a methyl group at δ 2.46 (s, H_2-11) and δ 21.7 (C-11) in the ^{1}H- and ^{13}C NMR spectra of **PR-EB-17** readily established the structure as 1,3-dihydroxy-8-methoxy-6-methylanthracene-9,10-dione, a known compound namely 1-O-methylemodin. The established structure was also confirmed by examining the 2D NMR spectra of **PR-EB-17** and comparing the data with previous reports (Ayer and Trifonov 1994).

Table 14. ^{1}H and ^{13}C NMR spectroscopic data of PR-EB-17, a) (in DMSO-d6, ^{1}H:500 MHz, ^{13}C:125 MHz)

Position	**δ_C (ppm)**	**δ_H (ppm), (J in Hz)**
1	160.6 s	-
2	119.8 d	7.43 d (1.5)
3	146.9 s	-
4	120.1 d	7.60 d (1.6)
4a	134.1 s	-
5	186.2 s	-
5a	110.0 s	-
6	107.2 d	7.03 d (2.4)
7	164.5 s	-
8	108.3 d	6.54 d (2.4)
9	164.5 s	-
9a	117.9 s	-
10	182.5 s	-
10a	134.6 s	-
11	21.7 q	2.46 s
1-OMe	56.5 q	3.93 s
7-OH	-	-
9-OH	-	13.28 s

a) Assignments are confirmed by 2D-COSY, HSQC, and HMBC experiments.

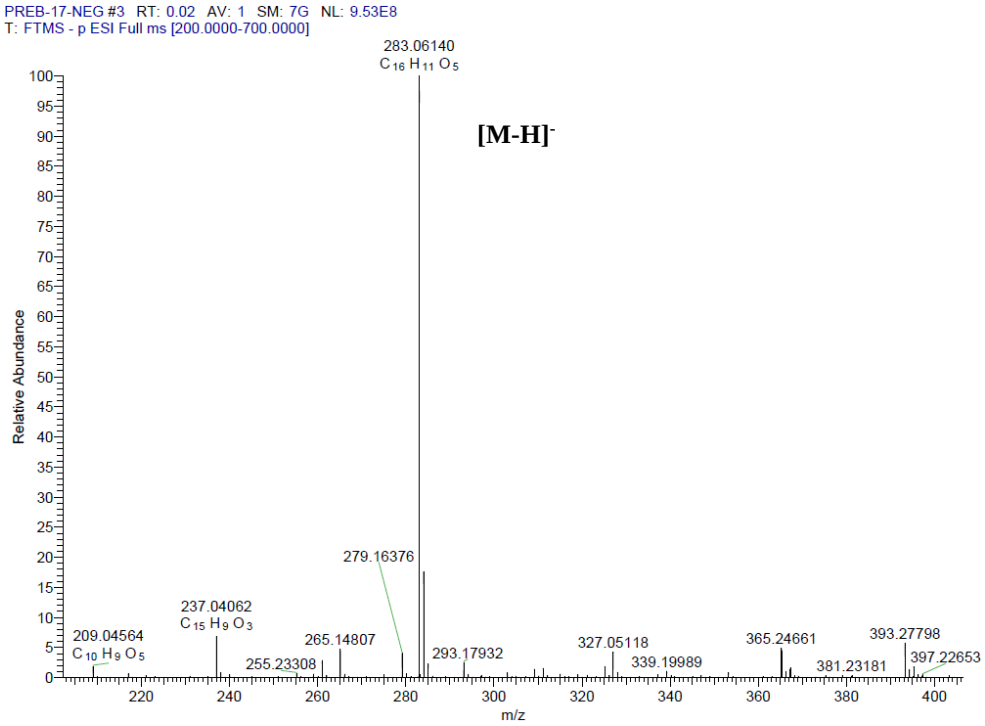

Spectrum 49. HR-ESI-MS Spectrum of PR-EB-17 (negative mode).

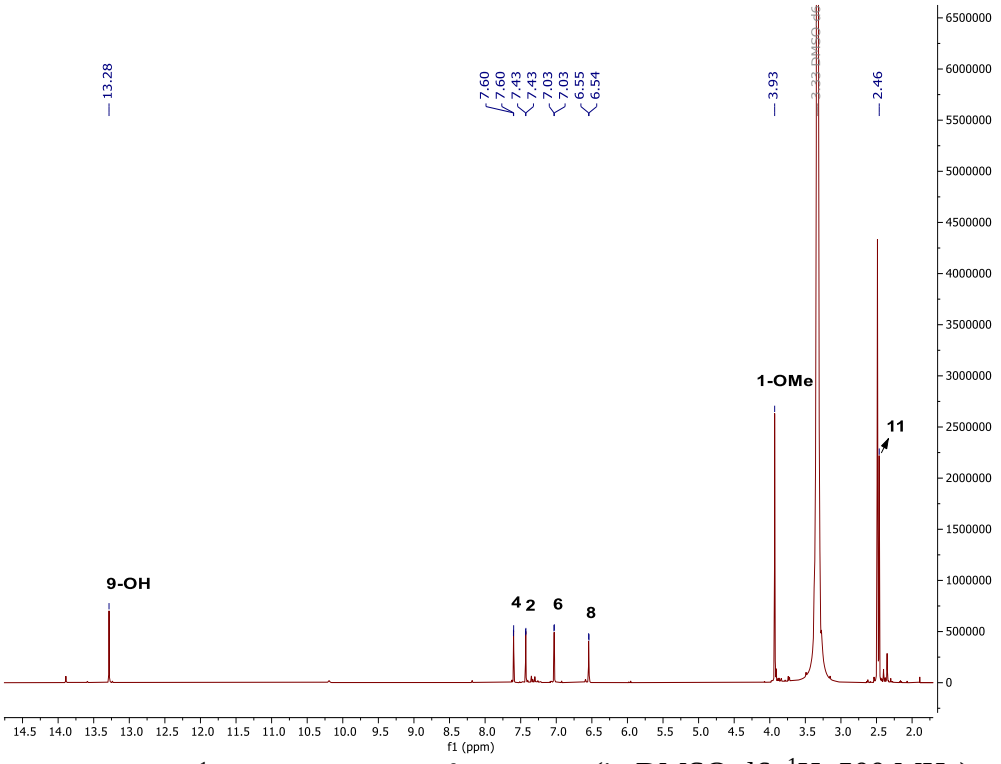

Spectrum 50. ^{1}H NMR Spectrum of PR-EB-17 (in DMSO-d6, ^{1}H: 500 MHz).

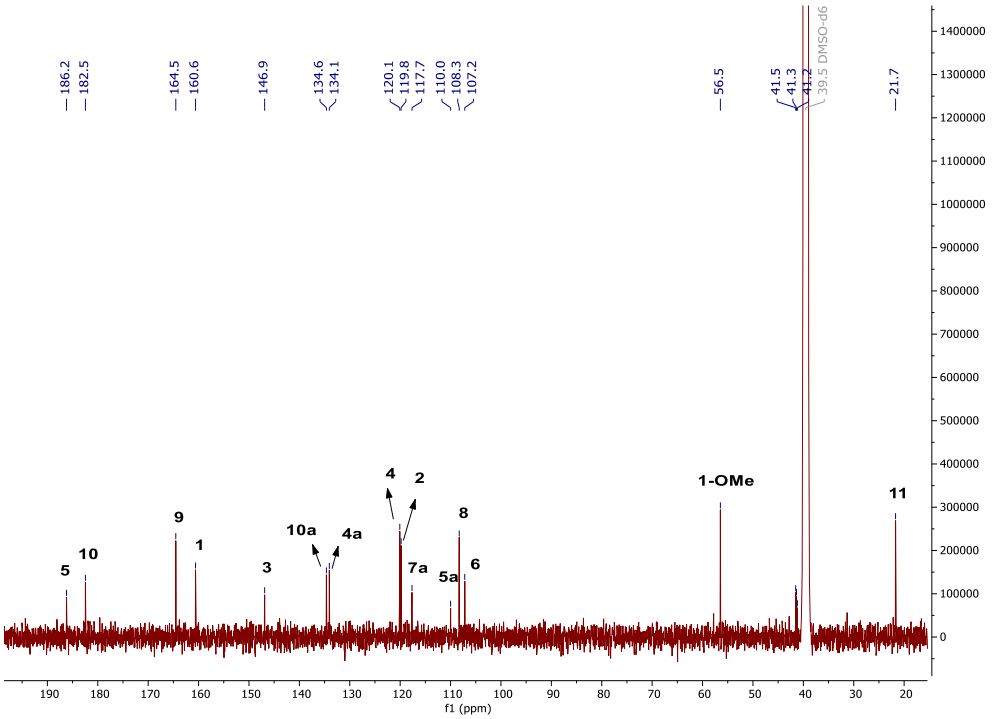

Spectrum 51. ^{13}C NMR Spectrum of PR-EB-17 (in DMSO-d6, ^{13}C:125 MHz).

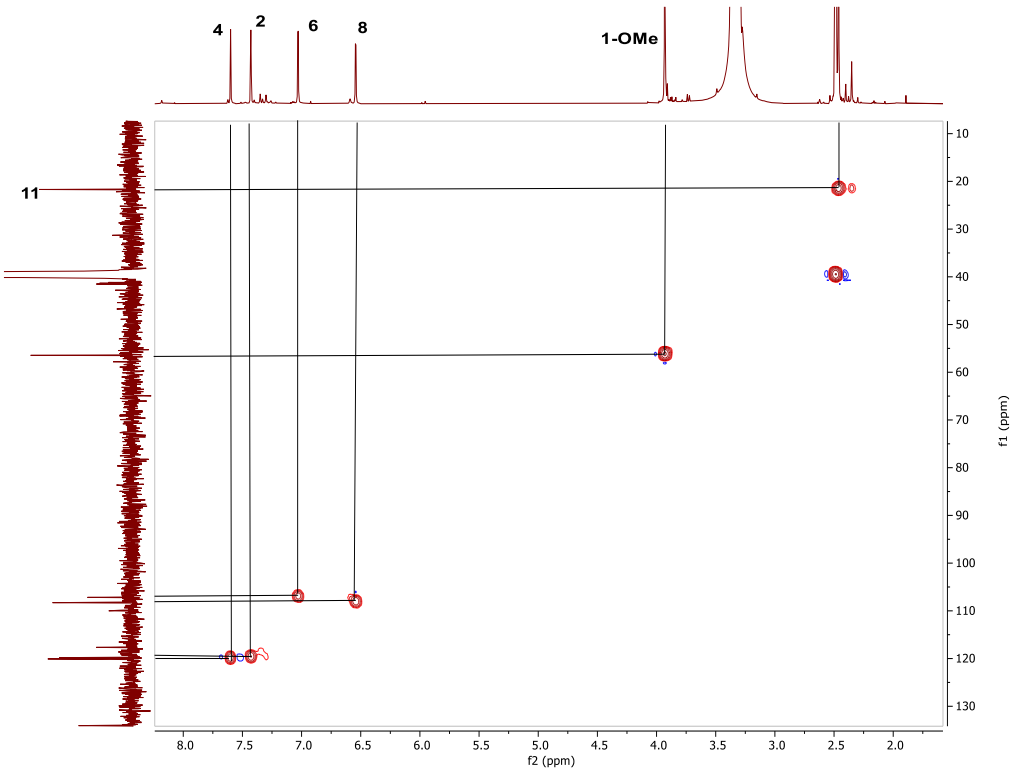

Spectrum 52. HSQC spectrum of PR-EB-17.

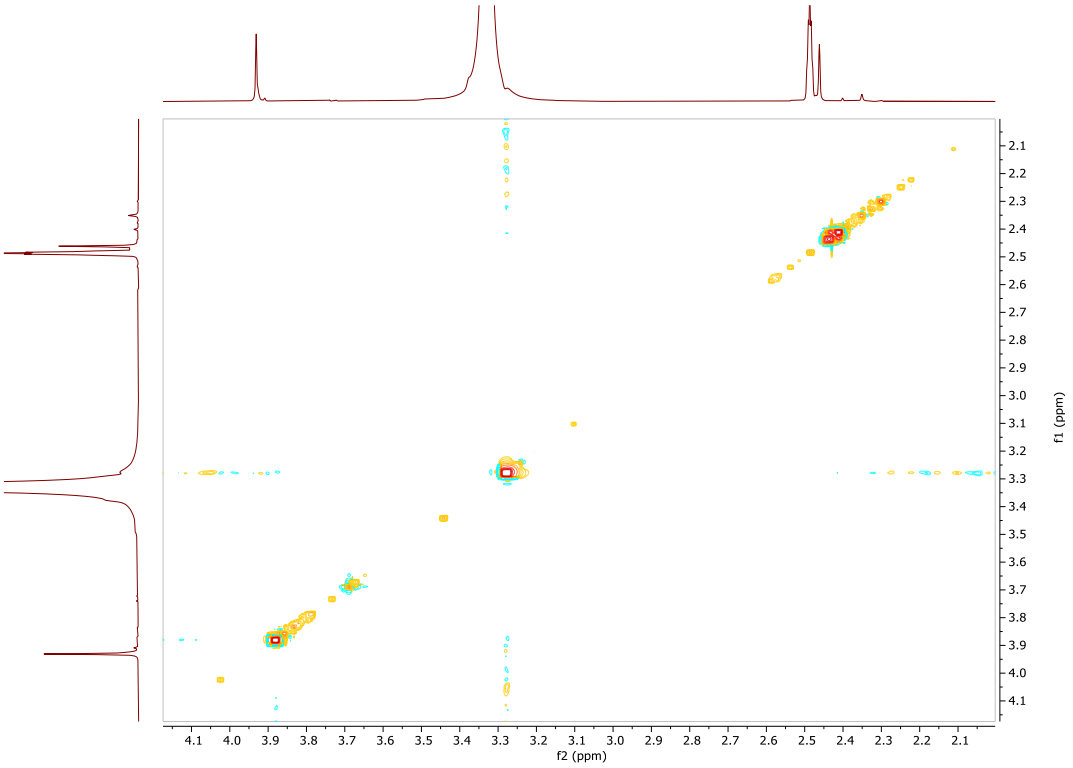

Spectrum 53. COSY spectrum of PR-EB-17.

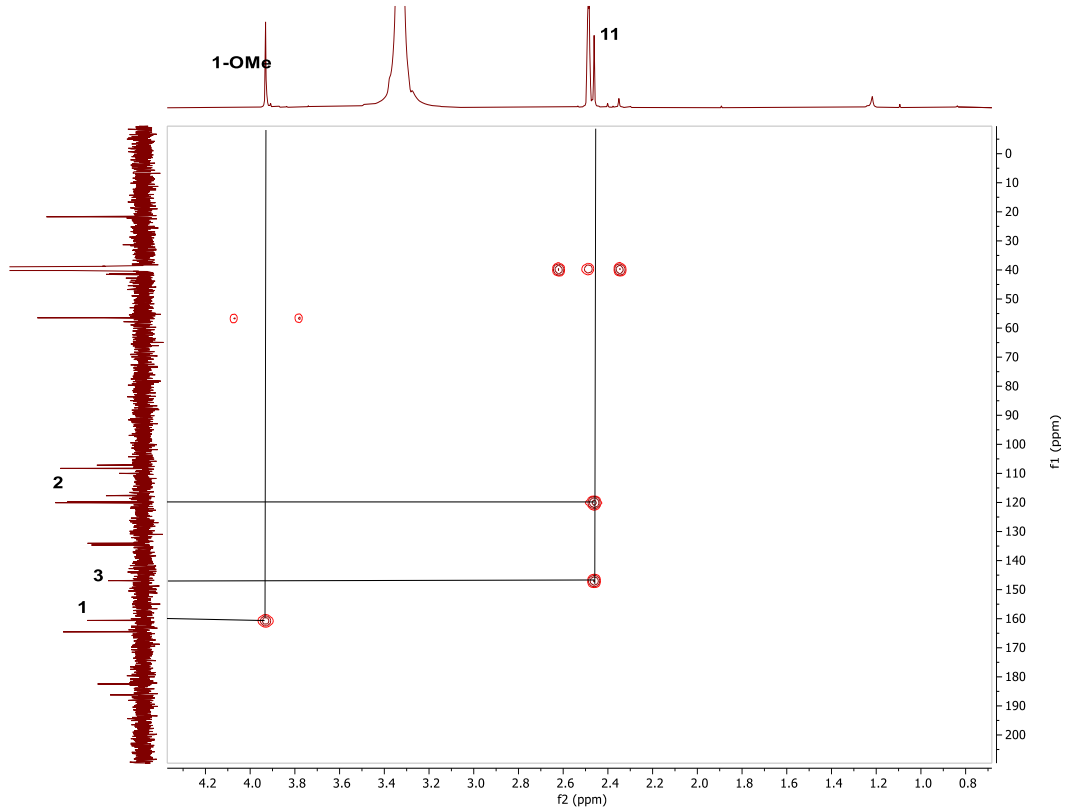

Spectrum 54. HMBC spectrum of PR-EB-17.

3.2. Results of bioactivity studies

The cytotoxic effects of all compounds and the EtOAc extract were investigated by MTT assay on three human prostate cell lines namely LNCap, PC3, Du145 and RPWE1. Cells were treated with different concentrations of the compounds for 48 h, and DMSO was used as control. Finally, the spectrophotometric absorbance was measured at wavelength of 590/690 nm. The data was analyzed by using GraphPad Prism to determine IC_{50} values of the compounds (Table 15).

Table 15. IC_{50} values of the isolated compounds.

	LNCaP	**PC3**	**Du145**	**RPWE-1**
PR-EB-01	26 μM	37.6 μM	24.7 μM	30.9 μM
PR-EB-03	>50 μM	>50 μM	>50 μM	ND
PR-EB-04	>50 μM	>50 μM	>50 μM	>50 μM
PR-EB-05	>50 μM	>50 μM	>50 μM	>50 μM
PR-EB-06	cytostatic	cytostatic	cytostatic	>50 μM
PR-EB-09	>50 μM	>50 μM	>50 μM	>50 μM
PR-EB-10	>50 μM	>50 μM	>50 μM	>50 μM
PR-EB-11	>50 μM	>50 μM	>50 μM	>50 μM
PR-EB-17	>50 μM	>50 μM	>50 μM	>50 μM
Extract	15 μg/ml	29.5 μg/ml	> 32 μg/ml	ND

3.2.1. Cytotoxic Activity Screening

The compounds except **PR-EB-01** did not show a promising cytotoxic effect (IC_{50} >50 μM). **PR-EB-01** exhibited cytotoxic effects towards all cell lines between 26 and 37.6 μM; however, its structurally close metabolite **PR-EB-06**, only revealed a cytostatic effect, preventing us from calculating the value of IC_{50} (Figures 21-24). Somehow, the presence of O-methyl group at C-11 position of **PR-EB-01** converts the cytostatic action of **PR-EB-06** into cytotoxic activity. This unexpected observation might be explained by physicochemical alterations that affect solubility, cell membrane penetration, distribution, the metabolization of the substance, or disturbing different target site(s)/pathway(s). Additionally, **PR-EB-01** was not selective towards human prostate cell lines. The selectivity between cancer cells and non-cancerous cells (therapeutic index) will be determined in due course.

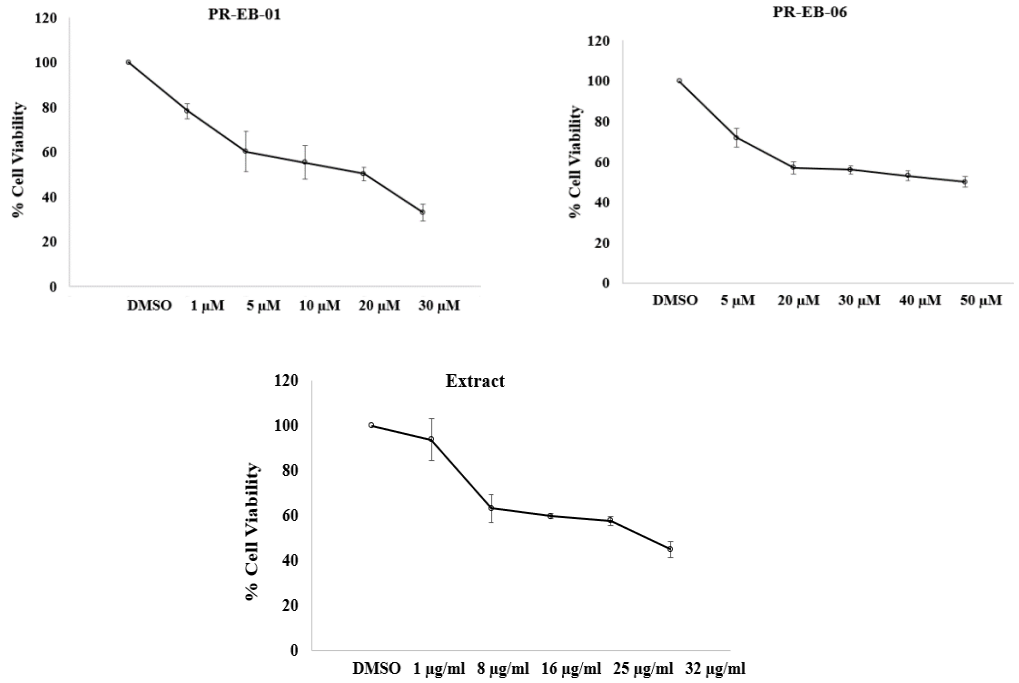

Figure 21. The cytotoxic effect of PR-EB-01, PR-EB-06 and the extract on the PC3 cell line at 48 h. Certain concentrations of compounds were subjected to wells in triplicate. DMSO is used as a control in all experiments. IC_{50} values were determined using GraphPad Prism.

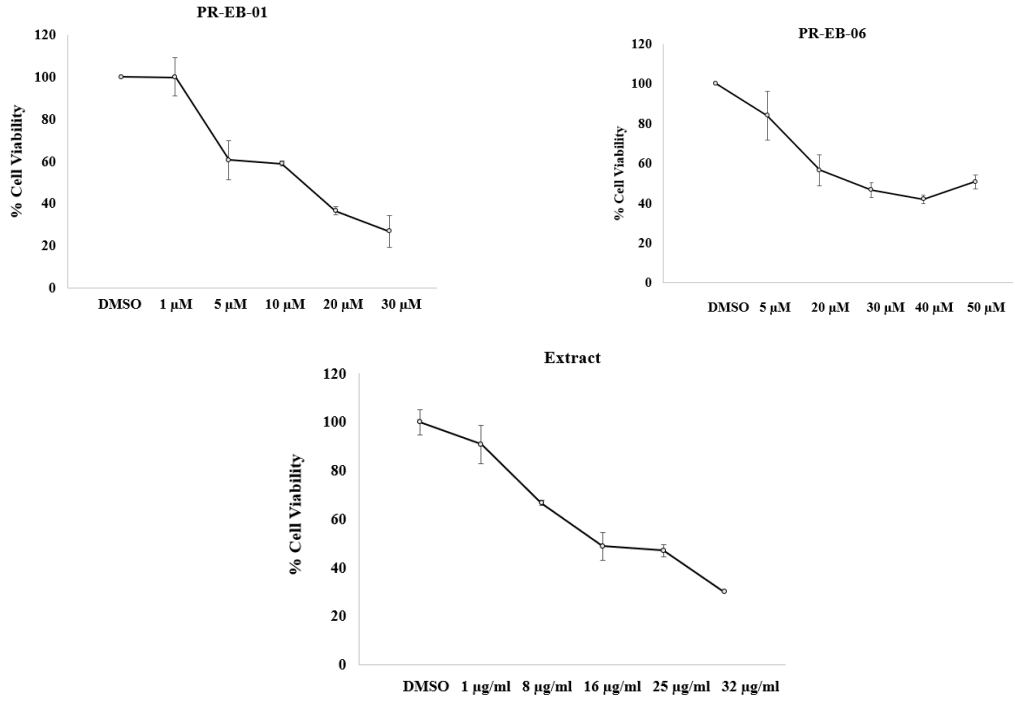

Figure 22. The cytotoxic effect of PR-EB-01, PR-EB-06 and the extract on the LNCaP cell line at 48 h. Certain concentrations of compounds were subjected to wells in triplicate. DMSO is used as a control in all experiments. IC_{50} values were determined using GraphPad Prism

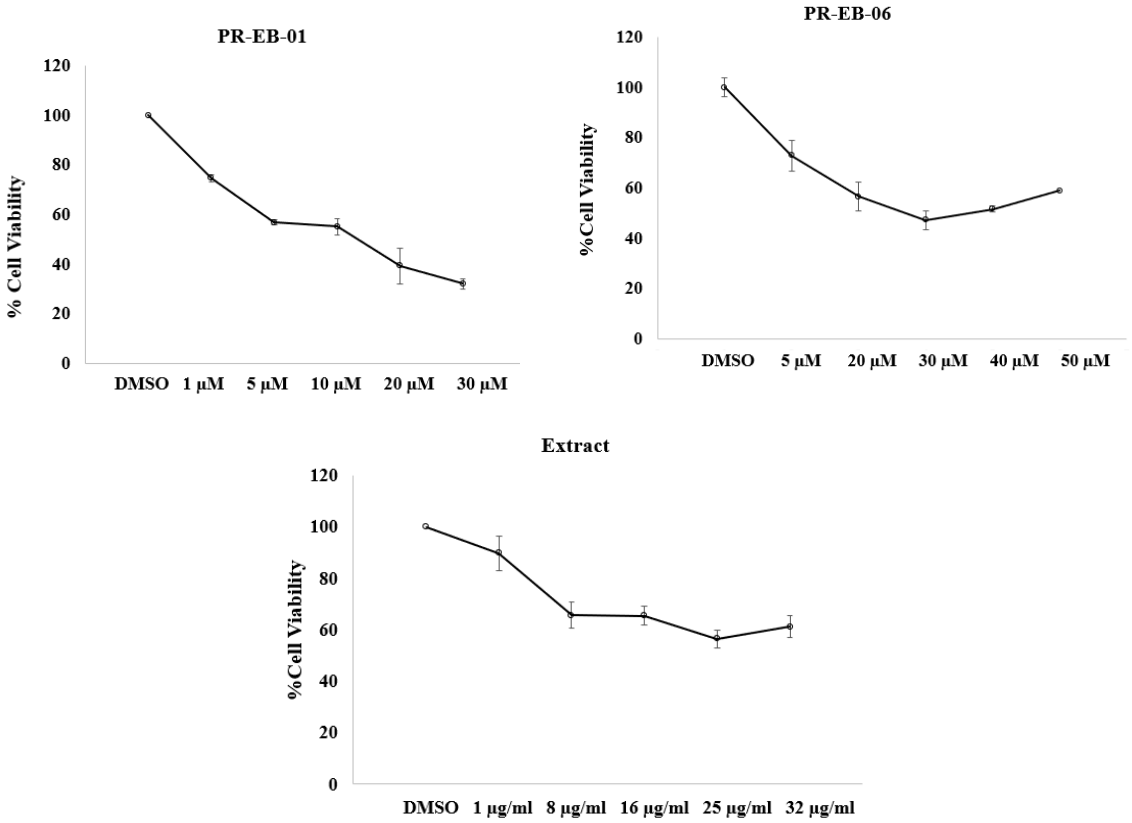

Figure 23. The cytotoxic effect of PR-EB-01, PR-EB-06 and the extract on the Du145 cell line at 48 h. Certain concentrations of compounds were subjected to wells in triplicate. DMSO is used as a control in all experiments. IC_{50} values were determined using GraphPad Prism.

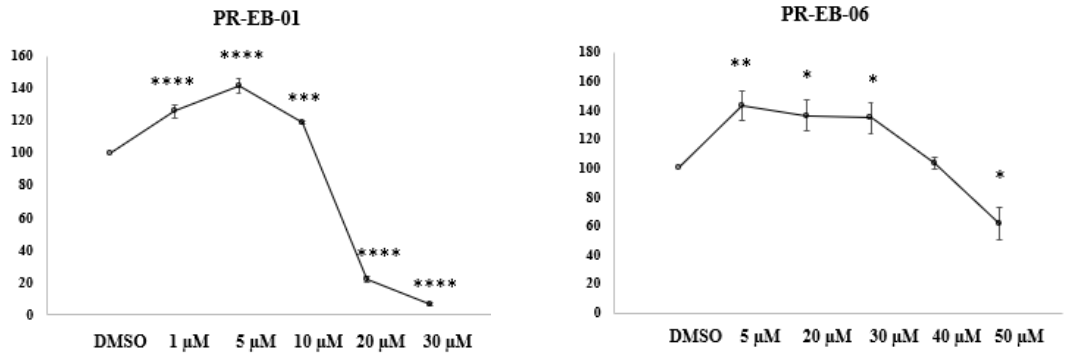

Figure 24. The cytotoxic effect of PR-EB-01 and PR-EB-06 on the RWPE-1 cell line at 48 h. Certain concentrations of compounds were subjected to wells in triplicate. DMSO is used as a control in all experiments. IC_{50} values were determined using GraphPad Prism.

The extract in a dose-dependent manner was as effective as **PR-EB-01** with similar IC_{50} values towards PC3 and LNCaP cell lines. In contrast, the extract exhibited lower activity IC_{50}> 32 μg/ml on the Du145 cell line, whereas **PR-EB-01** had an IC_{50} value of 24.7 μM. In the literature, **PR-EB-06** was reported to have cytotoxic activity against different cell lines (Shen et al. 2015); however, herein it was cytostatic. It somehow stopped the proliferation of all cell lines, as seen in Figures 21-24. According to the data given above, it was clear that the extract showed more consistent and significant results than most isolates. Thus, one should consider the possibility that the minor substances, which were not isolated during isolation studies due to their low amounts, would be contributing to the cytotoxic effect of the extract. In addition, none of the molecules possessing anthraquinone backbone showed activity on prostate cancer cell lines.

CHAPTER 4

CONCLUSION

The endophytic fungi are important microorganisms for producing a wide range of secondary metabolites. In the search for undescribed bioactive secondary metabolites, the endophytes are good candidates because of the biotic and abiotic factors to that they are exposed. These features lead to the biosynthesis of numerous and diverse compounds with a broad range of bioactivities. A previous study reported that 51% of biologically active compounds derived from endophytic fungi were previously unknown compounds (Strobel and Daisy 2003). As many natural products have been obtained, the potential of endophytic fungi has not yet been thoroughly examined to discover novel secondary metabolites, including *Penicillium* species.

This thesis, according to the data obtained from previous screening studies, aimed to isolate bioactive secondary metabolites from an endophytic fungus, namely *P. roseopurpureum* 1E4BS1. In fermentation cultures, the color of the broth changed after 20 days of incubation. According to the TLC results of the 7^{th} and 14^{th} days of EtOAc extracts, the primary molecule profile was not affected, while their amount increased. In the fermentation studies, the obtained broth was extracted with EtOAc, and the nine metabolites were isolated by chromatographic methods. The structures of the isolates were elucidated by spectral methods (1D-, 2D-NMR, and HR-ESI-MS). When the established structures were screened for novelty, five of them were turned out to be undescribed compounds. All the new compounds were anthraquinone-type metabolites. Additionally, the known compounds were identified as 11-methoxycurvularin (**PR-EB-01**, epimeric mixture), carviolin **(PR-EB-04)** (Aly et al. 2011; Elbanna et al. 2021), and 11-hydroxycurvularin (**PR-EB-06**, diastereoisomeric mixture) (Greve et al. 2008).

The compounds were screened by MTT assay for their cytotoxic effects against human prostate cancer cell lines. The macrolide **PR-EB-01** had the highest activity towards DU145, LNCaP, and PC3 cell lines, whereas the other macrolide **(PR-EB-06)** exhibited cytostatic effects. Moreover, **PR-EB-01** showed cytotoxicity in a dose-

dependent manner towards the RPWE-1 cell line with an IC_{50} value of 30.9 μM, so it was clear that **PR-EB-01** was not selective towards human prostate cell lines.

In addition, none of the anthraquinone molecules **(PR-EB-03, -04, -05, -09, -10, -11, and -17)** exhibited cytotoxic activity. From the structure-activity relationship point of view, observing the decisive activity difference between **PR-EB-01** and **PR-EB-06** was intriguing. This data implies that either the compounds target different site(s)/pathway(s) or their physicochemical character changes, affecting their solubility, cell membrane penetration, distribution, or metabolization properties. Further chemical (derivatization) and molecular mechanism studies are warranted to shed light on this issue.

REFERENCES

Abdelgaleil, S. A.M., M. M.G. Saad, N. R. Ariefta, and Y. Shiono. 2020. "Antimicrobial and Phytotoxic Activities of Secondary Metabolites from Haplophyllum Tuberculatum and Chrysanthemum Coronarium." *South African Journal of Botany* 128: 35–41. https://doi.org/10.1016/j.sajb.2019.10.005.

Alkhulaifi, Manal M., Amani S. Awaad, Hind A. AL-Mudhayyif, Monerah R. Alothman, Saleh I. Alqasoumi, and Sarah M. Zain. 2019. "Evaluation of Antimicrobial Activity of Secondary Metabolites of Fungi Isolated from Sultanate Oman Soil." *Saudi Pharmaceutical Journal* 27 (3): 401–5. https://doi.org/10.1016/j.jsps.2018.12.009.

Aly, Amal H., Abdessamad Debbab, Carol Clements, Ruangelie Edrada-Ebel, Barbora Orlikova, Marc Diederich, Victor Wray, Wenhan Lin, and Peter Proksch. 2011. "NF Kappa B Inhibitors and Antitrypanosomal Metabolites from Endophytic Fungus Penicillium Sp. Isolated from Limonium Tubiflorum." *Bioorganic and Medicinal Chemistry* 19 (1): 414–21. https://doi.org/10.1016/j.bmc.2010.11.012.

Assaf, Christelle El Hajj, Chrystian Zetina-Serrano, Nadia Tahtah, André el Khoury, Ali Atoui, Isabelle P. Oswald, Olivier Puel, and Sophie Lorber. 2020. "Regulation of Secondary Metabolism in the Penicillium Genus." *International Journal of Molecular Sciences* 21 (24): 1–26. https://doi.org/10.3390/ijms21249462.

Ayer, William A., and Latchezar S. Trifonov. 1994. "Anthraquinones and a 10-Hydroxyanthrone from Phialophora Alba." *Journal of Natural Products* 57 (2): 317–19. https://doi.org/10.1021/np50104a021.

Barrios-González, Javier. 2018. "Secondary Metabolites Production." *Current Developments in Biotechnology and Bioengineering*, 257–83. https://doi.org/10.1016/b978-0-444-63990-5.00013-x.

Bills, Gerald F., and James B. Gloer. 2016. "Biologically Active Secondary Metabolites from the Fungi." *Microbiology Spectrum* 4 (6). https://doi.org/10.1128/microbiolspec.funk-0009-2016.

2017. "Biologically Active Secondary Metabolites from the Fungi." *The Fungal Kingdom*, 1087–1119. https://doi.org/10.1128/9781555819583.ch54.

Bond, Carly, Yi Tang, and Li Li. 2016. “Saccharomyces Cerevisiae as a Tool for Mining, Studying and Engineering Fungal Polyketide Synthases.” *Fungal Genetics and Biology* 89 (April): 52–61. https://doi.org/10.1016/j.fgb.2016.01.005.

Brakhage, Axel A. 2013. “Regulation of Fungal Secondary Metabolism.” *Nature Reviews Microbiology* 11 (1): 21–32. https://doi.org/10.1038/nrmicro2916.

Brown, Alian G, Terry C Srnale, Trevor J King, Rainer Hasenkamp, and Ronald H Thompson. n.d. “Crystal and Molecular Structure of Compactin, a New Antifungal Meta-Bol Ite f Rorn Penicillium Brevicompactum.”

Chomel, Mathilde, Marie Guittonny-Larchevêque, Catherine Fernandez, Christiane Gallet, Annie DesRochers, David Paré, Benjamin G. Jackson, and Virginie Baldy. 2016. “Plant Secondary Metabolites: A Key Driver of Litter Decomposition and Soil Nutrient Cycling.” *Journal of Ecology* 104 (6): 1527–41. https://doi.org/10.1111/1365-2745.12644.

Cisneros-Zevallos, Luis. 2021. “The Power of Plants: How Fruit and Vegetables Work as Source of Nutraceuticals and Supplements.” *International Journal of Food Sciences and Nutrition* 72 (5): 660–64. https://doi.org/10.1080/09637486.2020.1852194.

Cox, Russell J. 2007. “Polyketides, Proteins and Genes in Fungi: Programmed Nano-Machines Begin to Reveal Their Secrets.” *Organic and Biomolecular Chemistry* 5 (13): 2010–26. https://doi.org/10.1039/b704420h.

Cox, Russell J., Elizabeth Skellam, and Katherine Williams. 2018. “Biosynthesis of Fungal Polyketides.” In *Physiology and Genetics*, 385–412. Springer International Publishing. https://doi.org/10.1007/978-3-319-71740-1_13.

Daley, D. K., K. J. Brown, and S. Badal. 2017. *Fungal Metabolites*. *Pharmacognosy: Fundamentals, Applications and Strategy*. Elsevier Inc. https://doi.org/10.1016/B978-0-12-802104-0.00020-2.

Daniel, Stephen H. 2007. “Introduction.” *Reexamining Berkeley’s Philosophy*, 3–10. https://doi.org/10.5422/fordham/9780823251278.003.0001.

Demain, A. L., and A. Fang. 2000. “The Natural Functions of Secondary Metabolites.” *Advances in Biochemical Engineering/Biotechnology* 69: 1–39. https://doi.org/10.1007/3-540-44964-7_1.

Deng, Zhangshuang, Aiping Deng, Dan Luo, Dachun Gong, Kun Zou, Yan Peng, and Zhiyong Guo. 2015. “Biotransformation of (-)-(10E,15S)-10,11-

Dehydrocurvularin." *Natural Product Communications* 10 (7): 1277–78. https://doi.org/10.1177/1934578x1501000735.

Dreyfuss, M. M., and I. H. Chapela. 1994. "Potential of Fungi in the Discovery of Novel, Low-Molecular Weight Pharmaceuticals." *Biotechnology (Reading, Mass.)*. https://doi.org/10.1016/b978-0-7506-9003-4.50009-5.

"EF as a Source." n.d.

Elbanna, Ahmed H., Zeinab G. Khalil, Paul v. Bernhardt, and Robert J. Capon. 2021. "Neobulgarones Revisited: Anti and Syn Bianthrones from an Australian Mud Dauber Wasp Nest-Associated Fungus, Penicillium Sp. CMB-MD22." *Journal of Natural Products* 84 (3): 762–70. https://doi.org/10.1021/acs.jnatprod.0c01035.

Fleming, Alexander. 1929. "A. Fleming,1929- Antibacterial Action of Cultures of a Penicillium.Pdf." *The British Journal of Experimental Pathology*.

Frisvad, Jens C, Jørn Smedsgaard, Thomas O Larsen, and Robert A Samson. 2004. "Mycotoxins, Drugs and Other Extrolites Produced by Species in Penicillium Subgenus Penicillium." *IN MYCOLOGY*. Vol. 49.

Gaber, Yasser, Sophanit Mekasha, Gustav Vaaje-Kolstad, Vincent G.H. Eijsink, and Marco W. Fraaije. 2016. "Characterization of a Chitinase from the Cellulolytic Actinomycete Thermobifida Fusca." *Biochimica et Biophysica Acta - Proteins and Proteomics* 1864 (9): 1253–59. https://doi.org/10.1016/j.bbapap.2016.04.010.

Gloer, J B. n.d. "5 Applications of Fungal Ecology in the Search for New Bioactive Natural Products."

Greve, Hendrik, Peter J. Schupp, Ekaterina Eguereva, Stefan Kehraus, Gerhard Kelter, Armin Maier, Heinz Herbert Fiebig, and Gabriele M. König. 2008. "Apralactone A and a New Stereochemical Class of Curvularins from the Marine Fungus Curvularia Sp." *European Journal of Organic Chemistry*, no. 30 (October): 5085–92. https://doi.org/10.1002/ejoc.200800522.

Grijseels, Sietske, Jens Christian Nielsen, Jens Nielsen, Thomas Ostenfeld Larsen, Jens Christian Frisvad, Kristian Fog Nielsen, Rasmus John Normand Frandsen, and Mhairi Workman. 2017. "Physiological Characterization of Secondary Metabolite Producing Penicillium Cell Factories." *Fungal Biology and Biotechnology* 4 (1): 1–12. https://doi.org/10.1186/s40694-017-0036-z.

Gupta, Shubhpriya, Preeti Chaturvedi, Manoj G. Kulkarni, and Johannes van Staden. 2020. "A Critical Review on Exploiting the Pharmaceutical Potential of Plant

Endophytic Fungi." *Biotechnology Advances* 39 (May 2019): 107462. https://doi.org/10.1016/j.biotechadv.2019.107462.

Ha, Tran Minh, Wonmin Ko, Seung Jun Lee, Youn Chul Kim, Jae Young Son, Jae Hak Sohn, Joung Han Yim, and Hyuncheol Oh. 2017. "Anti-Inflammatory Effects of Curvularin-Type Metabolites from a Marine-Derived Fungal Strain Penicillium Sp. SF-5859 in Lipopolysaccharide-Induced RAW264.7 Macrophages." *Marine Drugs* 15 (9). https://doi.org/10.3390/md15090282.

Habtemariam, Solomon. 2019. "Introduction to Plant Secondary Metabolites—From Biosynthesis to Chemistry and Antidiabetic Action." In *Medicinal Foods as Potential Therapies for Type-2 Diabetes and Associated Diseases*, 109–32. Elsevier. https://doi.org/10.1016/b978-0-08-102922-0.00006-7.

He, Yi, Bin Wang, Wanping Chen, Russell J. Cox, Jingren He, and Fusheng Chen. 2018. "Recent Advances in Reconstructing Microbial Secondary Metabolites Biosynthesis in Aspergillus Spp." *Biotechnology Advances* 36 (3): 739–83. https://doi.org/10.1016/j.biotechadv.2018.02.001.

Hoffmeister, Dirk, and Nancy P. Keller. 2007. "Natural Products of Filamentous Fungi: Enzymes, Genes, and Their Regulation." *Natural Product Reports* 24 (2): 393–416. https://doi.org/10.1039/b603084j.

Hohlman, Robert M., and David H. Sherman. 2021. "Recent Advances in Hapalindole-Type Cyanobacterial Alkaloids: Biosynthesis, Synthesis, and Biological Activity." *Natural Product Reports*. Royal Society of Chemistry. https://doi.org/10.1039/d1np00007a.

Jamloki, Abhishek, Malini Bhattacharyya, M. C. Nautiyal, and Babita Patni. 2021. "Elucidating the Relevance of High Temperature and Elevated CO2 in Plant Secondary Metabolites (PSMs) Production." *Heliyon* 7 (8): e07709. https://doi.org/10.1016/j.heliyon.2021.e07709.

Jouda, Jean Bosco, Jean de Dieu Tamokou, Céline Djama Mbazoa, Prodipta Sarkar, Prasanta Kumar Bag, and Jean Wandji. 2016. "Anticancer and Antibacterial Secondary Metabolites from the Endophytic Fungus Penicillium Sp. CAM64 against Multi-Drug Resistant Gram-Negative Bacteria." *African Health Sciences* 16 (3): 734–43. https://doi.org/10.4314/ahs.v16i3.13.

Keller, Nancy P. 2019. “Fungal Secondary Metabolism: Regulation, Function and Drug Discovery.” *Nature Reviews Microbiology* 17 (3): 167–80. https://doi.org/10.1038/s41579-018-0121-1.

Khan, Abid Ali, Nafees Bacha, Bashir Ahmad, Ghosia Lutfullah, Umar Farooq, and Russell John Cox. 2014. “Fungi as Chemical Industries and Genetic Engineering for the Production of Biologically Active Secondary Metabolites.” *Asian Pacific Journal of Tropical Biomedicine* 4 (11): 859–70. https://doi.org/10.12980/APJTB.4.2014APJTB-2014-0230.

Kopp, Florian, and Mohamed A. Marahiel. 2007. “Macrocyclization Strategies in Polyketide and Nonribosomal Peptide Biosynthesis.” *Natural Product Reports*. https://doi.org/10.1039/b613652b.

Kozlovsky, A. G., G. A. Kochkina, V. P. Zhelifonova, V. Antipova, N. E. Ivanushkina, and S. M. Ozerskaya. 2020. “Secondary Metabolites of the Genus Penicillium from Undisturbed and Anthropogenically Altered Antarctic Habitats.” *Folia Microbiologica* 65 (1): 95–102. https://doi.org/10.1007/s12223-019-00708-0.

Kumar, Avnish, Monika Asthana, Ankur Gupta, Darshika Nigam, and Surabhi Mahajan. 2017a. *Secondary Metabolism and Antimicrobial Metabolites of Penicillium*. *New and Future Developments in Microbial Biotechnology and Bioengineering: Penicillium System Properties and Applications*. Elsevier B.V. https://doi.org/10.1016/B978-0-444-63501-3.00003-X.

2017b. “Secondary Metabolism and Antimicrobial Metabolites of Penicillium.” In *New and Future Developments in Microbial Biotechnology and Bioengineering: Penicillium System Properties and Applications*, 47–68. Elsevier. https://doi.org/10.1016/B978-0-444-63501-3.00003-X.

Liang, Qiren, Yongquan Sun, Binxun Yu, Xuegong She, and Xinfu Pan. 2007. “First Total Syntheses and Spectral Data Corrections of 11-α- Methoxycurvularin and 11-β-Methoxycurvularin.” *Journal of Organic Chemistry* 72 (25): 9846–49. https://doi.org/10.1021/jo701885n.

Ma, Chuanteng, Kaijin Zhang, Xianyan Zhang, Guowei Liu, Tianjiao Zhu, Qian Che, Dehai Li, and Guojian Zhang. 2021. “Heterologous Expression and Metabolic Engineering Tools for Improving Terpenoids Production.” *Current Opinion in Biotechnology*. Elsevier Ltd. https://doi.org/10.1016/j.copbio.2021.02.008.

Macheleidt, Juliane, Derek J. Mattern, Juliane Fischer, Tina Netzker, Jakob Weber, Volker Schroeckh, Vito Valiante, and Axel A. Brakhage. 2016. “Regulation and Role of Fungal Secondary Metabolites.” *Annual Review of Genetics* 50 (September): 371–92. https://doi.org/10.1146/annurev-genet-120215-035203.

Marinelli, Flavia, and Giorgia Letizia Marcone. 2019. *Microbial Secondary Metabolites*. *Comprehensive Biotechnology*. Third Edit. Vol. 3. Elsevier. https://doi.org/10.1016/B978-0-444-64046-8.00168-3.

Mazumder, Kishor, Yasmeen Nazim Ruma, Rasheda Akter, Asma Aktar, Mir Monir Hossain, Zinnat Shahina, Santosh Mazumdar, and Philip G. Kerr. 2021. “Identification of Bioactive Metabolites and Evaluation of in Vitro Anti-Inflammatory and in Vivo Antinociceptive and Antiarthritic Activities of Endophyte Fungi Isolated from Elaeocarpus Floribundus Blume.” *Journal of Ethnopharmacology* 273 (September 2020): 113975. https://doi.org/10.1016/j.jep.2021.113975.

Mosunova, Olga, Jorge C Navarro-Muñoz, and Jérôme Collemare. 2020. “The Biosynthesis of Fungal Secondary Metabolites: From Fundamentals to Biotechnological Applications.” *Reference Module in Life Sciences*, 1–19. https://doi.org/10.1016/b978-0-12-809633-8.21072-8.

Narmani, Abolfazl, Rémy Bertrand Teponno, Mahdi Arzanlou, Frank Surup, Soleiman E. Helaly, Kathrin Wittstein, Dimas F. Praditya, Asadollah Babai-Ahari, Eike Steinmann, and Marc Stadler. 2019. “Cytotoxic, Antimicrobial and Antiviral Secondary Metabolites Produced by the Plant Pathogenic Fungus Cytospora Sp. CCTU A309.” *Fitoterapia* 134 (February): 314–22. https://doi.org/10.1016/j.fitote.2019.02.015.

Newman, David J., and Gordon M. Cragg. 2020. “Natural Products as Sources of New Drugs over the Nearly Four Decades from 01/1981 to 09/2019.” *Journal of Natural Products* 83 (3): 770–803. https://doi.org/10.1021/acs.jnatprod.9b01285.

Ogbe, Abdulazeez A., Jeffrey F. Finnie, and Johannes van Staden. 2020a. “The Role of Endophytes in Secondary Metabolites Accumulation in Medicinal Plants under Abiotic Stress.” *South African Journal of Botany* 134: 126–34. https://doi.org/10.1016/j.sajb.2020.06.023.

2020b. “The Role of Endophytes in Secondary Metabolites Accumulation in Medicinal Plants under Abiotic Stress.” *South African Journal of Botany* 134 (November): 126–34. https://doi.org/10.1016/j.sajb.2020.06.023.

Oxford, Albert Edward, Harold Raistrick, and Paul Simonart. n.d. “XXIX. STUDIES IN THE BIOCHEMISTRY ,OF MICRO-ORGANISMS LX. GRISEOFULVIN, C17H1706CI, A METABOLIC PRODUCT OF PENICILLIUM GRISEO-FULVUM DIERCKX.”

Patil, Ravindra H., Mohini P. Patil, and Vijay Laxminarayan Maheshwari. 2016. “Bioactive Secondary Metabolites From Endophytic Fungi: A Review of Biotechnological Production and Their Potential Applications.” *Studies in Natural Products Chemistry* 49: 189–205. https://doi.org/10.1016/B978-0-444-63601-0.00005-3.

Rajagopal, Kalyanaraman, Meenambiga Ss, and ; Arulmathi. n.d. “Endophytic Fungi, A Versatile Organism for Modern Microbiological Research and Industrial Applications Chapter 4 Current Research in Microbiology.” www.openaccessebooks.com.

Rajagopal, Kalyanarman, Meenambiga SS, and Arulmathi R. 2019. “Endophytic Fungi , A Versatile Organism for Modern Microbiological Research And.” *Current Research in Microbiology*, 1–13. http://www.openaccessebooks.com/current-research-in-microbiology/endophytic-fungi-a-versatile-organism-for-modern-microbiological-research-and-industrial-applications.pdf.

Ramakrishna, Wusirika, Anuradha Kumari, Nafeesa Rahman, and Pallavi Mandave. 2021. “Anticancer Activities of Plant Secondary Metabolites: Rice Callus Suspension Culture as a New Paradigm.” *Rice Science* 28 (1): 13–30. https://doi.org/10.1016/j.rsci.2020.11.004.

Regueira, Torsten Bak, Kanchana Rueksomtawin Kildegaard, Bjarne Gram Hansen, Uffe H. Mortensen, Christian Hertweck, and Jens Nielsen. 2011. “Molecular Basis for Mycophenolic Acid Biosynthesis in Penicillium Brevicompactum.” *Applied and Environmental Microbiology* 77 (9): 3035–43. https://doi.org/10.1128/AEM.03015-10.

Rokas, Antonis, Matthew E. Mead, Jacob L. Steenwyk, Huzefa A. Raja, and Nicholas H. Oberlies. 2020. “Biosynthetic Gene Clusters and the Evolution of Fungal

Chemodiversity." *Natural Product Reports* 37 (7): 868–78. https://doi.org/10.1039/c9np00045c.

Sanchez, Sergio, and Arnold L. Demain. 2019. "Secondary Metabolites." *Comprehensive Biotechnology* 1 (1): 131–43. https://doi.org/10.1016/B978-0-444-64046-8.00012-4.

Schläger, Sabrina, and Birgit Dräger. 2016. "Exploiting Plant Alkaloids." *Current Opinion in Biotechnology*. Elsevier Ltd. https://doi.org/10.1016/j.copbio.2015.12.003.

Shen, Weiyun, Hongqiang Mao, Qian Huang, and Jinyan Dong. 2015. "Benzenediol Lactones: A Class of Fungal Metabolites with Diverse Structural Features and Biological Activities." *European Journal of Medicinal Chemistry*. Elsevier Masson SAS. https://doi.org/10.1016/j.ejmech.2014.11.067.

Siddhardha, Busi, and Himani Meena. 2020. *Microbial Secondary Metabolites: Natural Benediction Elements for Plants During Abiotic and Biotic Stress Conditions*. *Microbial Services in Restoration Ecology*. Elsevier Inc. https://doi.org/10.1016/b978-0-12-819978-7.00007-5.

Singh, Archana, Dheeraj K. Singh, Ravindra N. Kharwar, James F. White, and Surendra K. Gond. 2021a. "Fungal Endophytes as Efficient Sources of Plant-Derived Bioactive Compounds and Their Prospective Applications in Natural Product Drug Discovery: Insights, Avenues, and Challenges." *Microorganisms* 9 (1): 1–42. https://doi.org/10.3390/microorganisms9010197.

2021b. "Fungal Endophytes as Efficient Sources of Plant-Derived Bioactive Compounds and Their Prospective Applications in Natural Product Drug Discovery: Insights, Avenues, and Challenges." *Microorganisms*. MDPI AG. https://doi.org/10.3390/microorganisms9010197.

Strobel, Gary, and Bryn Daisy. 2003. "Bioprospecting for Microbial Endophytes and Their Natural Products." *Microbiology and Molecular Biology Reviews* 67 (4): 491–502. https://doi.org/10.1128/mmbr.67.4.491-502.2003.

Tallapragada, Padmavathi, and Rashmi Dikshit. 2017. *Microbial Production of Secondary Metabolites as Food Ingredients*. *Microbial Production of Food Ingredients and Additives*. Elsevier Inc. https://doi.org/10.1016/b978-0-12-811520-6.00011-8.

Tez, Doktora, Tez Dan, Erdal Bed, and Elif Esin Hame. 2016. “Septofusidium Berolinense ’ NİN BİYOAKTİF SEKONDER METABOLİT İÇERİĞİNİN.”

Thirumalanadhun, Vasavi, Lavanya Latha Yerraguravagari, Uma Maheswari, and Devi Palempalli. 2021. *Endophytic Microflora : The Fountainhead of Anticancer Metabolites — A Systematic Review*. *Recent Developments in Applied Microbiology and Biochemistry*. Elsevier Inc. https://doi.org/10.1016/B978-0-12-821406-0.00002-3.

Thirumurugan, Durairaj, Alagappan Cholarajan, Suresh S.S. Raja, and Ramasamy Vijayakumar. 2018a. “An Introductory Chapter: Secondary Metabolites.” *Secondary Metabolites - Sources and Applications*, 3–22. https://doi.org/10.5772/intechopen.79766.

2018b. “An Introductory Chapter: Secondary Metabolites.” *Secondary Metabolites - Sources and Applications*, 3–22. https://doi.org/10.5772/intechopen.79766.

2018c. “An Introductory Chapter: Secondary Metabolites.” In *Secondary Metabolites - Sources and Applications*. InTech. https://doi.org/10.5772/intechopen.79766.

Ullah, Asad, Asghari Bano, and Haleema Tariq Janjua. 2020. *Microbial Secondary Metabolites and Defense of Plant Stress*. *Microbial Services in Restoration Ecology*. Elsevier Inc. https://doi.org/10.1016/b978-0-12-819978-7.00003-8.

Vaishnav, Preeti, and Arnold L. Demain. 2011. “Unexpected Applications of Secondary Metabolites.” *Biotechnology Advances* 29 (2): 223–29. https://doi.org/10.1016/j.biotechadv.2010.11.006.

Vasundhara, M., M. Sudhakara Reddy, and Anil Kumar. 2019. *Secondary Metabolites from Endophytic Fungi and Their Biological Activities*. *New and Future Developments in Microbial Biotechnology and Bioengineering: Microbial Secondary Metabolites Biochemistry and Applications*. Elsevier B.V. https://doi.org/10.1016/B978-0-444-63504-4.00018-9.

Wang, Cai Yi, Hyun Jae Jang, Yoo Kyong Han, Xiang Dong Su, Seung Woong Lee, Mun Chual Rho, Heng Shan Wang, Seo Young Yang, and Young Ho Kim. 2018. “Alkaloids from Tetrastigma Hemsleyanum and Their Anti-Inflammatory Effects on LPS-Induced RAW264.7 Cells.” *Molecules* 23 (6). https://doi.org/10.3390/molecules23061445.

Wei, Jihua, and Bin Wu. 2020. “Chemistry and Bioactivities of Secondary Metabolites from the Genus Fusarium.” *Fitoterapia* 146 (June): 104638. https://doi.org/10.1016/j.fitote.2020.104638.

Yadav, Ajar Nath, Divjot Kour, Kusam Lata Rana, Neelam Yadav, Bhanumati Singh, Vinay Singh Chauhan, Ali Asghar Rastegari, Abd El Latif Hesham, and Vijai Kumar Gupta. 2019. *Metabolic Engineering to Synthetic Biology of Secondary Metabolites Production*. *New and Future Developments in Microbial Biotechnology and Bioengineering: Microbial Secondary Metabolites Biochemistry and Applications*. Elsevier B.V. https://doi.org/10.1016/B978-0-444-63504-4.00020-7.

Zhan, Jixun, and A. A.Leslie Gunatilaka. 2005. “Microbial Transformation of Curvularin.” *Journal of Natural Products* 68 (8): 1271–73. https://doi.org/10.1021/np0580309.

Zhan, Jixun, E M Kithsiri Wijeratne, Christopher J Seliga, Jun Zhangb, Elizabeth E Pierson, Leland S Pierson Iii, Hans D Vanettenb, and A A Leslie Gunatilakaa. 2004. “A New Anthraquinone and Cytotoxic Curvularins of a Penicillium Sp. from the Rhizosphere of Fallugia Paradoxa of the Sonoran Desert.” *JOURNAL OF ANTIBIOTICS*. Vol. 57.